Aus dem Lehrstuhl für Pathologie
Professor Dr. Evert
der Fakultät für Medizin
der Universität Regensburg

The role of E2F1 in cholangiocarcinoma
Potential therapeutic options

Inaugural- Dissertation
zur Erlangung des Doktorgrades der Medizin

der
Fakultät für Medizin
der Universität Regensburg

vorgelegt von Tabea Globuschütz

2023

Aus dem Lehrstuhl für Pathologie
Professor Dr. Evert
der Fakultät für Medizin
der Universität Regensburg

The role of E2F1 in cholangiocarcinoma
Potential therapeutic options

Inaugural-Dissertation
zur Erlangung des Doktorgrades der Medizin

der
Fakultät für Medizin
der Universität Regensburg

vorgelegt von Tabea Globuschütz

2023

Dekan: Prof. Dr. Dirk Hellwig

1. Berichterstatter: Prof. Dr. Matthias Evert

2. Berichterstatter: Prof. Dr. Tobias Pukrop

Tag der mündlichen Prüfung: 01.12.2023

Table of content

1. Introduction *5*

1.1 Cholangiocarcinoma **5**

1.1.1 Classification 5

1.1.1.a Subclassification of intrahepatic cholangiocarcinoma 7

1.1.1.b TNM classification 8

1.1.1.c Cells of origin 11

1.1.1.d Cancer stem cells 12

1.1.2 Epidemiology 12

1.1.3 Risk Factors 14

1.1.4 Clinical presentation, diagnosis, and treatment 15

1.1.4.a Intrahepatic cholangiocarcinoma (iCCA) 19

1.1.4.b Perihilar cholangocarcinoma (pCCA) 20

1.1.4.c Distal cholangiocarcinoma (dCCA) 21

1.2 Cell cycle **22**

1.2.1 Regulation of the cell cycle 23

1.2.2. Rb/E2F Pathway 26

1.3 E2F family of transcription factors **27**

1.4 Biology and function of E2F1 ..... **29**

1.5 E2F1 and its targets **31**

1.6 Structure and effects of HLM006474 ..... **34**

1.7 Aim of the work **35**

2. Material & Methods *36*

2.1.Material **36**

2.1.1 Equipment 36

2.1.2 Reagents 38

2.1.3 Cell lines 40

2.1.4 Primary Antibodies 40

2.1.5 Secondary Antibodies 41

2.1.6 Software 41

2.1.7 Patient Collective 42

2.2 Methods **44**

2.2.1 Cell culture 44

2.2.2 Transfection with RNAiMAx (Silencing) 45

2.2.3 RNA and protein isolation from 6-well-plates (Cellculture) 46

2.2.4 Protein Extraction 47

2.2.5 RNA Extraction 48

2.2.6 Bradford protein assay 48

2.2.7 Western Blot 49

2.2.8 Transcription into cDNA (complementary desoxyribonucleic acid) 50

2.2.9 Polymerase chain reaction (quantitative real time-PCR, q-RT-PCR) 51

2.2.10 Real-time Cell Analysis (RTCA) 53

2.2.11 Statistics 55

3. Results *57*

3.1 Protein levels - Western Blot Analysis **57**

3.2 RNA expression -Quantitative PCR-Analysis 64
3.3 Silencing of E2F1 in CCA-Cell lines 67
3.4 Real-time cell analysis under treatment with HLM006474 73
4. Discussion 78
4.1 E2F1 and regulation of its targets in CCA 78
4.2 Summary 87
4.3 Zusammenfassung 89
5. Attachment 91
5.1 List of figures 91
5.2 List of tables 93
5.3 List of abbrevations 95
5.4 Additional tables 98
6. References 101
7. Curriculum vitae I

Zusammenfassung

Das cholangiozelluläre Karzinom (CCA) ist ein äußerst aggressiver Tumor, welcher nach wie vor eine sehr schlechte Prognose hat, was unter anderem auf den oftmals späten Diagnosezeitpunkt und das bedingte Ansprechen auf die gängigen Therapieformen zurückzuführen ist.
Daher ist es notwendig an neuen therapeutischen Ansätzen zu arbeiten, um die Therapie und damit einhergehend auch die Prognose des CCA zu verbessern.
Fokus dieser Arbeit war der Transkriptionsfaktor E2F1, von dem bekannt ist, dass er beim Voranschreiten des Zellzyklus durch seine Stellung im Rb-Signalweg eine zentrale Rolle einnimmt. E2F1 beeinflusst die Expression vieler Gene bzw. tritt mit ihnen in Wechselwirkungen.
Durch die Einnahme einer solchen Schlüsselposition bei Zellteilung und Zellproliferation hat E2F1 auch bei der Proliferation von Tumorzellen eine große Bedeutung. In vielen Tumorentitäten wurde bereits eine Überexpression von E2F1 beschrieben, wenn die Rolle dennoch komplex scheint und es auch Tumorerkrankungen gibt auf die das nicht bzw. Gegenteiliges zu trifft.
Diese Arbeit lässt sich in zwei Versuchsbereiche aufteilen, basierend auf der Fragestellung, ob E2F1 im CCA therapeutisch genutzt werden kann.
Dafür wurden zum einen humane CCA Proben auf die Expression von E2F1 und einiger Zielgene (Cyclin E, Cyclin B1, MCM2, MCM7, c-Myc, Cyclin D1, SKP2 und FOXM1) untersucht, immer im direkten Vergleich mit gesunden Lebergewebe vom identischen Patienten. Auf Proteinebene konnten keine aussagekräftigen Ergebnisse erzielt werden, da sich keine deutlichen Expressionsunterschiede zwischen Tumorgewebe und tumorfreien Gewebe nachweisen ließen. Auf RNA-Ebene ließen sich zum Teil deutlichere Unterschiede herausarbeiten, wobei sich der erwartete Zusammenhang nur für E2F1 selbst und MCM2 auf signifikantem Niveau bestätigen ließ. Die meisten anderen Zielgene zeigten sogar widersprüchliche Expressionsmuster, wodurch sich abschließend kritisch ableiten lässt, dass die Untersuchung von 33 CCA Tumorproben in dieser Arbeit nicht dazu geführt hat, die Hypothese zu stützen, dass E2F1 ein vielsprechender therapeutischer Ansatzpunkt im CCA ist.

Der zweite große Versuchskomplex beinhaltete Zellkulturversuche mit vier CCA Zelllinien. Um hier die Abhängigkeit der Zielgene von E2F1 aufzuzeigen, wurde E2F1 mittels Silencing unterdrückt und dann die Expression der Zielgene darunter untersucht. Aus diesen Ergebnissen ließ sich ableiten, dass eine Unterdrückung von E2F1 die Expression der Zielgene deutlich beeinflusst, eine Unterdrückung über 50% ausgehend von der Expression in den Kontrollgruppen wurde hier für MCM2, MCM7, SKP2 und RRM2 nachgewiesen.

Des weiteren wurden die Zelllinien mit dem E2F1-Inhibitor HLM006474 in unterschiedlichen Konzentrationsstufen behandelt und anschließend ihr Wachstumsverhalten untersucht. Grundsätzlich kann anhand dieses Versuchmodells gesagt werden, dass die Anwendung von HLM006474 Auswirkungen auf das Wachstumsverhalten der CCA-Zelllinien hat, wobei der Unterschied zwischen 50 und 100 µM meist nicht mehr groß war. Zusammen mit den Ergebnissen aus den Silencing Versuchen, kann aber der Schluss gezogen werden, dass eine therapeutische Inhibierung von E2F1 zum einem möglich ist und zum anderen auch einige mit in die Tumorentstehung und-proliferation involvierte Gene beeinflussen dürfte.

Abschließend können die Ergebnisse dieser Arbeit dahingehend zusammengefasst werden, dass die Untersuchungen der humanen CCA Proben zwar keine eindeutigen Schlüsse über die Rolle von E2F1 und seine Zielgenen im CCA zulassen, aber die Zellkulturversuche dennoch zeigten, dass E2F1 im CCA Einfluss auf die Expression anderer Schlüsselgene hat. Eine Inhibierung von E2F1 durch HLM006474 beeinflusst das Wachstumsverhalten, so dass die Ergebnisse zumindest einen Ausgangspunkt dafür liefern, dass der Einsatz von HLM006474 weiter untersucht werden sollte. Neue Versuchsmodelle in vitro und in vivo sollten dafür zur Anwendung kommen und diese sollten auch um die Kombination mit bereits etablierten Therapieformen erweitert werden, um zu sehen, ob ein klinischer Einsatz von HLM006474 gute Ergebnisse in der Tumorbehandlung erzielen könnte und ein Einsatz im Menschen schlussendlich realisierbar wäre.

1. Introduction

1.1 Cholangiocarcinoma

Cholangiocarcinoma (CCA) includes a heterogeneous group of malignant tumors that can emerge at any point of the biliary tree (1). It is a rare tumor entity, accounting for less than 1.7% of all malignancies and 3% of all gastrointestinal tumors. Worldwide, CCA accounts for approximately 2% of cancer-related deaths (2). After HCC (hepatocellular carcinoma), CCA is the second most common malignancy of the liver, accounting for about 15% of all cases (2). Regarding incidence, there are significant geographic differences. Although many advances have been made in awareness, detection and diagnosis in recent years, the 5-year survival rate is still very low, ranging from 7-20% (3). Independent from the CCA classification, all CCAs are characterized by clinical aggressiveness and limited treatment options (4), which is why the research for further therapy options is crucial to improve the prognosis of this tumor disease.

1.1.1 Classification

The classification of CCA has been frequently modified. Most recently, a classification based on the anatomical location of the tumor in intrahepatic (iCCA) and extrahepatic (eCCA) has been established. Extrahepatic CCA has been further divided into perihilar (pCCA), also known as Klatskin tumor, and distal (dCCA). Intrahepatic CCAs are characterized by three main patterns of growth, which can be observed based on gross appearance (5): mass-forming (MF-iCCA), periductal infiltrating (PI-iCCA), and intraductal growing (IG-iCCA) (1, 5). Occurring in 65% of all iCCAs, the MF-Type is the most common type (1, 6). Histologically, it consists of adenocarcinoma cells with cholangiocellular differentiation surrounded by a rich desmoplastic stroma (6).
Most pCCA and dCCA are mucin-producing adenocarcinomas or papillary tumors (1, 7, 8). However, iCCAs are more heterogeneous (1); in general, they are adenocarcinomas with variable tubular structures, acinus formation, and micro papillary architecture (1, 7, 8). There are two different subtypes, classified by their anatomical origin along the intrahepatic biliary tree (5). There is bile ductular type (mixed) or "small-duct" type, originating from small intrahepatic bile ducts, and the bile duct type (mucinous) or "large duct" type, originating from large intrahepatic bile

ducts (5, 9-12). The histological classification is related to different clinicopathological features (5). Small duct type iCCAs show a nearly exclusively mass forming growth pattern (5, 9-12) and are associated with chronic liver diseases, like viral hepatitis and cirrhosis (13). No preneoplastic lesion as a precursor can be appreciated (3, 9-12).

In contrast, large duct type iCCAs display a mass-forming (MF), periductal infiltrating (PI), or intraductal growth pattern. Besides, these iCCAs are often associated with primary sclerosing cholangitis (PSC) and can show preneoplastic lesions as precursors (5,9-12). Furthermore, the bile duct type (mucinous) iCCAs show common characteristics with pCCA and pancreatic cancer (5)

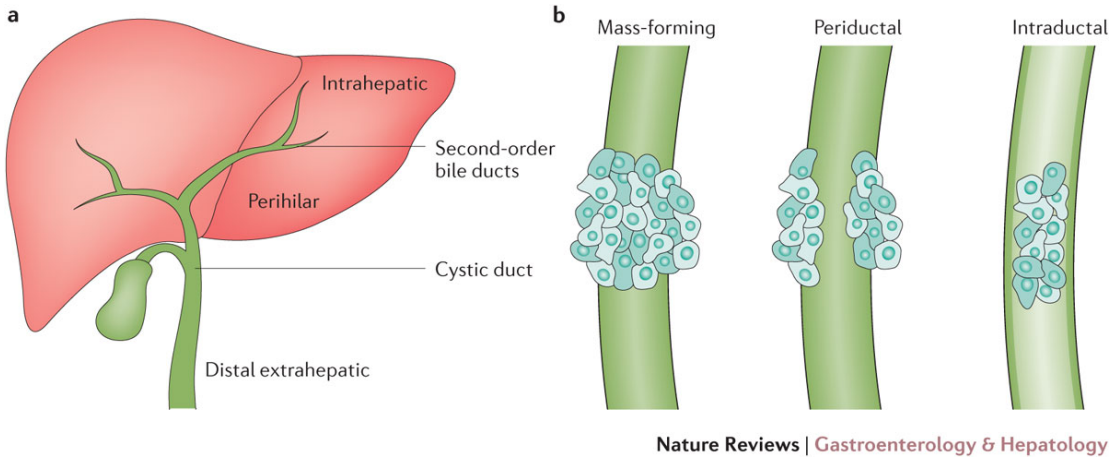

Figure 1: Classification and appearance of CCA

Source: Banales, J. M. *et al*. (2016) Cholangiocarcinoma: current knowledge and future perspectives consensus statement from the European Network for the Study of Cholangiocarcinoma (ENS-CCA). *Nat. Rev. Gastroenterol. Hepatol.* doi:10.1038/nrgastro.2016.51

The following table (Table 1) summarizes the different histopathological characteristics of small and large duct type iCCA.

1.1.1.a Subclassification of intrahepatic cholangiocarcinoma

	Small duct type	Large duct type
Main location and gross features	Peripheral hepatic parenchyma MF pattern	Proximal to hepatic hilar regions PI pattern, PI+ MF pattern
Risks	Non-biliary cirrhosis, chronic viral hepatitis	Primary sclerosing cholangitis, hepatolithiasis, liver fluke infection
Precursors	Unknown	Biliary intraepithelial neoplasia, intraductal papillary neoplasm
Histology	Small ductal components: tubular pattern with low columnar to cuboidal cells and desmoplastic reaction Ductular components: cuboidal epithelia showing ductular or cord-like-pattern with a slit-like lumen and desmoplastic reaction	Ductal or tubular pattern with columnar to cuboidal epithelium, with desmoplastic reaction
Mucin production	Non-mucin-secreting glands	Mucin-secreting glands
Perineural/Lymphatic invasion	-/+	++
Origins of cells	Small bile ducts and bile ductules; hepatic progenitor cells or transformed hepatocytes?	Intrahepatic large bile ducts and peribiliary glands
Common molecular features	IDH1/2 and BRAF mutation, FGFR2-fusions	KRAS mutations
Similar to	Adenocarcinoma component of combined hepatocellular cholangiocarcinoma	Perihilar cholangiocarcinoma

Table 1: Classification of small duct type and large duct type intrahepatic cholangiocarcinoma

Adapted from: WHO (World Health Organization) classification of Tumors, Digestive system tumors, 5th ed.;vol.1, pg. 254

1.1.1.b TNM classification

The UICC (Union for International Cancer Control) published the TNM classification of malignant tumors in close cooperation of numerous committees and continuous development. Among other things a uniform presentation is necessary to help clinicians in treatment planning, to derive an indication of prognosis, to facilitate the exchange of information between treatment centers, and also to contribute to the ongoing research in human cancers (14). Basically, the TNM classification consists of three components, where T describes the stage of the primary tumor, N the absence or presence of regional lymph node metastases, and M the absence or presence of distant metastases. Two classifications can be applied to all anatomic regions: On the one hand, the clinical classification (cTNM), which is based on findings obtained prior to treatment and based on clinical examination, imaging or other interventions, and on the other hand, the postoperative (pathological) classification (pTNM). These postoperative histopathologic findings are complementary to the findings obtained prior to treatment. A pathologic assessment requires surgical resection or biopsy. The clinical classification of the TNM classification is tabulated below.

For the pathological classification (pTNM) for the description of the primary tumor (pT) in general: pTX: primary tumor cannot be described, pT0: no histological evidence for primary tumor and pTis: carcinoma in situ, pT1-4: increasing size and/or local extension of the primary tumor on histological evaluation. For pathologic description of lymph nodes (pN): pNX: regional lymph nodes cannot be assessed histologically, pN0: no lymph node metastases histologically, pN1-pN3: increasing involvement of regional lymph nodes (16). For the description of distant metastases (pM): pM1: distant metastases confirmed microscopically, pM0 and pMX are not applicable categories.

Furthermore, a histopathological grading for the degree of differentiation (G) is established: GX: degree of differentiation cannot be determined, G1: well differentiated, G2: moderately differentiated, G3: poorly differentiated,G4: undifferentiated (14).

In addition, specific suffixes are used in special cases, where m indicates multiple primary tumors; y is used when initial multimodality therapy has already been given; r describes a recurrent tumor after a disease-free interval; and a indicates cases in which classification is by autopsy (14). Lymphatic vessel invasion (L), venous

invasion (V), and perineural invasion (Pn) may be indicated. Finally, the absence or presence of residual tumor is described by R: RX: presence of residual tumor cannot be described, R0: no residual tumor, R1: microscopic residual tumor, R2: macroscopic residual tumor (14).

Tables 2-4 show the current TNM classification of iCCA which is mainly investigated in this thesis.

Regional lymph nodes for right liver cholangiocarcinoma cover the hilar (common bile duct, hepatic artery, portal vein and cystic duct), periduodenal, and peripancreatic lymph nodes. For left liver intrahepatic cholangiocarcinoma, regional nodes are the hilar and gastrohepatic lymph nodes. iCCA further spreads into coeliac and/or periaortic and caval nodes, which already belong to the category of distant metastases (14).

T	Expansion primary Tumor
Tx	Primary Tumor cant be assessed
T0	No evidence of primary tumor
Tis	Carcinoma in situ (intraductal tumor)
T1	Solitary tumor 5 cm or less in greatest dimension without vascular invasion
T1b	Solitary tumor more than 5 cm in greatest dimension without vascular invasion
T2	Solitary tumor with intrahepatic vascular invasion or multiple tumors, with or without vascular invasion
T3	Tumor perforating the visceral peritoneum
T4	Tumor involving local extrahepatic structures by direct hepatic invasion

Table 2: Clinical TNM classification of tumors of the intrahepatic bile ducts : T- Primary Tumor

Source: UICC Classification of Malignant Tumors, 8th Edition

N	Regional lymoh nodes
Nx	Regional lymph nodes cannot be assessed
N0	No regional lymph node metastasis
N1	Regional lymph node metastasis

Table 3: Clinical TNM classification of tumors of the intrahepatic bile ducts: N- Regional Lymph Nodes

Source: UICC Classification of Malignant Tumors, 8th Edition

M	Distant metastasis
M0	No distant metastasis
M1	Distant metastasis

Table 4: Clinical TNM classification of tumors of the intrahepatic bile ducts: M- Distant Metastasis

Source: UICC Classification of Malignant Tumors, 8th Edition

Based on the TNM classification, iCCA is divided into 4 tumor stages, which also influence prognosis and treatment decisions. Table 5 shows the different stages according to UICC classification.

Stage 0	Tis	N0	M0
Stage I	T1	N0	M0
Stage IA	T1a	N0	M0
Stage IB	T1b	N0	M0
Stage II	T2	N0	M0
Stage IIIA	T3	N0	M0
Stage IIIB	T4 (Any T)	N0 (N1)	M0 (M0)
Stage IV	Any T	Any N	M1

Table 5: Stages classification according to UICC

Source: UICC Classification of Malignant Tumors, 8th Edition

1.1.1.c Cells of origin

iCCA is a histologically heterogeneous group of hepatobiliary malignancies and develops from biliary epithelial cells, and possibly hepatic progenitor cells or even mature hepatocytes. On the other hand, dCCA and pCCA develop from the biliary epithelium and peribiliary glands (15). It is assumed that the cell of origin is a normal cell that undergoes a series of mutations, ultimately leading to cancer development. Because of the different subtypes of CCAs, there might be a diverse cellular origin in every type of CCA (5). Cells of origin of the CCA could be hepatic stem cells, immature neural cell adhesion molecule positive (NCAM+) cholangiocytes, mature (NCAM-) interlobular cholangiocytes and peribiliary gland cells (5,16). Especially the iCCAs grow along or into the lumen of bile ducts, which is explained by their origin of biliary epithelial cells (BEC) (17). Another mechanism for the formation of iCCA could be the lineage conversion during malignant transformation of hepatocytes, which can be substantiated by the observation that activation of NOTCH signaling can cause a conversion from hepatocytes into BEC-like cells (17). There is a large inter- and intratumoral heterogeneity in CCAs, presumably caused by the interaction between distinct cell types and cells of origin (18). Experimentally, different cells of origin in iCCAs have been identified. Thus, a final determination of the origin of iCCA is still disputed, and further research is necessary to address this issue (2).

1.1.1.d Cancer stem cells

Cancer stem cells (CSCs) possess the ability for self-renewal (5) and malignant growth. They must be differentiated from the cells of origin, and they are not inevitably related to the stem cells (16). Some CSCs markers are expressed in the CCA, such as CD133, epithelial cell adhesion molecule (EpCAM), CD44, CD13, SOX2, and CD90, and over 30% of the tumor mass express CSCs markers (5). CSCs play an essential role in chemoresistance and tumor recurrence (5).

1.1.2 Epidemiology

CCAs are the most common biliary malignancy and the second most frequent hepatic tumor after hepatocellular carcinoma (HCC). They account for about 3% of all gastrointestinal tumors.

As concerns the frequency based on the different CCA types, 8% of the patients have an intrahepatic, 50% a perihilar, and 42% a distal tumor (19).

The epidemiology of CCA shows a vast geographical variation, which reflects the different exposures to risk factors (5, 20). In general, CCA is a rare cancer with an incidence of < 6 cases per 100.000 individuals (5). However, an exceptionally high incidence occurs in some countries, particularly in Asia, where it is often caused by liver fluke infection (5, 20). A worldwide progressive increase of iCCA up to the end of the past century, with a plateau in the last 10 years, has been described (5). In contrast to this observation, the incidence of pCCA and dCCA seems to be decreasing (5, 20).

The following figure shows the geographic differences in incidence (measured per 100,000 people):

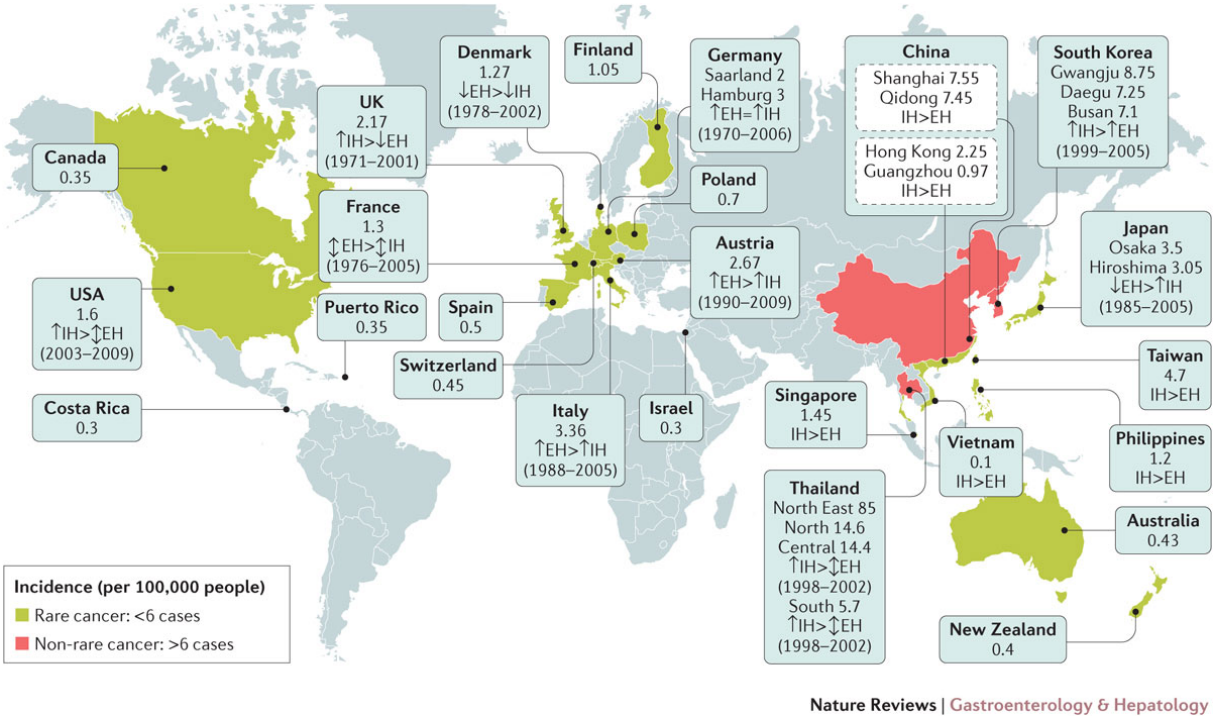

Figure 2: Worldwide incidence of cholangiocarcinoma

Source: Banales, J. M. *et al*. (2016) Cholangiocarcinoma: current knowledge and future perspectives consensus statement from the European Network for the Study of Cholangiocarcinoma (ENS-CCA). *Nat. Rev. Gastroenterol. Hepatol.* doi:10.1038/nrgastro.2016.51

It remains yet unclear whether the worldwide increasing incidence of iCCA is caused by the prevalence of cirrhosis and related risk factors or an increase in the diagnosis rate because of better screening programs (21).

The highest rates of CCA, which are related to age, are recorded in Hispanic and Asian populations (2.8-3.3 per 100.000) and the lowest in non-Hispanic white people and black people (both 2.1 per 100.000) (22). The development of CCA in childhood is unusual (23). The incidence in the male population is slightly higher than in the female population (15). In contrast to the increasing incidence of CCA in the last years, the 5-year survival rate has not increased in this period and is still about 10% (15). The mean age at the diagnosis is around 50 years and is unusual before 40 years except for patients with primary sclerosing cholangitis (PSC) (15). After the diagnosis, the median survival amounts to 24 months (15). From all cancer-related deaths worldwide, 13% are caused by hepatobiliary malignancies, and 10-20% of them are related to CCA (15).

1.1.3 Risk Factors

The majority of CCAs arise *de novo* without identifying risk factors (22). However, there are also established risk factors, which can be related to the geographic variation of incidence (15). In Southeast Asia, for instance, where the incidence rate of CCA is extremely high (15), the infection by the liver flukes (*Opisthorchis viverrini* and *Clonorchis sinensis*) is a prevalent risk factor (5), due to the ability of the two parasites to cause chronic inflammation of the biliary tract (15).

Especially in Europe and North America, PSC is a predisposing factor for CCA (15), mainly for pCCA (5). The lifetime prevalence for CCA for patients with PSC is between 5 -10% (24). About 50 % of the patients with PSC develop a CCA within 24 months after the diagnosis of PSC (22).

Another clinical and epidemiological relevant factor is the chronic infection by hepatitis B and hepatitis C virus and the possibly resulting in chronic liver disease or cirrhosis. Infections by hepatitis C display an increased association with CCA, especially in Europe and other Western countries (5). A hepatitis B infection is particularly significant in countries, where the prevalence of hepatitis B in general is high (5).

Further risk factors are structural changes in the biliary system, like extra- and intrahepatic cysts (24), cholelithiasis, choledocholithiasis (15) and hepatolithiasis or choledochal cystic diseases, like the Caroli disease (15), which consists of congenital, multifocal, and segmental dilation of the intrahepatic bile ducts (24).

There are also associations between developing a CCA and metabolic syndrome (5), alcohol and tobacco use, nonalcoholic fatty liver disease, and diabetes (21). Additional suspected risk factors are nitrosamine-contaminated food, asbestosis, dioxins, and vinyl chlorides (25).

All risk factors are characterized by chronic inflammation, which can be triggered by intrahepatic accumulation of bile acids in the absence of cholestasis (5). Nevertheless, most CCAs develop without the presence of chronic liver disease or other risk factors (5). CCA often develops in the context of inflammation and, for this reason, it can be divided into two different subtypes, the proliferation- and the inflammation-type (5). In the presence of sustained inflammation, cytokines, growth factors, tyrosine kinases, and bile acids can cause cholangiocarcinogenesis by triggering proliferation and apoptosis and modifications of the cell cycle (15). IL-6, an inflammatory mediator,

is secreted by CCA and possesses autocrine or paracrine effects on cholangiocytes' growth (5).

1.1.4 Clinical presentation, diagnosis, and treatment

In the early stages, CCA usually presents no symptoms (4). Consequently, all types of CCA are characterized by aggressiveness and a poor prognosis because of the late diagnosis.

Diagnosis is reached by the combination of clinical presentation and image findings (25). In terms of radiological imaging, contrast-enhanced ultrasound (CEUS), contrast-enhanced computer tomography (ce-CT), and contrast-enhanced magnetic resonance imaging (ce-MR) are mainly used. For histological classification, a biopsy is necessary, although there is a risk of metastasis seeding (26). If the diagnosis is confirmed, the staging is determined using mainly CT and MRI (magnetic resonance imaging) and 18-F-fluorodeoxyglucose positron emission tomography (18-FDG-PET) (25).

The most frequent CCA presentation is jaundice, marked by a yellowish or greenish pigmentation of the skin (25). The increased amount of conjugated bilirubin can also cause acholia/pale stools (25). Another frequent symptom of cholestatic diseases is pruritus, although it is not specific and associated with different systemic diseases (25).

Although there are different therapy strategies against this tumor type, complete surgical resection is the only treatment for the CCA with curative intent (5). Unfortunately, even after radical resection, the recurrence rate is high (up to 50% within the first 12 months) (19), and the 5-year overall survival is in the range of 25%-35% (28) (22-44% for iCCA, 11-41% for pCCA, and 27-37% for dCCA, respectively) (5). For patients with unresectable, metastatic, advanced, or recurrent CCAs, systemic therapy consists of palliative treatment (27).

Figure 3 outlines the current treatment recommendations for biliary carcinomas in Germany:

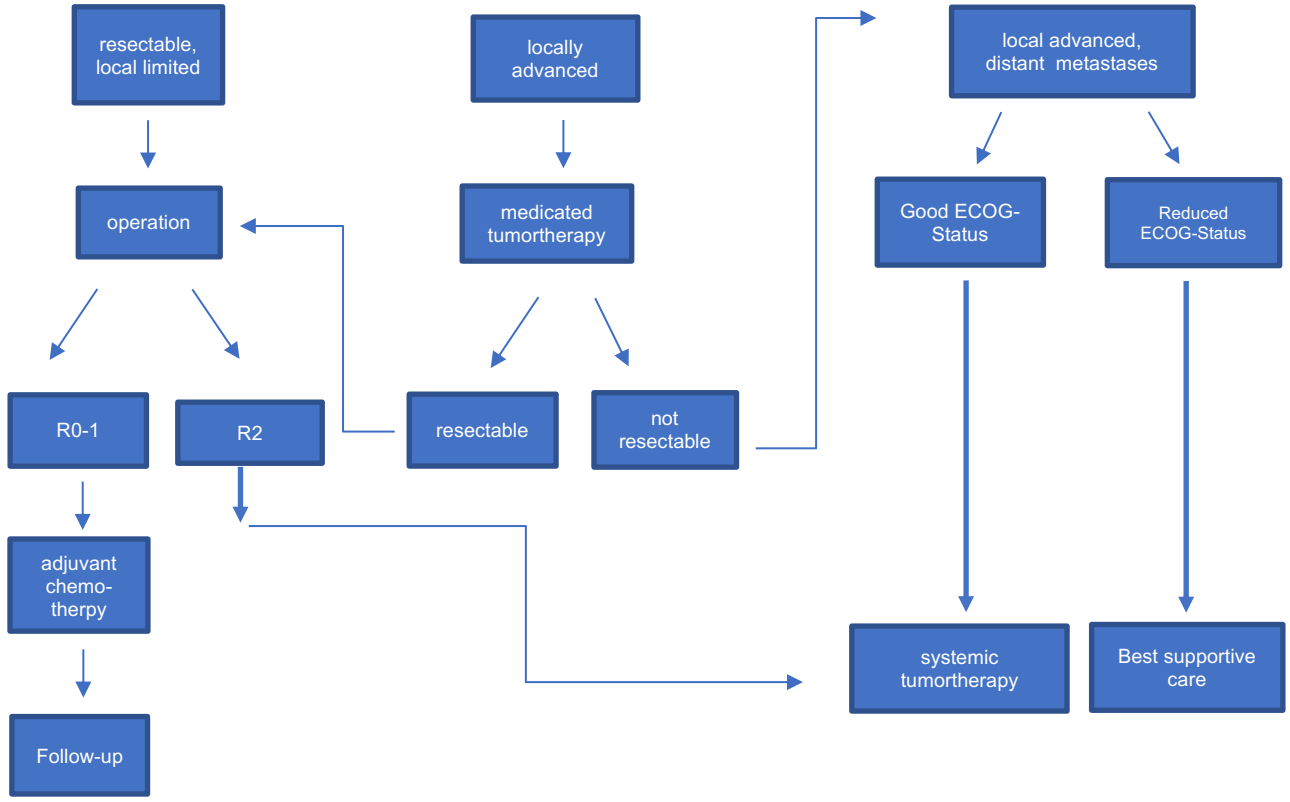

Figure 3: Therapeutic algorithmus biliary carcinoma

ECOG (Eastern Cooperative Oncology Group), ECOG Performance Status is attached in the appendix (5.4 Nr.1),

R0= Removal of the tumor in healthy, no tumor tissue detectable in the resection margin; R1= macroscopically completely removed, histopathologically small rests detectable in the resection margin, R2=larger macroscopically visible parts could not be removed

Source: Onkopedia Guideline, Biliary Carcinoma, October 2021

The main goal of the surgery is R0 resection combined with low post-operation mortality (26).

In an unresectable or metastatic stage, systemic chemotherapy is the most common palliative treatment (5). Gemcitabine combined with Cisplatin is the first-line treatment, as the progression-free and overall survival are higher than using gemcitabine alone (5). A meta-analysis from 2014 showed insufficient evidence for second-line chemotherapy, but selected cohorts of patients may benefit from it (29). In clinical practice, often a fluoropyrimidine-based regimen, when the gemcitabine-based treatment fails, is employed (5).

Although the use of adjuvant chemotherapy is still questioned, the BILCAP study (a phase 3 study) suggests the improvement of overall survival in patients with resected biliary tract cancer when capecitabine is used as adjuvant chemotherapy (30).

In contrast, a french randomized phase III trial (PRODIGE-12-ACCORD 18-UNICANCER GI), which included patients with intrahepatic, extrahepatic, and bile duct carcinomas, has so far shown no improvement in survival with adjuvant chemotherapy with gemcitabine and oxaliplatin compared with follow-up only (3, 31).

Also the randomized BCAT trial, recently showed no advantage between adjuvant therapy with gemcitabine or follow-up only in patients with extrahepatic biliary carcinoma (3, 32). Currently, additional studies are still recruiting, which should hopefully yield more fundamental conclusions about the benefits of adjuvant therapy in the future.

Mainly due to the high recurrence rate, there is often a need for local adjuvant therapy. Although there is currently no standard for adjuvant radiochemotherapy, since no randomized phase III trials are available, meta-analyses describe the benefit of both adjuvant radiotherapy, especially in the case of positive lymph node status, and adjuvant radiochemotherapy (3, 33, 34).

External-beam radiation therapy (EBRT), such as 3D conformal radiotherapy (3D-CRT) or intensity-modulated radiotherapy (IMRT), is used (35).

Neoadjuvant therapy concepts are partly already used individually. Especially when it comes to achieving a possible resectbale status. Clinical studies are currently underway to establish possible therapy concepts (3).

In Stage IV (see Figure 3) palliative systemic therapy with gemcitabine and cisplatin is the therapy of choice, if the general condition permits and a best supportive care

concept in case of reduced general condition. In case of non-response or progression during systemic therapy, molecularly stratified therapies are now available, which is why a molecular genetic or molecular pathological examination is recommended before starting therapy. In the meantime, therapies for patients with proven genetic alterations have already been approved in the second line (3). Thus, for patients with FGFR2 gene fusion/rearrangement, the tyrosine kinase inhibitor Pemigatinib is approved (36). Entrectinib or Larotrectinib are available for patients with NTRK alterations (3). For off-label use, there is also the possibility of targeting patients with an IDH (isocitrate dehydrogenase)1 mutation with Ivosidenib, clinical studies showed a benefit in progression-free survival (2).

One reason why target- and immunotherapy are becoming more important, also in research, is the poor response of CCA to conventional chemotherapy regimens.Thus, an urgent need of modern pharmacology is to understand the mechanisms of chemoresistance (MOC) in this tumor type (5). Several MOC have been identified in CCA: change of drug concentration by a reduced uptake (MOC1a) or by an enhanced efflux (MOC1b); different ratios between the active drug, prodrug, and the inactive metabolites (MOC2); change in molecular targets of antitumor drugs related to a different response to the chemotherapy (MOC3); the inability of tumor cells to repair DNA (deoxyribonucleic acid) lesions that are caused by the drug (MOC4); an imbalance between apoptosis and survival of tumor cells (MOC5) (27).

In an inoperable stage, local therapy procedures such as direct ablative and transarterial procedures are applied. Direct ablative procedures include radiofrequency ablation (RFA), microwave ablation (MWA), and CT-guided high-dose brachytherapy, starting at a tumor size of 3 cm.

Transarterial procedures include transarterial chemoembolization (TACE), selective internal radiotherapy, intraarterial chemotherapy, and chemosaturation (3).

Some special features of the diagnosis and treatment of each subtype of CCA are outlined in the following sections.

1.1.4.a Intrahepatic cholangiocarcinoma (iCCA)

iCCA arises from the intrahepatic biliary tract, and patients often show an intrahepatic mass forming lesion (MF) (24). The MF- type is the most frequent iCCA (5). The MF-type usually spreads along the veins and lymphatic vessels. Besides, a superficially spreading type, which does not invade the liver parenchyma but goes along the biliary duct lumen and has a better prognosis than other CCAs, has been described (24). CT and MRI are used to diagnose, with iCCA showing the contrast agent's uptake in the arterial and venous phases (24). Differential diagnosis of iCCA versus HCC is still a problem because there are no specific markers to differentiate between them (5). Despite diagnostic options, the diagnosis is an incidental finding in 20-25% of cases (5). As already mentioned, iCCA develops more frequently in patients with chronic liver disease, such as an infection by hepatitis B or hepatitis C, or an infection by a liver fluke, than the pCCA (5). Patients often show unspecific, heterogeneous symptoms like malaise, cachexia, abdominal pain, fatigue, and jaundice (5, 24).

Carbohydrate antigen 19-9 (CA19-9) is a serum marker of CCA, with 62% sensitivity and 63% specificity. However, testing CA19-9 should be associated with other diagnostic tools to identify individuals with iCCA (24). CA19-9 levels >1000 U/ml point to the presence of metastatic disease (35). Immunohistochemical markers such as Cytokeratin (CK) 19 and 7 are helpful in difficult histologic cases, especially for mixed tumors (HCC-CCA) (24). As mentioned before, surgical resection is the only potentially curative therapy for iCCA, with the goal of a complete R0-resection and the preservation of an adequate portion of the liver (26). Patients with metastatic disease or nodal involvement beyond the hepatoduodenal and gastro-hepatic ligament show lower benefits from a resection (26). The 5-year survival of patients after resection is about 60 % (17).

Patients with unresectable iCCA who undergo liver transplantation show, in general, a poor 5-year survival (25%) (26) and a rapid tumor recurrence (5). Consequently, liver transplantation is generally not indicated for iCCA patients (26).

For iCCA that is too large for percutaneous ablation, transarterial chemoembolization (TACE) and transarterial radioembolization (TARE) can be applied (5). Also, it has been shown that in patients with an unresectable iCCA, use of TACE in association

with cisplatin improves the survival of the patients. Radiofrequency ablation also seems to provide benefits for this group of patients (5).

1.1.4.b Perihilar cholangocarcinoma (pCCA)

pCCAs can develop at any point from the second-order biliary ducts upwards (24). The most frequent subtype of the pCCA is the periductal-infiltrating tumor, although it can also show up as a nodular form (24). Usually, pCCAs spread by perineural invasion and lymphatic metastasis (24).

When pCCAs develop in the major bile ducts, they can cause cholestasis and display symptoms earlier than the iCCA. About 90% of the patients have painless jaundice, 10% have cholangitis, and 56% have unspecific systemic symptoms, such as malaise, abdominal pain, nausea, anorexia or weight loss (24).

A typical radiological sign for the pCCA is a bile duct stricture (5). Cillo et al.(26) described in their work the diagnostic workup that, besides the presence of a constriction in the liver hilum, the diagnosis of a pCCA requires one of the following:

1. Biopsy or cytology positive for cancer cells
2. Polysomy by fluorescent in situ hybridization (FISH)
3. Mass forming lesion on CT or MRI at the stricture
4. CA 19-9 above 100 U/ml

The evaluation of the serum levels of CA19-9 is less specific for the detection of pCCA than iCCA (15). In case of uncertain diagnosis, patients undergo further examinations, such as endoscopic retrograde cholangiopancreatography (ERCP), magnetic resonance cholangiopancreatography (MRCP), and several other procedures (cytology, brushing, FISH). Nonetheless, about 40% of the patients undergo surgery without a definitive diagnosis (5).

MRCP has replaced the ERCP in diagnosing this tumor type (26).

Similar to iCCA, the resection of pCCA is the only curative option. Helpful for the decision is the Bismuth-Clorette classification (15) and the AJCC (American Joint Committee on Cancer) classification system, which assesses the local extent and the peripheral spreading of the tumor (26). The surgical resection of the pCCA often requires a radical hemi-hepatectomy, which has a relevant impact on the patient's

performance status and the function of the remaining liver (26). In the presence of obstructive cholangitis, percutaneous biliary drainage (PBD) is necessary (28). After resection, the risk of post-hepatectomy liver failure (PHLF) is elevated. Portal vein embolization decreases the risk of PHLF, because of compensatory hypertrophy from the remaining liver, by occluding the portal vein from the resected liver (26). After resection, the recurrence rate is high, and the 5-year survival ranges from 13% to 40% (37).

A neo-adjuvant chemo-radiation followed by liver transplantation has also been discussed as a curative option (15). Liver transplantation of patients with pCCA effectively cures the underlying liver disease (26); patients with PSC, for example, need liver transplantation often more than surgical resection (15).

Some loco-regional treatments are under investigation as alternative options in the absence of distant metastatic disease (26). These treatments consist mainly of hepatic arterial infusion pumps, irreversible electroporation, and photodynamic therapy (26).

1.1.4.c Distal cholangiocarcinoma (dCCA)

dCCA involves the distal common bile duct (38) and can arise at any point between the insertion of the cystic duct and the ampulla of Vater (15). Due to its anatomic location, it is often difficult to differentiate between dCCA and pancreatic adenocarcinoma (38). Like patients with early pancreatic cancer, dCCA patients exhibit painless jaundice and laboratory findings according to biliary obstruction (15). dCCA can originate from intraductal papillary neoplasm and biliary intraepithelial neoplasia as precursor lesions (15).

The diagnosis of dCCA is achieved similar to that described for the diagnosis of pCCA (35) .

Surgical resection of dCCA typically requires a pancreaticoduodenectomy (Whipple procedure) (35). The 5-year survival of patients with dCCA is about 23%; if an R0 resection is performed, the 5-year survival is about 27% (35).

1.2 Cell cycle

The cell cycle is a complex process with different phases (Figure 4), which depends on many regulatory proteins to correct DNA duplication and the production of two identical daughter cells. Morphologically, the cell cycle can be subdivided into the M (mitotic) phase and the interphase. The M-phase includes mitosis and cytokinesis when the chromosomes and cytoplasm are split into two daughter cells. Mitosis is composed of five steps: prophase, prometaphase, metaphase, anaphase, and telophase (39). The interphase includes G1-, S-, and G2-phases. DNA replication takes place in the S-phase. The interval between mitosis and DNA replication is called G1-phase, and G2- phase marks the period between the completion of DNA replication and mitosis (39).

Checkpoints are control stations between cell cycle stages. The checkpoints send inhibitory signals to the cell cycle system when an internal or external problem occurs (39). There are four different checkpoints (39):

1. Restriction point: in G1-phase, sensitive to physiological status of the cell and interaction with extracellular matrix.
2. DNA- damage checkpoints: in G1-, S-, G2-phase, block cell-cycle progression and can trigger apoptosis.
3. DNA- replication checkpoint: detects incorrect DNA replication forks, can stabilize stalled replication forks.
4. Spindle assembly checkpoint (metaphase checkpoint): delays chromosome separation until all chromosomes are in the correct position to the mitotic spindle.

As mentioned above, the cell cycle is highly regulated. Characteristic for cancer is uncontrolled cell proliferation, which can be due to somatic mutations, infection by viruses, or genetic predisposition (40). Somatic mutations related to cancer are mainly relevant when they affect genes responsible for cell growth and cell proliferation or DNA repair. There are two different groups of genes in this context, controlling cell growth and cell proliferation. On the one hand, the proto-oncogenes, which stimulate growth and differentiation processes, and on the other hand, the tumor suppressor

genes, which inhibit these processes. Consequently, activating mutations of proto-oncogenes and inactivation of tumor suppressor genes are responsible for carcinogenesis and many of them lead to carcinogenic cell cycle dysregulation (40).

1.2.1 Regulation of the cell cycle

The cell cycle is controlled by complexes that consist of cyclins, cyclin-dependent kinases (CDKs), and CDK inhibitors (CKIs) (Table 6,7). CDKs have a serine/threonine-specific catalytic core (41): they build complexes with subunits of cyclins and are activated by phosphorylation and initiate transition to the next cell cycle step. CKIs can inhibit CDKs so that the cell cycle can be stopped when they detect incorrect DNA.

Kinase	Cyclin (or other partners)	Function
CDK 1	A, B1, B2	G2- → M-phase transition
CDK 2	A, E	G1- → S transition
CDK 3		Poorly understood
CDK 4, CDK 6	D1-D3	Phosphorylation of the retinoblastoma protein (pRb)
CDK 5	P35	Neuronal differentiation
CDK 7	H	RNA Polymerase II transcription and DNA repair
CDK 8	C	Regulation of RNA Polymerase II
CDK 9	T	Regulation of RNA polymerase II transcription

Table 6: CDKs and their cyclin partners (39)

Source: Cell Biology, Pollard TD et al., Vol. 2

CKI	Inhibiton target	Function
CKI: P21	most CDK-cyclin complexes	induced by p53 tumor suppressor, cell cycle arrest after damage
CKI: P27	most CDK-cyclin complexes	cell cycle arrest in response to growth suppressors like TGF-ß
CKI: P57	most CDK-cyclin complexes	Important in the development of the palate

Table 7: CKIs

Source: Cell Biology, Pollard TD et al., Vol. 2

Cyclins have many functions in the regulation of the cell cycle. Before a cell can reach the next step in the cell cycle, the cyclin levels of the previous phase decrease, and the cyclin of the next phase in the cell cycle is synthesized (42).

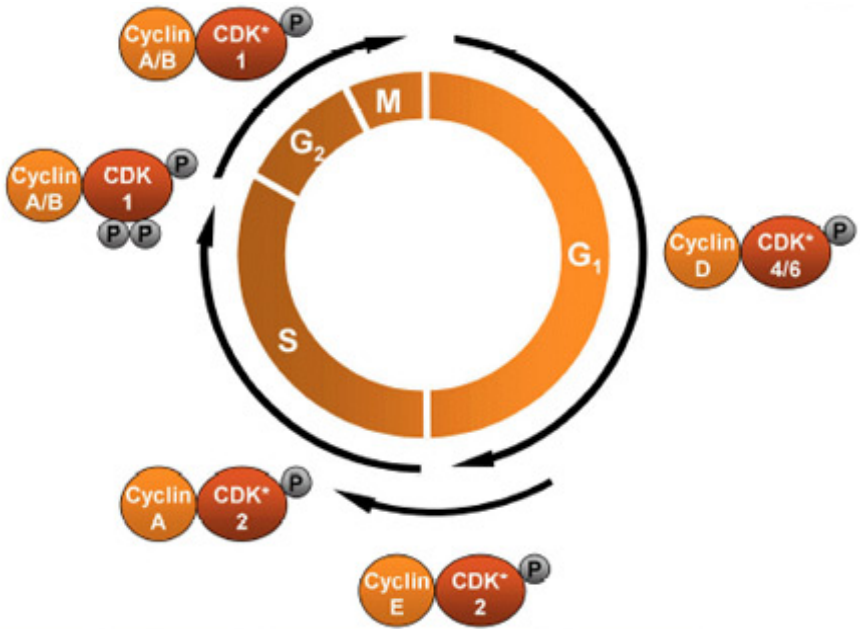

Figure 4: Cell cycle

Source: https://www.chemie.uni-l.de/fachrichtungen/lmctox/eisenbra/forschung/cyclin.html

A critical tumor suppressor in the control of the cell cycle is the retinoblastoma protein (p(phosphorylated)Rb). At the end of the G1-phase, hypophosphorylated Rb is bound to the transcription factor E2F1. In this bound form E2F1 is inactive and transcription is slowed down or stopped. When Rb is phosphorylated, the chemical binding between pRb and E2F1 is disrupted, and E2F1 is released (Figure 5). This step is necessary

for the cell cycle progression. There are also different negative regulators, including the p16 and the p21 families (42).
Figure 5 shows the E2F1 related transcription.

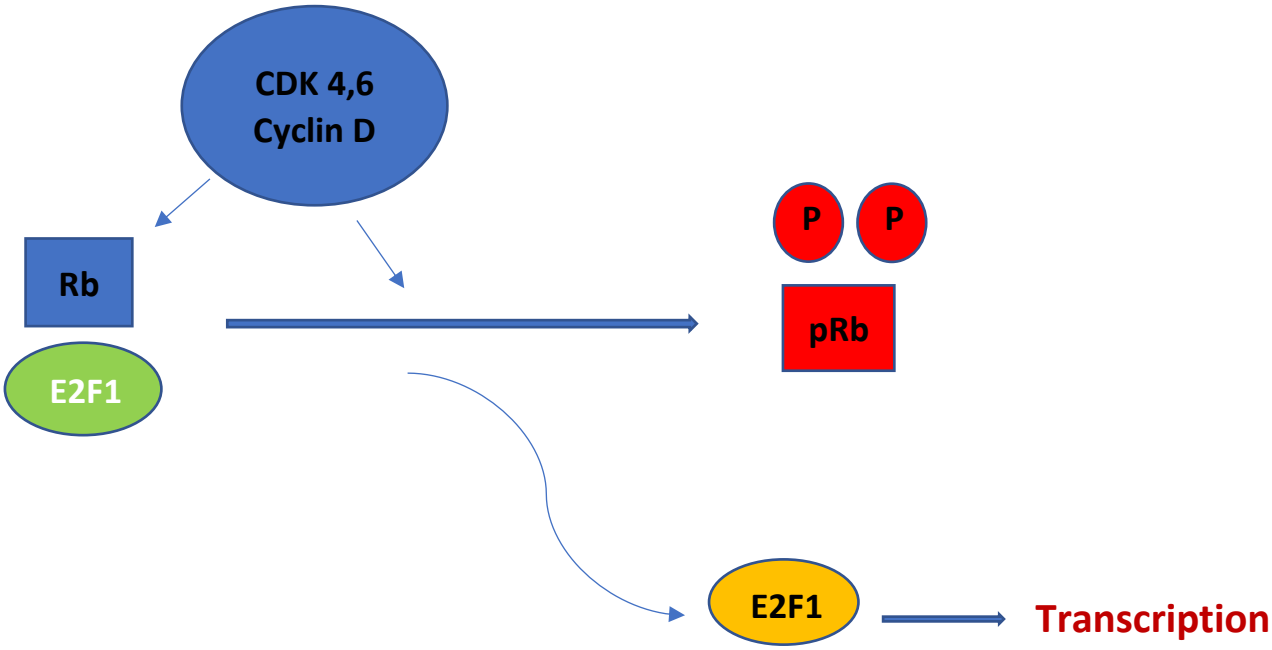

Figure 5: E2F1 related Transcription

For instance, proteins from the p21 family bind to cyclins and prevent phosphorylation of Rb by CDKs. The p53 protein induces the expression of p21, thus triggering cell cycle arrest (43). During the replication, cells are dependent on growth factors, and the point after which the cells are no longer under the impact of growth factors is referred to as the restriction point (42). As mentioned above, the restriction point is the first checkpoint in the cell cycle, so if the DNA replication started, it must be finished. After the restriction point, the S-phase progression is not controlled by extracellular signals like growth factors (44). When DNA replication is completed, and the cells finish the S-phase, they go into G2-phase and prepare for mitosis, without the control of growth factors (44). At this point, internal checkpoints evaluate the presence of DNA damage. The mitosis progress after the G2-phase depends on pathways that check the

microtubule function and the correct chromosomal separation. Thus, the beginning of the G1-phase is the only period in the cell cycle that depends on growth factors (44). It has been proposed that for passing the restriction point, an accumulation of labile proteins (R-proteins) is necessary (45). R-proteins are sensitive to growth factors (44), and an accumulation of a certain amount is necessary for the transition from the restriction point to the S-phase (45). One hypothetical R-protein is Cyclin D1 that leads different mechanisms to G1/S progression (44). As mentioned above, the phosphorylation of Rb by Cyclin D-CDK 4/6 leads to E2F1 release and at least to activation of Cyclin E and A. Cyclin E builds a complex with CDK2, which also works on the phosphorylation of Rb. The activation of the Cyclin E-CDK 2 complex is necessary for independence from growth factors (44) and the progression to the S-phase. Overall, at the restriction point, different up- and down-regulation processes come together and build feedback loops. Another transcription factor, which takes part in regulating the restriction point, is C-myc. C-Myc is involved in many processes such as cell proliferation, survival, and metabolism (46).

Numerous molecular pathways act in somatic cells allowing the cell to enter the S-phase of the cell cycle. When the cell starts the division cycle, cell cycle checkpoints monitor this process. Main regulation mechanisms are the Rb pathway, the C-myc proto-oncogene as a central regulator, and the Rb-E2F axis (47). Also crucial for the regulation during the G1/S checkpoint is the silencing of Cdc25A and the sustained activation of the p53 tumor suppressor (47).

1.2.2. Rb/E2F Pathway

RB1 (the gene encoding Rb protein) is a critical tumor suppressor gene, and the E2F1 transcription factor is the main target of the growth suppressing function of pRb (48). The Rb protein is a vital tumor suppressor and controls the transition from the G1- to the S-phase of the cell cycle. Rb is active in the dephosphorylated form and binds E2F1 until phosphorylation by CDKs. pRb belongs to the group of pocket proteins, which have pockets to bind their target molecules. Only once the release of E2F1 is finished, the cell cycle can enter into the S-phase. Thus, the Rb/E2F pathway takes part in controlling cell proliferation.

A connection between the accumulation of p53-induced apoptosis and the Rb/E2F1 pathway has been established. Specifically, the loss of pRb function induces the accumulation of E2F1 and the ARF/Mdm2/p53 pathway (48). The regulation of this and other molecular pathways are embedded in a sensitive system; thus, it is not surprising that oncogenic mutations impair the pathway's normal function (48). In many human tumors, a large spectrum of modifications, particular deletions, mainly affecting pRb, have been identified. Another frequently mutated gene in the Rb/E2F pathway is the p16 cyclin kinase inhibitor, which regulates Cyclin D/CDK4 kinase activity (48). The overactivity of unhindered Cyclin D/CDK 4 leads to E2F1 accumulation.

1.3 E2F family of transcription factors

The E2F proteins are a group of transcription factors that play a pivotal role in the cell cycle, especially in G1-phase, when the cell is about to enter the S-phase and go into DNA replication. E2F proteins can be divided into subgroups based on their main function, structures, and interacting partners. To date, eight E2F (E2F1-8) genes have been identified, which are shown in Table 8.

The first group includes the E2F1-3a genes: They can be defined as “activators” since they promote the transcription during the transition from the G1- to the S-phase (49). This group of activators is bound to pRb. Thus, the loss of E2Fs of this group results in cell cycle arrest (50). The gene locus of E2F3 can be divided into two different parts, which means two different proteins are encoded: E2F3a belongs to the group of activators and is superficially expressed in S-phase, while E2F3b is a repressor of the transcription and constantly expressed during the cell cycle (49). The second group of E2Fs includes E2F3b, E2F4, and E2F5; they act as transcription repressors (49). E2F6, E2F7, and E2F8 also belong to the repressors group, but in contrast to E2F3b, E2F4, and E2F5, they do not bind to pocket proteins. E2F4 mainly binds to p107 and p130, and E2F5 to p130 (49). E2F6 is part of a multi-subunit complex (51). How E2F7 and E2F8 repress the expression of genes and, therefore, the transcription, is less understood, but it seems that they act differently from the other E2Fs (51).

The function of the various E2F genes are summarized in Table 8.

E2F1 gene	Cell cycle	Transcription	Pocket proteins	Biological function	Special functions
E2F1	activators	Promote transcription	-	Apoptosis/ Proliferation	-
E2F2	activators	Promote transcription	-	Apoptosis/ Proliferation	-
E2F3a	activators	Promote transcription	-	Apoptosis/ Proliferation	-
E2F3b	repressors	-	-	-	-
E2F4	repressors	-	Binds to pocket proteins p107 and p130	Differentiation	-
E2F5	repressors	-	Binds to p130	Differentiation	-
E2F6	repressors	-	Part of a subunit complex	Development Differentiation	-
E2F7	repressors	directly repress transcription of transcription factors like E2F1	no binding to pocket proteins	-	Key role in polyploidization of placenta and liver cells (52)
E2F8	repressors	directly repress transcription of transcription factors like E2F1	no binding to pocket proteins	-	Key role in polyploidization of placenta and liver cells (52)

Table 8: E2F family genes and role in cell cycle, transcription, and other biological features

1.4 Biology and function of E2F1

E2F1 is a master regulator of the cell cycle but also a controller of apoptosis induced by DNA damage and the checkpoint response (53). E2F1 has a single DNA binding domain and needs to heterodimerize with the dimerization partner (DP1/DP2) to forge an effective DNA bond and recruit other transcription factors (53). A group of pocket proteins can inhibit the E2F1-DP1/2 heterodimers: pRB, p109, and p130 (53). The Rb proteins are corepressors of E2F transcription factors (54) and operate via two mechanisms: they block the transcriptional activation domain of E2F1 (53). In addition, they are also thought to recruit histone deacetylases to E2F1-responsive promoters, thus repressing gene expression (54). The structure of E2F1 is shown in Figure 6.

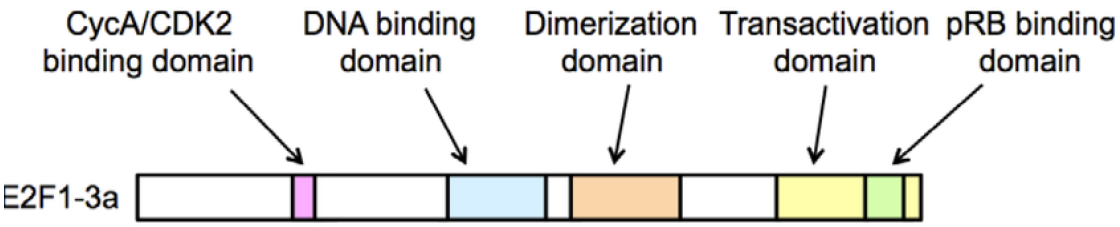

Figure 6: Structure of E2F1

Source: Ozono, E., Yamaoka, S., Ohtani, K., 2013, 'To Grow, Stop or Die? – Novel Tumor-Suppressive Mechanism Regulated by the Transcription Factor E2F', in Y. Cheng (ed.), Future Aspects of Tumor Suppressor Gene, IntechOpen, London. 10.5772/54510., Figure 4

As mentioned above, a crucial point in the cell cycle is the restriction point, after which the cells complete cell cycle and go into S-phase. It is assumed that E2F1 is a mediator of the transition from G1- to S-phase. This regulatory role has been proven by the finding that a prolonged overexpression of E2F1 leads to G1 checkpoint activation and apoptosis to avoid redundant DNA synthesis (53). The inhibition of E2F1 is induced through negative feedback from the product of E2F1 target genes (53). Involved proteins, including Cyclin E and Cyclin A, have different cell cycle peaks. They show a delayed expression, so Cyclin E is always expressed before Cyclin A (53), necessary for transition into the S-phase.

Due to the many functions of E2F1 and the target genes in the cell cycle progression, it is easy to envisage that E2F1 acts as a tumor promoter (53). Thus, it is not surprising that E2F1 is overexpressed in most tumor types. Mutations in the E2F1 gene are rare, and the COSMIC database lists 43 somatic mutations (53). Overexpression of CDK4/6

can lead to E2F1 pathway overactivation; besides, some viruses, including the human papillomavirus or the adenovirus, can perturb the binding pRb-E2F1 binding, leading to E2F1 deregulation (53). Another possible mechanism leading to a perturbed E2F1 is the loss of function of pRB due to mutations or phosphorylation-dependent inactivation (55).

Besides cell cycle regulation, E2F1 promotes DNA repair and apoptosis, thus possessing tumor suppressor functions as well (53). E2F1 induces apoptosis through the p53 pathway, p73 induction, and the intrinsic apoptotic pathway (53, 56). However, it has been shown that E2F1 can also block apoptotic signals via the PI3K/AKT pathway and promotes DNA repair (53).

It has been known for some time that the E2F transcription factors are connected to cancer development. Higher expression levels of E2F family genes have been found in different tumor tissues (57). A higher level of E2F1 expression linked to poor prognosis could be detected in hepatocellular carcinoma and lung adenocarcinoma (57). In cervical cancer, E2F1 has a prognostic role; indeed, high expression of E2F1 is a favorable factor (58). In thyroid cancer, a higher expression is also linked to a better prognosis (59). In liver, endometrial, renal, and pancreatic cancer, in contrast, high levels of E2F1 are associated with an unfavorable prognosis (60). Similarly, E2F1 target genes play a role in forming pulmonary metastases (61). In prostate cancer, a recent study showed that increased expression of E2F1 is associated with a higher Gleason score and thus a higher pathological stage. Those patients also showed a shorter recurrence-free interval (62).

1.5 E2F1 and its targets

In addition to the role of E2F1 itself and some target genes interacting with E2F1 in CCA, especially some cyclins and their kinases are presented in 1.2.1. This work focusses on Cyclin D1, Cyclin B1 and Cyclin E1.

A direct link between E2F1 and Cyclin D1 and E1 has been previously unraveled by the discover of putative E2F1 transcription binding sites in Cyclin D1 and Cyclin E1 promoters (63). Cyclin D1, which binds to the CDKs 4/6, enables the phosphorylation of Rb, which is necessary to release the transcription factor E2F1. Cyclin D1 and its gene CCDN1 with its function in cell proliferation is known as an oncogene (64). For instance, in esophageal squamous cell carcinoma, it has been demonstrated by immunohistochemistry that the combined upregulation of E2F1 and Cyclin D1 in the tumor tissue is an indicator of tumor progress and the prognosis of the patients (65).

As with Cyclin D1, the role of Cyclin E has already been highlighted under 1.2.1.

Cyclin E1, which binds to CDK2, causes the transition from G1- to S-phase. An increased Cyclin E1 concentration is associated with the development of cancer in many tumor entities, and its overexpression is also documented as a negative prognostic factor for example in ovarian cancer (66), breast cancer (67) and non-small cell lung cancer (68).

As another important cell cycle regulator, the role of Cyclin B in CCA is also attempted to be elucidated in this work. Cyclin B1 builds a complex with CDK1 and controls the entrance of the cell into mitosis. Cyclin B1 overexpression was revealed in many tumors, such as colorectal cancer (69), non-small cell lung cancer (70), and breast cancer (71), to name just a few. Besides this, it was observed that a high expression level of Cyclin B1 leads to chromosome instability (72), which promotes malignancy.

The CCBN1-gene encodes Cyclin B1. The resulting protein is involved in mitosis and forms a complex with p34 to build the maturation-promoting factor (MPF), which is necessary for controlling of G2/M- transition phase in the cell cycle. (73)

Previous studies showed that E2F1 had an impact on genes that regulate mitotic entry like Cyclin B1. Therefore, mitotic inhibitors may affect tumors with overexpression of E2F1 (74). Conversely, E2F1 could also reduce the cancer-promoting properties of

Cyclin B1. Recent studies in prostate cancer suggest that inhibition and stimulation of E2F1 and Cyclin B1 are modulated through CD437 (75).

c-Myc and its relationship to E2F1 in the CCA was also examinated in this thesis.

c-Myc is a transcription factor located on chromosome 8 and a protooncogene encoding a phosphoprotein that plays a role in cellular transformation, apoptosis, and cell cycle progression (76). The role of E2F1 is complex, and overexpression of E2F1 can have promoting or inhibitory effects on carcinogenesis. The interaction of E2F1 and c-Myc on carcinogenesis is similarly complex. Studies in colorectal cancer showed that overexpression of E2F1 triggers apoptosis and leads to upregulation of c-Myc (77). Another investigation revealed that E2F1 is an antiapoptotic factor by inhibiting c-Myc driven apoptosis via activation of PIK3CA/AKT/mTOR and c-Myc/COX-2 pathways (78). The interaction of E2F1 and c-Myc might also result in a negative feedback mechanism, and the failure of this mechanism triggers cell immortality and carcinogenesis (79).

Another E2F1 target gene is SKP2 (S-phase kinase-associated protein 2), an F-box containing protein, which has a critical role in the G1/S transition, and its overexpression has been shown to correlate with tumor aggressiveness (80). The F-box is composed of 50 amino acids and mediates protein-protein interactions. It was first described as a component of the SCF ubiquitin-ligase complexes (81). It has been shown that SKP2 has oncogenic potential and is upregulated in epithelial carcinogenesis (82). Higher SKP2 gene expression occurs in many human tumor cell lines, and it is considered an E2F1 target (80).

Another focus in this work is on two proteins encoded by genes belonging to the highly conserved mini-chromosome maintenance proteins (MCM) group MCM2 and MCM7.

As a part of a hexametric protein complex, MCM2 and MCM7 are important components of the pre-replication complex and are thus involved in forming the replication fork, which is necessary for genome replication (83).

MCM2 as mentioned is a member of the family of MCM proteins. MCM2 is regarded as a proliferation and prognosis marker similar to the KI-67 proliferation index in breast cancer (84), it is also suggested as a marker for proliferation and prognosis in oral melanoma (85), gastric cancer (86), and colorectal cancer (87). Also in ovarian cancer, MCM2 is being explored as a possible therapeutic target (88).

MCM7 belongs to the same family of highly conserved mini-chromosome maintenance proteins as MCM2.

It turned out that the Cyclin D1-dependent kinase CDK4 is associated with MCM7, and it plays a role by inactivating the tumor suppressor protein RB1/Rb (89). For instance, a direct association between MCM7 levels and poor prognosis has been demonstrated in HCC (90).

MCM7 takes a part in regulating Cyclin D1 by the MCM7-MAPK signaling pathway. Studies in hepatocellular carcinoma show that the MCM7-Cyclin D1 pathway contributes to cancer progression and acts as a biomarker for prognosis in HCC (90). Also, in prostate cancer could be shown that MCM7 is involved in cancer progression, growth, and invasion (91).

E2F1 promotes the expression of MCM2-7, which is necessary to build the preinitiation complex for the following DNA-Replication (53), which is why they are examined in this thesis.

FOXM1 (Forkhead box transcription factor M1) is a gene that encodes for a protein involved in cell proliferation. FOXM1 acts as a transcriptional activator and regulates the expression of Cyclin B1 and Cyclin D1 (92) and is thus also closely related to E2F1. FOXM1 had multiple functions at the cellular level in proliferation, differentiation, angiogenesis, apoptosis, and DNA damage repair. By modulating different cancer hallmarks, FOXM1 could be identified as an oncogene (93). E2F1 is known for regulating FOXM1 expression. For instance, E2F1-driven FOXM1 expression is responsible for epirubicin resistance in breast cancer (94).

Another target gene of E2F1 examined here is RRM2 (ribonucleotide reductase regulatory subunit M2). It encodes for two different subunits of the ribonucleotide reductase, which is necessary to form deoxyribonucleotides from ribonucleotides. RRM2 has a critical role in many cancer types regarding apoptosis, cell proliferation, invasion, and migration. In cervical cancer for example, inhibition of RRM2 expression is being investigated as a new therapeutic approach (95). Also in breast cancer, RRM2 inhibition was found to blunt the metastatic properties of cancer cells (96). It has been shown that E2F1 and RRM2 are simultaneously elevated in many cancers, in which E2F1 promotes cell proliferation, migration, and metastasis by activating RRM2 (97). Investigations in prostate carcinoma showed that overexpression of RRM2 is

associated with a poor patient prognosis and that its inhibition might be a therapeutic target (98). Similarly, inhibition of E2F1 by tyrosine kinase inhibitors has been shown to suppress RRM2 expression as well as enhance apoptosis and increase the efficacy of chemotherapy in gastrointestinal cancer (99). The inhibition of RRM2 or the downregulating of its expression could help overcome chemotherapy resistance or enhance its efficacy of chemotherapy (100). Since chemoresistance also plays a major role in CCA, the inhibition of E2F1 by HLM006474 could also cause downregulation of RRM2 and may increase the efficacy of chemotherapy in this tumor.

pE2F1, Rb, and pRB were repeatedly tested, however no qualitatively adequate results could be obtained by the tested antibodies. For this reason, the results from these proteins are not included in the report.

1.6 Structure and effects of HLM006474

HLM006474 is a small moelcule E2F Inhibitor, which controls the biological activity of E2F genes by blocking the E2F pathway (101). It has a crystal structure, which binds the E2F4/DP2 heterodimer (Figure 7) (102). Multiple studies suggest that targeting E2F1 might be a therapeutic option in different cancer types. In vitro studies have demonstrated that administration of HLM006474 to lung cancer cells severely inhibits their growth (101). Similarly, it has been shown that HLM006474 inhibits cell proliferation and induces apoptosis in a preclinical melanoma model (102). The biochemical IC50 (i.e. the concentration of an inhibitor required to block cells in vitro by 50%) is 29.8 µM tested in cell line A375, a cell line isolated from the skin of a 54-patient with malignant melanoma.

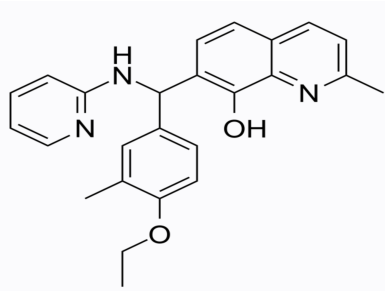

O=oxygen, H=hydrogen, N=nitrogen

Figure 7: Structure of HLM00647

Source:https://www.medchemexpress.com/hlm006474.html?utm_source=google&utm_medium=CPC&utm_campaign=Germany&utm_term=HY-16667&utm_content=HLM006474&gclid=EAIaIQobChMIwfqaqP3S-wIVmZ3VCh0mXwHjEAAYASAAEgIJQvD_BwE

1.7 Aim of the work

CCA is a highly aggressive tumor with few therapeutic options. Thus, new molecular targets should be identified to treat this devastating disease.

This work focuses on cell biology mechanisms in iCCA, specifically the transcription factor E2F1, as well as some target genes that are directly regulated by E2F1 at the cell biological level. For this purpose, a cohort of human iCCA samples was studied, complemented by translational experiments in four different human CCA cell lines.

In particular, studies to elucidate the protein and RNA expression of E2F1 and respective target genes were performed. Western blots were done to measure the expression at the protein level and PCR (polymerase chain reaction) experiments were performed to determine the expression at RNA level.

Furthermore, E2F1 was suppressed and the effect on its target genes was monitored. E2F1 inhibition was also investigated by monitoring growth behavior of cells (xCELLigence experiments) treated by the inhibitor (HLM006474). By performing this series of experiments we expected to elucidate the carcinogenic role of E2F1 and potential therapeutic effects of its pharmacologic inhibition in human iCCA.

2. Material & Methods

2.1.Material

2.1.1 Equipment

The following table shows an complete overview of the laboratory equipment and utensils used.

Product Name	Company
5424R Centrifuge	Eppendorf Vertrieb Deutschland GmbH
5430 Centrifuge	Eppendorf Vertrieb Deutschland GmbH
5810 R Centrifuge	Eppendorf Vertrieb Deutschland GmbH
8-Kanal Pipette	Starlab
Aspirator	Starlab
Bolt 4-12% Bis-Tris Plus 1.0 mm ´ 15 well	Invitrogen (ThermoFisher Scientific)
C100 Touch Thermal Cycler CFX96 Real Time System	Bio-rad Technologies
Cellculture Flask , 550 ML, 175 CM²	Greiner Bio-one GmbH
Cellculture Flask, 250 ML, 75CM²	Greiner Bio-one GmbH
Cellculture Flask, 50 ML, 25 CM²	Greiner Bio-one GmbH
ChemiDoc MP Imaging Sytem	Bio-Rad Laboratories GmbH
Citerion Blotter with Plate Electrodes	Bio-Rad Laboratories GmbH
CO2-incubator ICO105med	VWR
Combitips advanced 1,0ml, Eppendorf Biopure, 100Stk.	Eppendorf Vertrieb Deutschland GmbH
Computer	HP
Concentrator Plus	Eppendorf Vertrieb Deutschland GmbH
Counting Slides, Dual Chamber for Cell Counter	Bio-Rad Laboratories, Inc.
DynaMag TM-2	ThermoFisher Scientific Biosciences GmbH
E-Plate 16 PET	Agilent Technologies, Inc.
Fastgene Magna Stand 1,5ml	Nippon Genetics
Freezer	Liebherr
MiCroplate reader Fluostar	BMG Labtech
MiCroscopE Olympus	Olympus
Mini Gel Tank	ThermoFisher Scientific Biosciences GmbH
Mixer RM1	Starlab
Multipette E3	Eppendorf Vertrieb Deutschland GmbH
Nitrocellulose Membrane 0,2 um	Bio-Rad Laboratories GmbH
Optically clear Heat seal	Bio-Rad Laboratories GmbH
Orbital Shaker	Starlab
Pipette 10 ml, Graduation 1/10 ml	Greiner Bio-one GmbH
Pipette 5 ml Graduation 1/10 ml	Greiner Bio-one GmbH
Pipettee 25 mL, Graduation 2/10 ml	Greiner Bio-one GmbH
Pipette (Research Plus 3)	Eppendorf Vertrieb Deutschland GmbH
Plate Centrifuge	Axygen

Power Pac HC	Bio-Rad Technologies
Protein LoBind Tubes, Protein LoBind, 0.5 mL, PCR clean	Eppendorf Vertrieb Deutschland GmbH
Protein LoBind Tubes, Protein LoBind, 1.5 mL, PCR clean	Eppendorf Vertrieb Deutschland GmbH
Protein LoBind Tubes, Protein LoBind, 2.0 mL, PCR clean	Eppendorf Vertrieb Deutschland GmbH
Protein LoBind Tubes, Protein LoBind, 5.0 mL, PCR clean	Eppendorf Vertrieb Deutschland GmbH
PX1 PCR Plate Sealer	Bio-Rad Laboratories GmbH
Smart BlockTM, 1,5 ml	Eppendorf Vertrieb Deutschland GmbH
Nitrogen Tank	AirLiquide
T100 Thermal Cycler	Bio-Rad Laboratories GmbHBio-Rad Technologies
TC20 Autocell Counter & Cell Count Kit	Bio-Rad Laboratories GmbH
Thermomixer C	Eppendorf Vertrieb Deutschland GmbH
Transferpette-8 electronic	Brand
Transferpette-8 electronic 0,5-10µl	Brand
Transferpette-8 electronic 15-300µl	Brand
Transferpette-8 electronic 15-300µl	Brand
Tubes 50 ML, PP, 30/115 MM	Greiner Bio-one GmbH
Tubes, 15 ML, PP, 17/120 MM,	Greiner Bio-one GmbH
UV Cabinet	Biosan
VertiCal Stand autoclave	Tuttnauer
Waterbath	Memmert
xCELLIgence DP Bundle inClusive Control Unit, Software, ACcessory Kit	OLS Omni Life Science

Table 9: List of Equipment

2.1.2 Reagents

Following table shows consumables, such as reagents, buffers etc.

Product Name	Company
10x Binding Buffer #00-0055	Invitrogen
10X RT Buffer (High-Capacity cDNA Reverse Transcription Kit with RNase Inhibitor, #4374967)	Applied BiosystemsTM (ThermoFisher Scientific)
10X RT Random Primers (High-Capacity cDNA Reverse Transcription Kit with RNase Inhibitor, #4374967)	Applied BiosystemsTM (ThermoFisher Scientific)
ACTB TaqMan Assay VIC-MBG-PL	ThermoFisher Scientific Biosciences GmbH
Bolt Welcome Pack B (4-12%, 15Well)	Fisher Scientific
Bolt LDS Sample Buffer (4X)	ThermoFisher Scientific Biosciences GmbH
Bolt Sample Reducing Agent (10X)	ThermoFisher Scientific Biosciences GmbH
Clarity MaxTM Western ECL Substrate	Bio-Rad Laboratories, Inc.
Cyclin B1 (CCNB1) Human TaqMan™Gene Expression Assay (FAM)	ThermoFisher Scientific Biosciences GmbH
Cyclin D1 Human TaqMan™Gene Expression Assay (FAM)	ThermoFisher Scientific Biosciences GmbH
Cyclin E1 TaqMan™Gene Expression Assay (FAM)	ThermoFisher Scientific Biosciences GmbH
Dako Wash Buffer 10X	Dako Wash Buffer 10X
Dimethyl sulfoxide (DMSO)	Merck KGaA
DMEM High Glucose medium w/o L-glutamine w/o sodium	Anprotec
dNTP 100 mM (High-Capacity cDNA Reverse Transcription Kit with RNase Inhibitor, #4374967)	Applied BiosystemsTM (ThermoFisher Scientific)
Dulbecco's Phosphate Buffered Saline w/o Magnesium, w/o Calcium	Anprotec
E2F1 Human TaqMan™Gene Expression Assay (FAM)	ThermoFisher Scientific Biosciences GmbH
E2F1 Inhibitor, HLM006474	EMD Millipore Corp
E2F1 Silencer ™ Pre-Designed siRNA	ThermoFisher Scientific Biosciences GmbH
Ethanol	Carl Roth GmbH + Co. KG
Fetal calf serum	Anprotec
FOXM1 Human TaqMan™ Gene Expression Assay (FAM)	ThermoFisher Scientific Biosciences GmbH
GAPDH TaqMan® Gene Expression Assay, VIC-MGB	ThermoFisher Scientific Biosciences GmbH
Halt Protease & Phosphatase Inhibitor Cocktail (100X) #87786	ThermoFisher Scientific Biosciences GmbH
HEPES Buffer 1 M	Anprotec

High-Capacity cDNA Reverse Transcription Kit with RNase Inhibitor, #4374967	Applied BiosystemsTM (ThermoFisher Scientific)
L-Glutamine 100X	Anprotec
Lipofectamine® RNAiMAX Transfection Reagent	Life Technologies (ThermoFisher Scientific)
Loading Dye	Bio-Rad Laboratories GmbH
MCM2 TaqMan™ Gene Expression Assay (FAM)	ThermoFisher Scientific Biosciences GmbH
MCM7 Human TaqMan™ Gene Expression Assay (FAM)	ThermoFisher Scientific Biosciences GmbH
miRNeasy Mini Kit	Qiagen GmbH
MultiScribe Reverse Transcriptasem (High-Capacity cDNA Reverse Transcription Kit with RNase Inhibitor, #4374967)	Applied BiosystemsTM (ThermoFisher Scientific Biosciences GmbH)
Nitrocellulose MembranE 0,2 um	BioRad Laboratories GmbH
Novex NuPAGE MES SDS Running Buffer (20X)	Invitrogen (ThermoFisher Scientific Biosciences GmbH)
Novex SeeBlue Plus Prestained Standard (1X)	Invitrogen (ThermoFisher Scientific Biosciences GmbH)
Nuclease-Free Water	Ambion (ThermoFisher Scientific Biosciences GmbH)
NucleoSpin RNA Plus, Mini kit for RNA purification with DNA removal column (#740984.250)	Macherey-Nagel
Opti-MEM® I Reduced Serum Medium	ThermoFisher Scientific Biosciences GmbH
Penicillin-Streptomycin Solution 100X	Anprotec
PierceTM Protein-Free T20 (TBS) Blocking Buffer	ThermoFisher Scientific Biosciences GmbH
Ponceau solution	Sigma-Aldrich, Inc.
Protein Assay Dye Reagent Concentrate	Bio-Rad Laboratories, Inc.
RNase Inhibitor (High-Capacity cDNA Reverse Transcription Kit with RNase Inhibitor, #4374967)	Applied BiosystemsTM (ThermoFisher Scientific Biosciences GmbH)
RPMI 1640, w/o L-Glutamine	Anprotec
RRM2 Human TaqMan™Gene Expression Assay (FAM)	ThermoFisher Scientific Biosciences GmbH
Silencer select negative Control	Life Technologies GmbH
SKP2 Human TaqMan™Gene Expression Assay (FAM)	ThermoFisher Scientific Biosciences GmbH
Sodium Pyruvate 100 mM	Anprotec
T-Per Tissue Protein Extraction Reagent #78510	ThermoFisher Scientific Biosciences GmbH
TaqMan Fast Advanced Master Mix	Applied BiosystemsTM (ThermoFisher Scientific Biosciences GmbH)
TaqMan™ Gene Expression Assay Gene Name: MYC (FAM-MGB)	ThermoFisher Scientific Biosciences GmbH
Tris Buffered Saline with Tween® 20 (TBST-10X)	Cell Signaling Technology
Trypan blue solution 0.4%	Sigma-Aldrich, Inc.
Trypsin-EDTA 10X	Anprotec

Table 10: List of reagents

2.1.3 Cell lines

Table 11 shows four CCA cell lines, used in this study.

Cell line	Company/Source
HUCCT1	RIKEN (The Institute of Physical and Chemical Research)
KKU-156	Xin Chen Lab, San Francisco, UCSF
KKU-213	Sekisui XenoTech, LLC
RBE	RIKEN (The Institute of Physical and Chemical Research)

Table 11: CCA cell lines

KKU-213 (JCRB1557) is a human mixed (papillary and non-papillary) intrahepatic cholangiocarcinoma cell line, established from the biliary tract, isolated from a 58-year old patient, cultivated in DMEM (Dulbecco's modified Eagles medium)-medium.
KKU-156 is an intrahepatic cholangiocarcinoma cell line isolated from a 58-years old male patient cultivated in DMEM-medium. RBE is an intrahepatic cholangiocarcinoma cell line from a 64-year old female patient, cultivated in RPMI-1640 medium and HUCCT1 (JCRB0425) is an intrahepatic cholangiocarcinoma cell line isolated in a 56-year old male patient and cultivated in RPMI- 1640 medium.

2.1.4 Primary Antibodies

Table 12 shows the primary antibodies used in this work.

Antibody	Company	Catalog Number	Host
C-MYC	Cell Signaling	13987S	rabbit
CYCLIN D1	Cell Signaling	2922S	rabbit
MCM2	Cell Signaling	3619	rabbit
MCM7	Cell Signaling	3735	rabbit
SKP2	abcam	ab183039	rabbit
CYCLIN B1	Santa Cruz	sc-752	rabbit
E2F-1	Santa Cruz	sc-251	mouse
RRM2	Cell Signaling	65939	rabbit
CYCLIN E	Abcam	ab7959	rabbit
GAPDH	Proteintech	10494-1-AP	rabbit

Table 12: Primary antibodies

2.1.5 Secondary Antibodies

Table 13 lists the secondary antibodies used in this work.

Antibody	Company
HRP, GOAT ANTI-RABBIT IGG	Dianova
HRP, GOAT ANTI-MOUSE IGG	Dianova

Table 13: Secondary antibodies

2.1.6 Software

Table 14 summarizes the software used in this thesis.

Name	Version	Company
SPSS	25.0.0.2	IBM SPSS Statistics
CFX MaestroTM Software	4.1.2433.1219	Bio-Rad Laboratories, Inc.
GraphPad Prism	8.0	GraphPad Software
ImageLab	6.0.1	Bio-Rad Laboratories, Inc.
Microsoft Excel	16.30	Microsoft Corp.
Microsoft Powerpoint	16.30	Microsoft Corp.
Microsoft Word	16.30	Microsoft Corp.
Omega	5.50 R4	BMG LABTECH GmbH
Omega MARS	3.32 R5	BMG LABTECH GmbH
RCTA	2.1.0.	ACEA Biosciences, Inc.

Table 14: Software

2.1.7 Patient Collective

The tissue samples were provided by the Institute of Pathology of the University of Regensburg. Data collection and sample conservation were based on the positive ethics vote 16-316-101 from date 16.11.2016. The patient population comprises tumor samples from patients with cholangiocarcinoma who underwent surgery at the University Hospital of Regensburg between 2007 and 2018. Both tumor-free liver tissue and tumor tissue were examined from each patient so that two tissue samples are accounted for by each patient. With 33 patients, this resulted in a total of 66 samples to be examined. However, the material from patient number 6, i.e., samples 11 and 12, could not be used for Western blot analysis, as too little protein could be obtained. Thus, only 32 patients were examined in the study. The main clinicopathological features of the patients are summarized in Table 15.
In both Western blotting and real-time-PCR, the samples were processed and evaluated according to Tables 15 and 28.
Table 28 is attached in the appendix (5.4 Nr. 2) and shows the numbering of the samples and the respective assignment of tumor and non-tumor sample of each patient.

PAT. NR.	sample-Nr.	sex, age at resection	pathological TNM-Classification	Grading	classification
1	1,2	m, 78	pT2a, L0, V1, R0, pN1 (4/6), Pn1; G2	G2	iCCA
2	3,4	f, 81	pT3, L0, V0, R1, Pn1; G3	G3	iCCA
3	5,6	m, 52	rpT2b, L0, V0; G2	G2	iCCA
4	7,8	f, 44	pT1, L0, V0, R0 (lokal); G2	G2	iCCA
5	9, 10	m, 70	pT1, L0, V0, R0; G3	G3	iCCA
6	11,12	m, 58	pT2b, L0, V0, R0; G2	G2	iCCA
7	13,14	m, 50	pT1, L0, V0, R0; G2	G2	iCCA
8	15,16	m, 62	pT2b, L0, V0, R0, pN0 (0/2); G2	G2	iCCA
9	17,18	m, 75	pT1, L0, V0, Rx; G2	G2	iCCA
10	19,2	m, 65	pT2, L0, V1, pN0 (0/3), R0; G3	G3	iCCA
11	21,22	m, 83	pT2, V1, L0, pN0 (0/4), R0 (lokal); G2	G2	iCCA
12	23,24	m, 78	pT2, L0, V0, R0; G2	G2	iCCA
13	25,26	f, 64	pT1b, L0, V0, R0; G2	G2	iCCA
14	27,28	f, 74	(y)pT1b, L0, V0, R0; G2	G2	iCCA
15	29,30	f, 69	pT1, L0, V0, R0; G3	G3	iCCA
16	31,32	f, 67	pT2, L1, V1, pN1 (5/6), R0; G3	G3	iCCA
17	33,34	f, 64	pT2, L0, V1, pN0 (0/10), R0 (local); G2	G2	iCCA
18	35,36	f, 77	R0 (lokal); G3	G3	iCCA
19	37,38	m, 58	pT2, L1, V1, pN0 (0/1), R0 (local); G3	G3	iCCA
20	39,40	m, 70	pT3, L0, V0, pN1 (2/10), R1; G3	G3	iCCA
21	41,42	m, 69	pT3, L0, V0, pN1 (2/5), R1; G3	G3	iCCA
22	43,44	f, 51	pT1, L0, V0, R0 (local); G2	G2	iCCA
23	45,46	f, 69	ypT1, L0, V0, pN0 (0/1), R0 (local); G2	G2	iCCA
24	47,48	m, 66	pT2a, L0, V1, Pn1, R0 (local); G3	G3	iCCA
25	49,50	f, 71	rpT2b, L0, V0, R0 (locall); G3	G3	iCCA
26	51,52	f, 27	pT3, L1, V1, pN1 (4/6), Pn1; G3	G3	iCCA
27	53,54	m, 69	pT1, L0, V0, pN0 (0/1), R1; G2	G2	iCCA
28	55,56	m, 69	pT2b, L0, V0, R0 (local); G2	G2	iCCA
29	57,58	f, 55	pT2b, L1, V1, pN1 (3/5), R0 (local); G3	G3	iCCA
30	59,60	m, 48	ypT3, L1, V1, ypN1 (3/3), M1 (PER), Pn1, R1	-	iCCA
31	61,62	m, 32	pT1, L0, V0, pN1 (3/10), R0 (local); G3	G3	iCCA
32	63,64	f, 78	ypT1, L0, V0, Pn1, R1	-	iCCA
33	65,66	f, 59	pT1, L0, V0, R1; G2	G2	iCCA

Table 15: Clinicopathological features of the patients

Legend: m=male, f=female, p=pathological,y = after muldimodal therapy, for pTNM-classification see 1.1.1.b, iCCA= intrahepatic cholangiocarcinoma

2.2 Methods

2.2.1 Cell culture

The HUCCT1 and RBE cell lines were cultivated in RPMI-1640-medium and KKU-213 and KKU-156 in DMEM (Dulbecco's modified Eagles medium)-high glucose- medium. Both media (in 500 ml) bottles were shifted with 50 ml (milliliter) fetal calf serum (FCS), 5 ml L-Glutamine (100X, 200 mM (millimolar)), 5 ml Penicillin-Streptomycin (Solution 100X), 5 ml HEPES Puffer (1M), and 5 ml Sodium Pyruvate (100 mM, 100X) before using, they were stored at 4°C (Degree Celsius) and thawed in 37°C water bath before use. Cell lines were thawed from cyroconservation for a few minutes in a water bath and suspended in 10 ml of medium in a 50 ml falcon. Subsequently, cells were centrifuged for 5 minutes at 500 rpm (revolutions per minute), the supernatant was discarded after the centrifugation, and the cell pellet was resuspended in a fresh medium. Depending on the flask's size 30 ml of medium where used when seeded in 175 cm^2 flasks and 10 ml of medium when seeded in 75 cm^2 flasks. Afterward, the cells were placed in the incubator with 37°C, 5% CO^2- admission, and 95% humidity for the growth phase. Working with the cells took place only in clean rooms on laminar airflow workbenches for sterile working conditions.

After 3 to 4 days, the medium was changed, and when they were confluent, they were split into new flasks to grow until there were enough cells for the different experiments. For this purpose, the cells had to be counted based on the Trypan blue method. Before counting cells needed to be detached with a 2x Trypsin-EDTA (Ethyldiamintetraacetat) (10ml of 10x Trypsin/EDTA and 40 ml of Phosphate Buffered Saline (PBS)) mixture. At first, the old medium had to be discarded, and cells had to be washed in PBS. Therefore the same amount of PBS like medium before were added. After removing the PBS, 2ml of Trypsin/EDTA were added to the 75cm² flasks and 5ml to the 175cm² flasks. Following the administration of Trypsin, the cells have to be incubated for a short time (RBE and HUCCT1 for 3-5 minutes, KKU-213 and KKU-156 for 7-10 minutes) in this solution. After the cells were detached, some medium was added to the flasks for Trypsin inactivation. Subsequently, the suspension was transferred to 50 ml falcons and centrifuged for 5 minutes at 500 rpm. After discarding the supernatant and adding 10 ml medium, the pellet was resuspended, and the cells were ready to be counted. As mentioned before, the Trypan Blue method was used for this scope. This

method is based on the fact that living cells have intact cell membranes that delimit different dyes, like Trypan Blue, whereas dead cells assimilate the dyes. The cell counting kit (BioRad) and the TC20 Autocell Counter (BioRad) were used, where 10 ml of the cell suspension were mixed with 10 µl (microliter) of Trypan Blue and 10 µl of this mixture was added to the chamber slide from the kit and inserted into the TC20 Autocell Counter, which displays the number of cells per ml after a short time.
Cells that were not needed underwent cyroconservation. Specifically 2 million cells were freezed in 2µl of freezing medium (70% Medium, 20% FCS, 10% DMS0).

2.2.2 Transfection with RNAiMAx (Silencing)

Transfection means taking up external RNA (ribonucleic acid) into the cells to change the expression of specific genes. Conversely, it's possible to knock out some genes with siRNA (small interfering RNA). In this study the method of lipofection has been used, which means that synthetic cationic lipids interact with the DNA of the cells, building complexes, and in the end, fuse with the cell membrane to set the RNA into the cells. To deliver siRNA into the cells Lipofectamine RNAiMAX Transfection Reagent (ThermoFisher) has been unsed. The cells were plated in 6-well plates in the amount of 500.000 cells/well the day before the experiment. In this study, a specific siRNA against human E2F1 has been used. Specifically, three different solutions were prepared:

1. CTRL (Control) (Optimem™-Medium)
2. Scramble (Optimem™-Medium + neg. control siRNA)
3. siRNA (Optimem™-Medium + siRNA)

In the first step, the Transfection-mix was prepared (single volume):

1.: 100µl Optimem™- + 5µl RNAiMax

For the scramble (single volume):

2.: 100 µl Optimem™-+ 20µl neg. siRNA (E2F1) (5µM)

For the siRNA (single volume):

3.: 100µl Optimem™- + 20µl siRNA (5µM)

The solutions were incubated at room temperature for 10 minutes. Subsequently:

- ➔ Add 100 µl from 1. to 2. and 3.
- ➔ Incubate again for 10 minutes at room temperature
- ➔ Discard the medium from the cells in the 6- well-plate
- ➔ Add 1,8 ml of Optimem™- medium to each well
- ➔ Add 200 µl of Optimem™-meidum to control-well
- ➔ Add 200 µl of 2. For the scramble-well
- ➔ Add 200 µl of 3. to the siRNA-well
- ➔ Incubate the 6-well-plate again for 48h

2.2.3 RNA and protein isolation from 6-well-plates (Cellculture)

For harvesting the cells from the 6-well-plate, a lysis buffer was prepared (single volume): 10ml T-Per Tissue Protein Extraction Reagent (Thermo Fisher) +100µl HALT-Protease & Phosphatase Exhibitor (Thermo Fisher). Subsequently, the lysis buffer was cooled on ice. The 6-well-plates were prepared for the cell harvesting; thus, the medium was discarded, and the wells were washed with 2 ml PBS. After discarding the PBS, 300 µl of Trypsin/EDTA (same as in 2.2.1) were added to each well, and the cells were incubated for a short time, depending on the cell line, as described in 2.2.1. When the cells were detached, 300 µl PBS were added, and the cells were transferred into 1,5 ml Eppendorf cups, which were centrifuged for 5 minutes at 2500g. Next, the supernatant was discarded. Once the RNA was extracted, the pellets were freezed at -80°C.

The pellets from protein isolation were resuspended in 100 µl of the prepared lysis buffer. They were placed on ice for 30 minutes while vortexing them every 5 to 10

minutes. Next, the pellets were centrifuged for 30 minutes at 4°C at 20000g. Subsequently, the supernatant was transferred to a new tube, and the pellet was eliminated. The suspension was frozen at -20°C, or proceeded to the next step to evaluate protein concentration.

2.2.4 Protein Extraction

The samples from 33 patients with CCA were collected at the Institute of Pathology of the University of Regensburg. Liver tissues with tumor and tumor-free tissues were examined from each patient to compare the tumor tissue with the corresponding tumor-free tissue. The tumor samples were taken by pathologists as part of the diagnostic workup and preserved for this purpose. The RNA was isolated and provided from the laboratory.

The protein extraction was performed by using the Bullet Blender. For this purpose, the tissue was cut into pieces of 2x2x2cm to 4x4x4cm and put in the Beads-Lysis-Cup (Biostep GmbH). Subsequently, 100-250µl T-Per Lysis Buffer+Inhibitors (10 ml Lysis Buffer + 100µl inhibitors) was added to the tissue pieces. The Bullet Blender was used for 3 minutes at a speed of 8. Afterward, the samples were placed on the rotator mixer in the cold room at 4°C for 30-60 minutes. After centrifugation at 4°C for 5 minutes at full speed, the supernatant was transferred to a new Eppendorf tube. This step was followed by three centrifugations for 30 minutes at full speed (rcf 20.000xg) at 4 °C. Finally, the supernatant was transferred to a new Eppendorf Tube again.

2.2.5 RNA Extraction

RNA extraction was performed following the manufacturer's instructions using the NucleoSpin™ RNA Plus Kit (Mini kit for RNA purification with DNA removal column, Machery-Nagel). In the first step, the sample was homogenized and digested in the lysis buffer. After transferring the solution into a gDNA removal column followed by centrifugation at 11.000g for 30 seconds, the column was discarded. A binding buffer was added, then transferring the lysate in an RNA Plus Column and another centrifugation at 11.000g for 15 seconds. Several washing steps with a washing buffer and in total three more centrifugations at 11.000g were performed. Subsequently, the RNA was eluted by adding 30µl RNase-free water twice and centrifuging at 11.000g for 1 minute each. RNA concentration was measured by using the spectral fluorometer DS-11FX from Biozym. If the RNA was not used immediately, it was stored at -80 °C. The obtained RNA was transcribed into cDNA.

2.2.6 Bradford protein assay

The Bradford protein assay was used to measure the protein concentration. This assay is based on the color change from brown to blue caused by binding protein structures to Coomassie dye under acidic conditions (103). A spectrophotometer can measure this color change; the Fluostar Omega™ was used for this purpose. For the assay, the preparation of specific standards is necessary; for this work there was bovine serum albumin (BSA) 2mg/ml used. 10 µl of diluted protein samples (1:10) were added to a 96-well plate, and 190 µl of Bradford reagent (Bio-Rad Technologies) were added and incubated for 15 minutes. A measure in a dilution series of c (concentration)= 1000, 500, 125, 62,5, 31,25 µg/µl, always applied in triplets, was performed simultaneously for a standard curve of BSA. Subsequently, the photometric evaluation was conducted using the Fluostar Omega™, and the exact protein concentration could be determined, which is necessary to continue with the Western Blotting.

2.2.7 Western Blot

Western Blot is a method for the detection of proteins. The protein mixture is separated by electrophoresis on the basis of size and charge in the carrier matrix. The separated protein bands are then transferred to a carrier membrane, where they are accessible for antibody detection. The bands on the membrane can then be visualized by chemiluminescence (104). To separate the proteins SDS-Page (sodium dodecyl sulfate-polyacrylamide gel electrophoresis) was used. SDS was added to the samples (prepared as listed in 2.2.3), so they developed a negative charge proportional to their weight. Further, a reducing agent was added so that the disulfide bonds could be broken. A sample batch was prepared for this purpose, and 8 µl of it were added to each sample, so the total amount of protein was 10 µg. Samples were briefly pretexted and centrifuged and then heated for 10 minutes at 71 degrees at 300 rpm in a Thermomixer (Eppendorf). For the running of samples, the running buffer was diluted by mixing 50 ml SDS Running Buffer (VWR International, 20%) with 950 ml Millipore Water. Running buffer was added to a Mini Gel Tank (Thermo Fisher). For the electrophoresis, the Bolt ™ 4 to 12% (percent), Bis-Tris Mini Protein-Gel was used. The gel's first row was always loaded with 5µl of the Novex™SeeBlue™Plus2 Prestained Standard and then always 10 µl of the corresponding sample and then running for one hour at 135-150V (Volt). After the run was finished, the gels were prepared for the transfer. For this there were put on a nitrocellulose membrane (BioRad) and built into a blot tank (Criterion Blotter with Plate Electrodes from BioRad), filled up with Transfer buffer (BOLT™Transfer Buffer 20X, Life Technologies), and then a second run was started for 2,5-3 hours by 0,3 A and 60 V in the cold room. After the transfer phase, the membrane was secured and dyed in Ponceau Red (VWR International) for membrane staining; subsequently, the membrane was cut into smaller pieces based on the proteins' size to be evaluated. To wash out the Ponceau Red solution, the membrane slices were washed in TBS (tris-buffered saline)-Tween 20 (Cell Signaling). Afterwards, the pieces were placed in protein blocking buffer (Pierce™ Protein-Free T20 (TBS) Blocking Buffer) for a minimum of one hour on an orbital shaker at room temperature. After the blocking and a renewed washing, the primary antibody was added at the dilution suggested in the datasheet and incubated overnight at 4 °C. The following day, the primary antibody was recovered, and the

secondary antibody was added. Depending on whether the primary antibody was derived from rabbit or mouse, the appropriate secondary antibody was prepared in a 1:10000 or 1:5000 solution in Blocking Buffer. The secondary antibody was incubated for at least one hour at room temperature on the orbital shaker. Subsequently, the secondary antibody can be discarded, and several more washes were employed. To evaluate the membranes, they were treated with a chemiluminescent ECL (enhanced chemiluminescence) substrate solution (Clarity Max Western ECL, BioRad). For the exposure and measurement, the slices were placed in the Chemidoc Imaging system (BioRad) to generate the protein bands' image. For all 32 patients (n=32), a tumor sample and a non-tumor sample from the liver tissue were examined. GAPDH (Glycerinaldehyd-3-phosphate-Dehydrogenase) was used as a loading reference (housekeeper); initially, ß-Actin (ACTB) was used, but it turned out to be regulated. The samples of patients no. 12, 19, 25, and 31 did not show a clear signal in the housekeeper, and in the antibodies tested and could therefore not be evaluated. Thus, in most cases, a population of 28 samples is considered in the following evaluation. The evaluation of the bands was performed using the ChemiDoc MP Imaging System by detecting chemiluminescence. The mean and standard deviation calculation was performed using the normalization factor, which was determined using the software Image Lab from BioRad-Laboratories.

2.2.8 Transcription into cDNA (complementary desoxyribonucleic acid)

When the RNA was isolated from the cell culture or human samples, it had to be transcribed into cDNA to perform quantitative real time polymerase chain reaction (qRT-PCR). First, the RNA concentration is measured to work with the same concentration for all samples; for this purpose, the spectral fluorometer DS-11FX from Biozym™ was used. Usually, a concentration of 1 µg (microgram) RNA per 10 µl is desired; if the measured concentration was lower, the solution had to be adapted to the lowest RNA concentration. For the transcription, the High Capacity cDNA Reverse Transcription Kit with RNAse Inhibitor (Applied Biosystems by Thermo Fisher Scientific) was used, and the instructions from the manual were followed.

For each sample with isolated RNA, the following master mix (The ratio in which the individual components of the High Capacity cDNA Reverse Transcription Kit with RNAse inhibitor should be mixed for sample preparation) was prepared (Table 16):

Component	Batch per sample
RT Buffer (10X)	2,0 µl
dNTP Mix (100mM, 25X)	0,8µl
RT Random Primers (10X)	2,0 µl
Multiscribe Reverse Transcriptase	1,0 µl
RNase Inhibitor	1,0 µl
Nuclease free water	3,2 µl
Total volume	**10 µl**

Table 16 Composition of the master mix

The master mix was stored on ice, while 10 µl of it were pipetted into PCR tubes. 10 µl of RNA (with 1µg diluted RNA) were then pipetted to the master mix and mixed, so the total volume per tube was 20 µl. The tubes were sealed and placed in the cycler (T100 Thermal Cycler BioRad™). In the cycler, the following program was always followed (Table 17):

	Step 1	Step 2	Step 3	Step 4
Temperature	25 °C	37 °C	85°C	4 °C
Running Time	10 min.	120 min.	5 min.	Infinite hold

Table 17: Device settings of the T100 Thermal cycler for rewriting RNA into cDNA

If the DNA was not used immediately, it was frozen at -20 °C.

2.2.9 Polymerase chain reaction (quantitative real time-PCR, q-RT-PCR)

PCR is a method to measure the expression level of target genes by exponential amplification.

Transcribed cDNA from cell lines and human cholangiocarcinoma samples was subjected to quantitative RT-PCR. For this purpose, the CFX96™ Real-Time System

(Bio-Rad Laboratories GmbH.) and the TaqMan™ Fast Advanced Master Mix were used. A TaqMan™ gene expression assay contains the TaqMan™ Fast Advanced Master Mix, TaqMan ™ probes for the targets (in this case for E2F1, MCM2, MCM7, Cyclin D1, Cyclin E, c-Myc, SKP2, FOXM1, Cyclin B1, and RRM2 TaqMan™ Gene Expression Assays FAM or Vic) and GAPDH as a housekeeper. A list of the targets and the corresponding assays is attached in the appendix (under 5.4 Nr. 3).

Thus, 1 µl of cDNA was added to 9 µl of a qRT-PCR master mix prepared according the following scheme (Table 18):

Component	Volume (µl)
TaqMan™ Fast Advanced Master Mix	5.0
TaqMan™ Gene Expression Assay for the Target	0.5
TaqMan™ Gene Expression Assay for the housekeeper	0.5
Nuclease-free water	3.0

Table 18: Master mix composition of the target gene in direct comparison to the housekeeper gene

The cDNA and the master mix were pipetted in triplets in a PCR-microplate. All preparations were performed on ice. The PCR-microplate was sealed by using a PX1™ PCR Plate Sealer (Bio-Rad Laboratories GmbH). The plate was inserted into CFX96™ Real-Time System, and the following program was performed:

PCR cycles	conditions
1	95 °C for 2 minutes
40	94°C for 30 seconds
40	55°C for 30 seconds
40	72°C for 40 seconds
	Cooldown to 4 °C

Table 19: Device settings of the CFX96™ Real-Time System for a run

In this case, GAPDH was measured as a reference gene to allow relative quantification. The CT- (cycle threshold) value indicates the intersection of the

amplification curve with a threshold line at which the fluorescence signal significantly exceeds the background fluorescence for the first time (105).
The calculation was performed by the delta-CT method, where the differential expression of two samples is expressed as n-fold expression with the delta-CT value. Methodologically, first, the ΔCT(cycle threshold)-value was calculated;

The values are the result of the following formula:

$$\Delta CT \text{ (delta-CT)} = CT_{\text{Target gene}} - CT_{\text{Reference gene}}$$

The relative expression difference between the sample, normalized to the reference gene, is represented by the arithmetic formula of the $\mathbf{2}^{-\Delta CT}$.
Finally, the values from the tumor tissue were compared with those from the tumor-free tissue.
To calculate the deltadelta- CT value, the delta-CT value of the sample to be tested is subtracted from that of a positive control.
In the human samples examined, there was no positive control or callibrator, which is why the delta-CT values of the tumor and non-tumor samples are compared here in arrithmized form. For the cell lines, there was a control group, but for overview purposes, the delta-CT values were also statistically compared and for the human samples, an average of the delta-CT values from the group of tumor-free samples was calculated as the control value. For the sake of completeness, the deltadelta-CT values are listed in the appendix (5.4 Nr. 4, 5).

2.2.10 Real-time Cell Analysis (RTCA)

Real-time Cell Analysis (RTCA) performed with the xCELLigence™ is based on the measurement of impedance-dependent signals to evaluate cellgrowth behaivors. The experiments were performed using an xCELLigence RTCA DP instrument, including the RTCA 2.1.0 software from ACEA Biosciences. Sixteen well-plates were used for the measurements. In this study, four different CCA cell lines (KKU-213, KKU-156, RBE, and HUCCT1) were treated with HLM006474 at three different concentrations each (20, 50, and 100 μM).

The following schedule was generated for the measurements in the instrument (Table 20):

Step	Sweeps	Interval	Total time
1.	1	1 minute	00:00:10
2.	100	1 hour	25:42:31
3.	500	15 minutes	151:29:35

Table 20: The settings in the RTCA 2.1.0 software for the measurements of cell lines growth after the treatment with HLM006474 with xCELLigence™

In the beginning, a background measurement was always performed; specifically, 100 µl of the corresponding medium (DMEM or RPMI) was pipetted into each well. After the instrument had performed the background measurement automatically, 10.000 cells of the related cell lines, dissolved in 100 µl medium were pipetted into each well. The plate was left under the hood at 37 °C for 30 minutes so that the cells could sink to the bottom during this time. In the next step, the cells were measured for 24 hours without treatment. For the last step, 100 µl of medium were discarded from the wells, and treatment was added. For this purpose, the 10µM stock solution of HLM006474 was diluted in the medium suitable for the cell line so that the concentrations 20,50 and 100 µM were administered. After 24 hours, the inhibitor was applied at different concentrations, and the impedance measurement was continued. A control measurement with the solvent inhibitor (DMSO,1%) was performed at the same time for comparison. The individual concentrations were plotted in duplets.
The inhibitor was administered at concentrations of 20, 50, and 100 µM (micromolar) for each cell line.The monitoring lasted 48 hours after the point of treatment (inhibition with HLM006474)

The measured impedance was converted by the software RTCA into the CI (cell index). The CI can be used as a dimension of adhesion. In simple terms, the greater the cell index, the higher the adhesion. Conversely, the cell index decreases in the absence of living cells. Therefore, this method can be used to investigate the complex cellular behaviors and drug responses (106), as in this case, the behavior of four CCA cell lines after treatment with the E2F1 inhibitor HLM006474.

Besides the cell index, another point in the data evaluation was the IC50. IC50 was calculated also by the software RTCA; the IC50 indicates the mean inhibitory concentration, i.e. the concentration of an inhibitor at which the half-maximal inhibition is observed. So the concentration is indicated, which is necessary to achieve 50% inhibition in vitro.

2.2.11 Statistics

Statistical analysis was performed using SPSS Statistics software, Microsoft Exel, and Graphpad.

A mean and standard deviation were calculated for each of the available data from the Western blot experiments. Excel was first used to calculate the means and standard deviations. It was then necessary to determine which statistical test procedure could be used to compare the means, for this purpose it was first checked whether the data were normally distributed. A test for normal distribution of the samples was performed using the Kolmogorov-Smirnov, or the Shpiro-Wilk-test, which assumes with the null hypothesis that data are normally distributed. For values of $p<0.05$ in the Komogorov-Smirnov or the Shapiro-Wilk-test, a significant deviation from the normal distribution must be assumed and it must be assumed that the data are not normally distributed .

For the data from the Western blots and PCR tests, it had to be assumed after testing for normal distribution that they are not normal distributed. For these data, the non-parametric Mann-Whitney-U test was used for statistical analysis. By evaluation with SPSS, the Mann-Whitney-U test gives two p-values, the exact and the asymptotic. The exact p-value cannot always be calculated, in these cases the asymptotic p-value is used.The significance level is set at 5%, i.e. p-values <0.05 are considered significant.

To determine the correlation between E2F1 and the other targets, Spearman correlation was used for non-normally distributed data. To interpret the correlation coefficient ($|\rho|$), Cohen's guidelines are often used: $|\rho|= 0.10$: low, weak correlation, $|\rho|= 0.30$:medium/moderate correlation, and $|\rho|= 0.50$: large, strong correlation. Here, the p-value is also given to indicate whether the correlation coeffizient is singnificantly different from 0, again the significance level is $p<0.05$. The PCR data from the cell

culture experiments, can be considered as normally distributed, in this case the parametric unpaired t-test is applied for comparison, also here the significance level is set to 5% in the following. For the unpaired t-test, variance homogeneity is a prerequisite, therefore the Levene test of variance equality is performed. The significance level is set to 0.05, if the value is <0.05 there is no variance homogeneity and it must be assumed that the variances are not equal, to assess the statistical significance, the two-sided p-value is given, also here the significance level is set to 0.05.

3. Results

3.1 Protein levels - Western Blot Analysis

The levels of E2F1 and its target genes in the collection of intrahepatic cholangiocarcinoma samples were assessed to determine the importance of the E2F1 pathway in this aggressive tumor.

In the following chapter, the results of the Western blot are shown in figure a). The bands represent the result of the analysis of the chemiluminesecence signal. In addition, the result of the statistical evaluation between the values of the tumor and the tumor-free tissue is shown, the significance level is expressed by the p-value. Figure b) shows the absolute protein levels in tumor and tumor-free tissue normalized against GAPDH. For the group of tumor-free samples and those from tumor tissue, a mean value and the standard deviation were calculated in each case. The following values describe the mean value and the standard deviation behind it in parentheses.

For the expression of E2F1, a value of 1,219 (±1,08) was found in the tumor tissue and a value of 1,028 (±0,58) in the tumor-free tissue (Figure 8a/b).

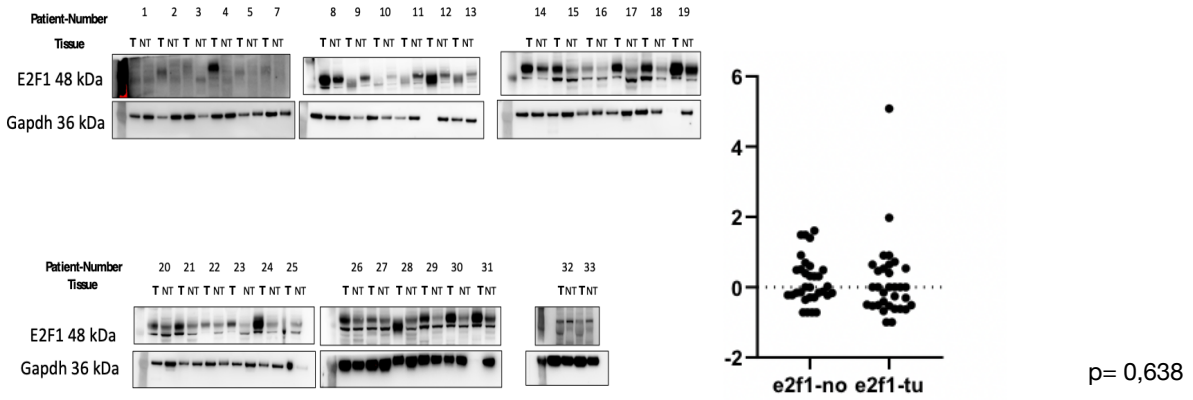

Figure 8a: E2F1 and GAPDH levels in 33 human cholangiocarcinoma samples

left: Western Blot analysis by evaluation with the ChemiDoc MP Imaging System and the Image Lab software. (Patient Nr.6 with samples 11 and 12 are missing because the samples were insufficient) GAPDH, with a protein size of 36 kDa, was used as a reference. E2F1 has a protein size of 48 kDa. Abbreviations: T= Tumor, NT= No Tumor, kDa= Kilodalton, **right:** graphical representation of expression in tumor and tumor-free tissue, statistic evaluation between tumor and non-tumor tissue; here shown the p-value

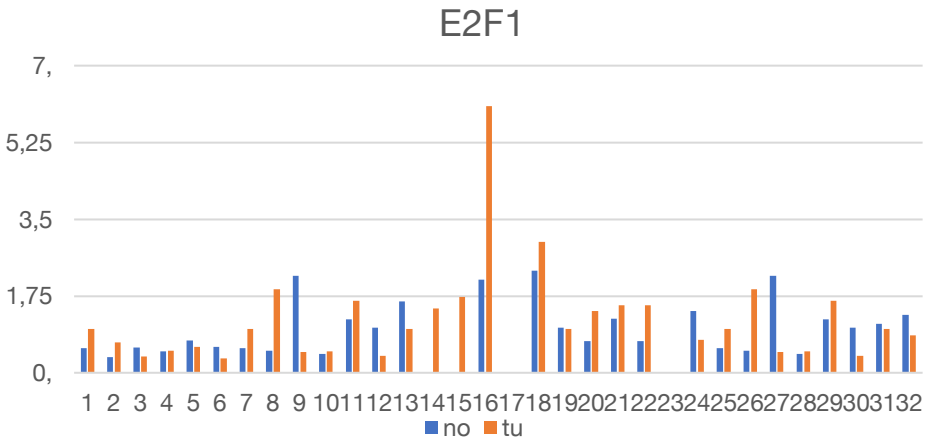

Figure 8b: Protein levels of E2F1 in pairs in tumor tissue and tumor-free tissue (= normal)
Values were normalized with GAPDH

When comparing the expression of C-Myc, a mean value of 1,32 (± 0,88) could be determined in the tumor tissue and 1,35 (±0,76) in tumor-free tissue (Figure 9).

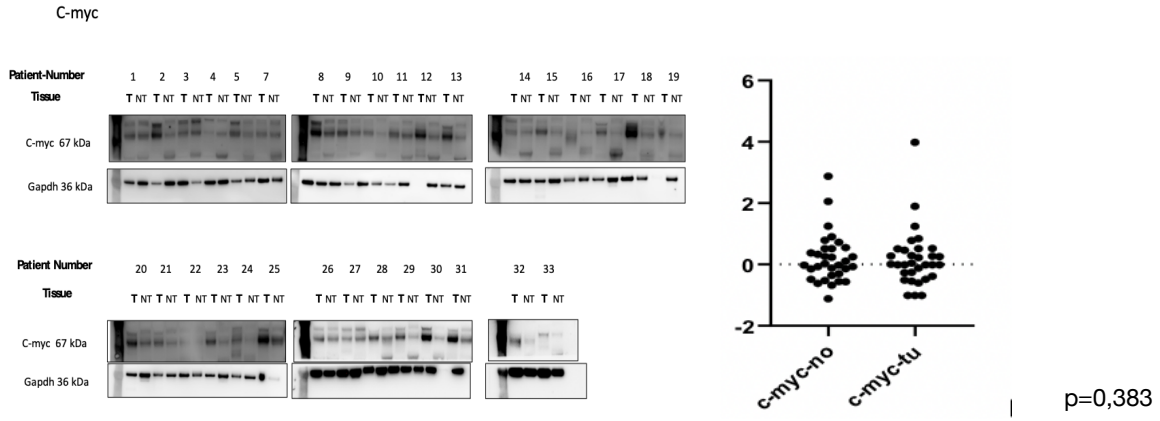

Figure 9a: C-Myc and GAPDH levels in 33 human cholangiocarcinoma samples

left: Western Blot analysis by evaluation with ChemiDoc MP Imaging System and the Image Lab software (Patient Nr.6 with samples 11 and 12 are missing because the protein amount of these samples was not sufficient). GAPDH, with a protein size of 36 kDa, was used as a reference. C-Myc has a protein size of 67 kDa. Abbreviations: T= Tumor, NT= No Tumor, kDa= Kilodalton, **right:** graphical representation of expression in tumor and tumor-free tissue statistic evaluation between tumor and non-tumor tissue; here shown the p-value

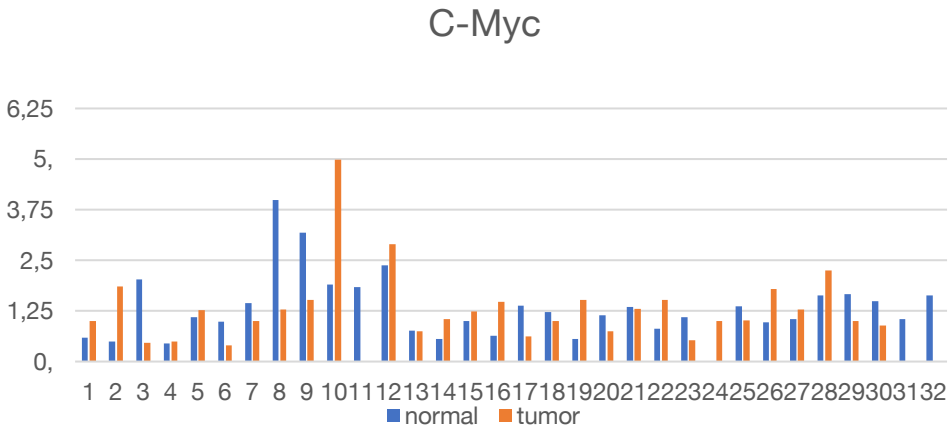

Figure 9b: Protein levels of C-Myc in pairs in tumor tissue and tumor-free tissue (= normal)
Values were normalized with GAPDH

Cyclin D1 expression has a value of 1,268 (±0,88) in the tumor tissue and 1,272 (±0,86) in the tumor-free tissue (Figure 10).

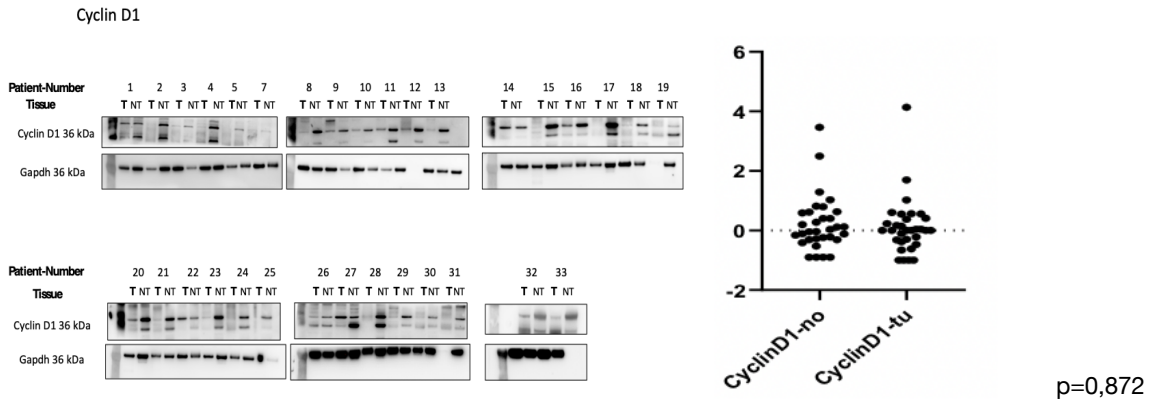

Figure 10a: Cyclin D1 and GAPDH levels in 33 human cholangiocarcinoma samples

left: Western Blot analysis by evaluation with ChemiDoc MP Imaging System and the Image Lab software (Patient Nr.6 with samples 11 and 12 are missing because the samples were insufficient). GAPDH, with a protein size of 36 kDa, was used as a reference. Cyclin D1 has a protein size of 36 kDa. Abbreviations: T= Tumor, NT= No Tumor, kDa= Kilodalton, **right:** graphical representation of expression in tumor and tumor-free tissue statistic evaluation between tumor and non-tumor tissue; here shown the p-value

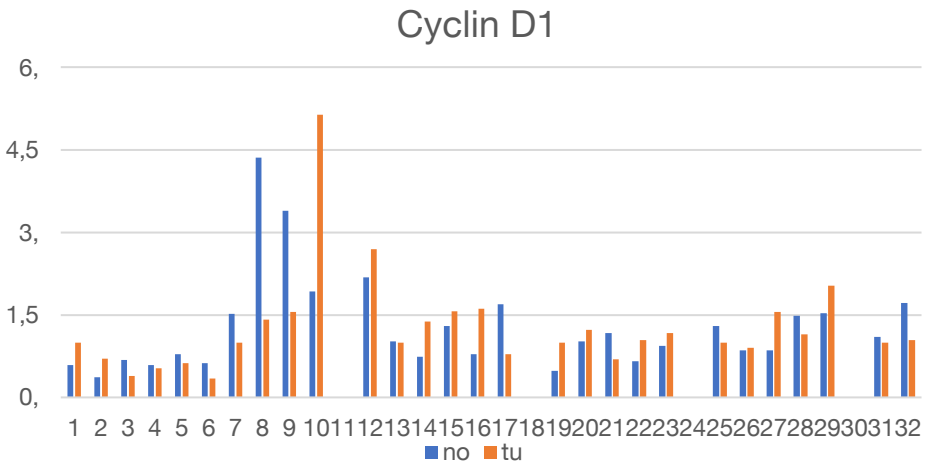

Figure 10b: Protein levels of Cyclin D1 in pairs in tumor tissue and tumor-free tissue (=normal) Values were normalized with GAPDH

The examination of the expression of MCM 2 showed a value of 1,229 (±0,60) in the tumor tissue and a value of 1,180 (±0,53) in the tumor-free tissue (Figure 11).

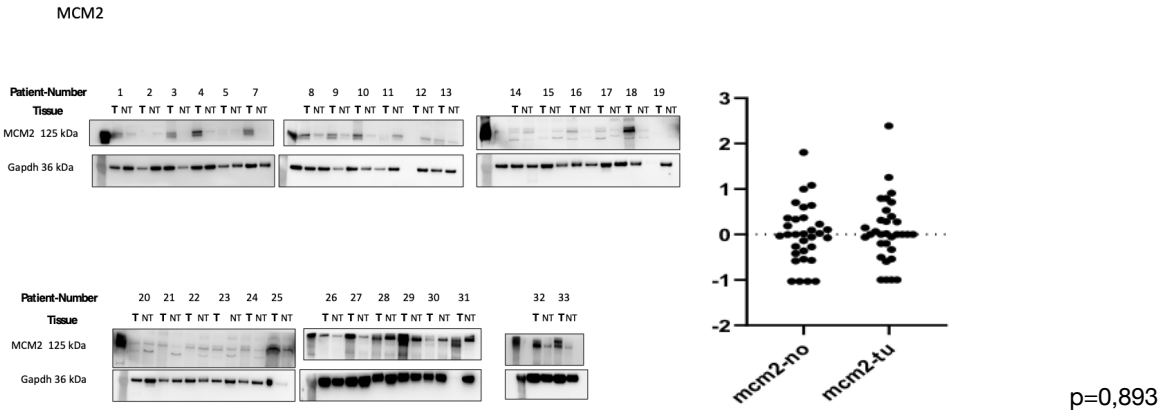

Figure 11a: MCM2 and GAPDH levels in 33 human cholangiocarcinoma samples

left: Western Blot analysis by evaluation with ChemiDoc MP Imaging System and the Image Lab software (Patient Nr.6 with samples 11 and 12 are missing because the samples were insufficient). GAPDH, with a protein size of 36 kDa, was used as a reference. MCM2 has a protein size of 125kDa. Abbreviations: T= Tumor, NT= No Tumor, kDa= Kilodalton**, right:** graphical representation of expression in tumor and tumor-free tissue statistic evaluation between tumor and non-tumor tissue; here shown the p-value

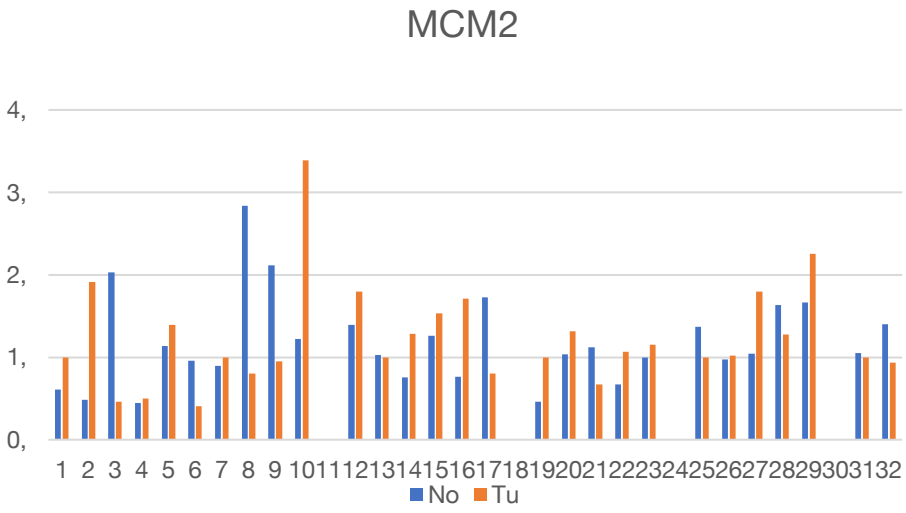

Figure 11b: Protein levels of MCM2 in pairs in tumor tissue and tumor-free (= normal). Values were normalized with GAPDH

Measurement of MCM7 expression showed a value of 1,694 (±1,150) in the tumor tissue and 1,558 (±0,76) in tumor-free tissue (Figure 12).

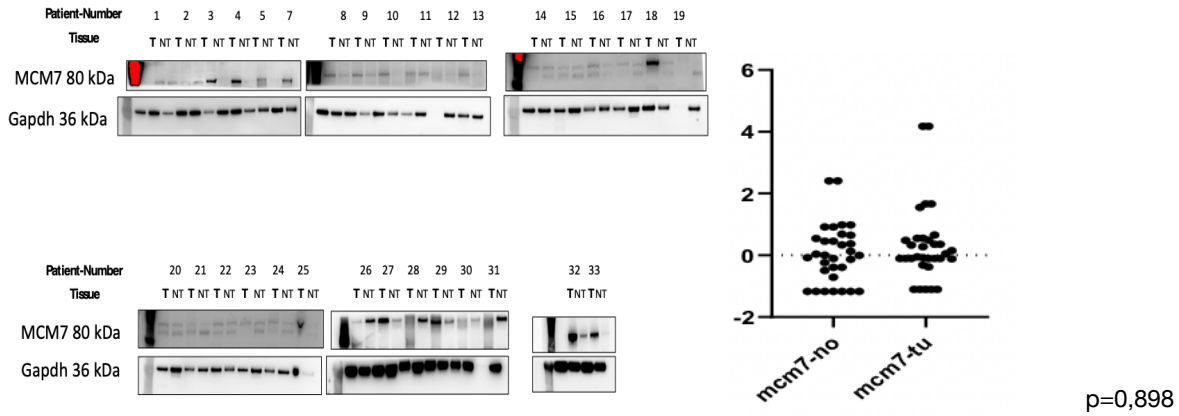

Figure 12a: MCM7 and GAPDH levels in 33 human cholangiocarcinoma samples

left: Western Blot analysis by evaluation with the ChemiDoc MP Imaging System and the Image Lab software (Patient Nr.6 with samples 11 and 12 are missing because the samples were insufficient) . GAPDH, with a protein size of 36 kDa, was used as a reference. MCM7 has a protein size of 80 kDa. Abbreviations: T= Tumor, NT= No Tumor, kDa= Kilodalton**, right:** graphical representation of expression in tumor and tumor-free tissue, statistic evaluation between tumor and non-tumor tissue; here shown the p-value, red color is caused by the high contrast, which is necessary for detection of the bands

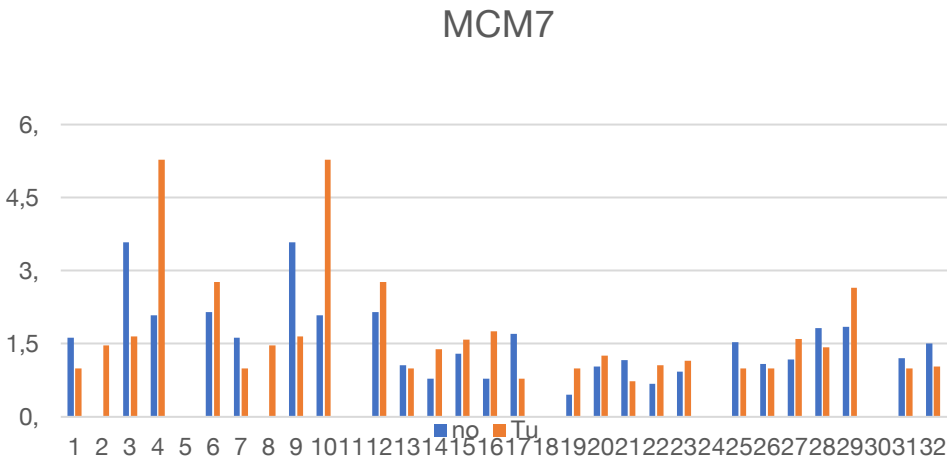

Figure 12b: Protein levels of MCM7 in pairs in tumor tissue and tumor-free tissue (= normal). Values were normalized with GAPDH

A value of 1,143 (±0,504) was obtained for Cyclin E expression in tumor tissue and of 1,06 (±0,46) in tumor-free tissue (Figure 13).

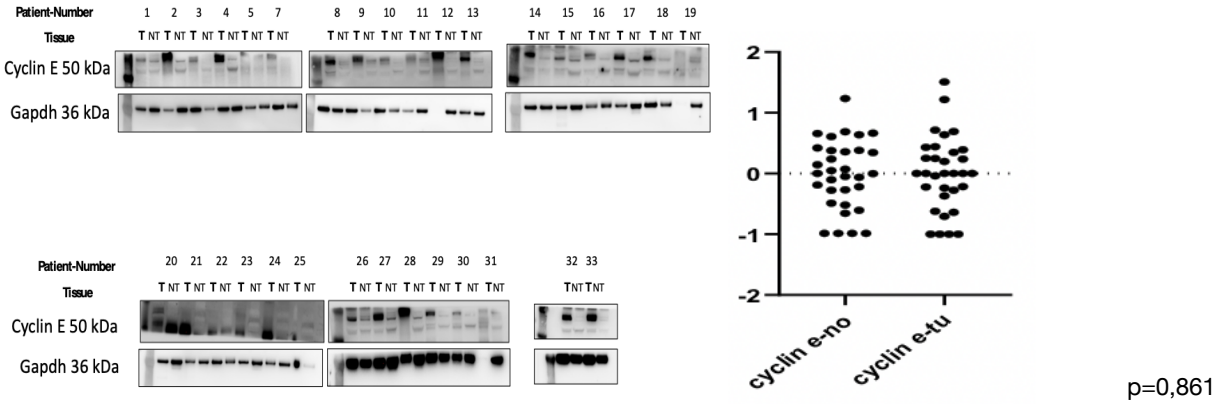

Figure 13a: Cyclin E and GAPDH levels in 33 human cholangiocarcinoma samples

left: Western Blot analysis by evaluation with ChemiDoc MP Imaging System and the Image Lab software (Patient Nr.6 with samples 11 and 12 are missing because the samples were insufficient). GAPDH, with a protein size of 36 kDa, was used as a reference. Cyclin E has a protein size of 50 kDa. Abbreviations: T= Tumor, NT= No Tumor, kDa= Kilodalton**, right:** graphical representation of expression in tumor and tumor-free tissue statistic evaluation between tumor and non-tumor tissue; here shown the p-value

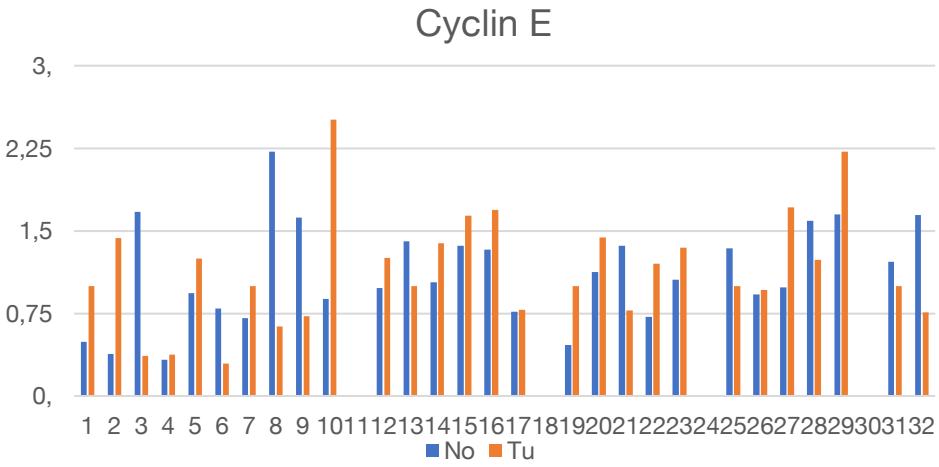

Figure 13b: Protein levels of Cyclin E in pairs in tumor tissue and tumor-free tissue (=normal). Values were normalized with GAPDH

The table below shows the statistical evaluation of the results from the Western blot experiments. The Whitney U-test was used for statistical evaluation, the asymptotic p-value indicates the significance level.

	E2F1	Cyclin-D1	c-Myc	MCM2	MCM7	Cyclin-E
p-value	0,638	0,872	0,383	0,893	0,898	0,861

Table 21: Statistical evaluation of the Western Blot, *p<0.05

As a result, none of the investigated cell cycle members and targets showed any significant difference in protein amount between the tumor samples and the normal tissue. Contrary to the previous assumption, no overexpression of E2F1 was detected at the protein level in the human CCA samples. In addition, there were no relevant differences between the tumor and non-tumorous tissue, for the co-investigated genes either.

3.2 RNA expression -Quantitative PCR-Analysis

As no relevant changes were detected at the protein level, we wanted to investigate whether this also holds true regarding gene expression.

After RNA was isolated from the samples and transcribed into cDNA as described above, PCR was performed.

Table 22 presents the RNA expression of the investigated genes, indicated in each case are the mean values and standard deviations (of the $2^{-\Delta CT}$ values) from the tumor tissue and the tumor-free tissue, as well as the p-value, which indicates significant differences between the two groups.

A significant increase in RNA expression in tumor tissue compared to tumor-free tissue was demonstrated for E2F1, MCM2 and Cyclin E. For MCM7, SKP2, Cyclin B1 and RRM2, expression were higher in tumor tissue albeit not at a significant level.
Contrary to expectations, RNA expression of Cyclin D1, c-Myc and FOXM1 were significantly increased in tumor-free tissue.

	Tumor		Non-Tumor		
target	**mean-value**	**standarddeviation**	**mean-value**	**standarddeviation**	**p-value**
E2F1	0,02085	0,01694	0,01385	0,01111	0,033*
MCM2	0,04198	0,03478	0,02877	0,01372	0,029*
MCM7	0,11061	0,07377	0,10678	0,10033	0,509
Cyclin D1	0,93031	1,01174	1,25665	1,07331	0,008*
Cyclin E	0,01503	0,01609	0,00671	0,00385	0,04*
c-Myc	0,2059	0,1355	0,39854	0,37455	0,005*
SKP2	0,08516	0,07111	0,1233	0,07991	0,012*
FOXM1	0,0134	0,01466	0,16999	0,95141	0,01*
Cyclin B1	0,05816	0,04875	0,03371	0,02755	0,852
RRM2	0,06173	0,05447	0,05451	0,04894	0,493

Table 22: PCR results, *p<0.05

Table 23 shows the statistical evaluation of the $2^{-\Delta CT}$ values calculated by the Mann-Whitney U test. Significant values are marked with an *.

	E2F1	MCM2	MCM7	CYC D1	CYC E1	Cmyc	SKP2	FOXM1	RRM2	Cyc B1
p-value	0,033*	0,029*	0,509	0,008*	0,04*	0,005*	0,012*	0,01*	0,493	0,852

Table 23: Statistical evaluation of the PCR results, p- values calculated by Mann-Whitney- U-Test, *p<0.05

The figures below show the comparison between the tumor samples and the tumor-free tissue. It is shown that the RNA expression of E2F1 was significantly higher in tumor tissue than in tumor-free tissue, which was as expected in contrast to the protein level studies, the same could be shown for MCM2 and Cyclin E. As Figure 14 shows, contrary to expectation, RNA expression for Cyclin D1, c-Myc and FOXM1 was higher in tumor-free tissue.

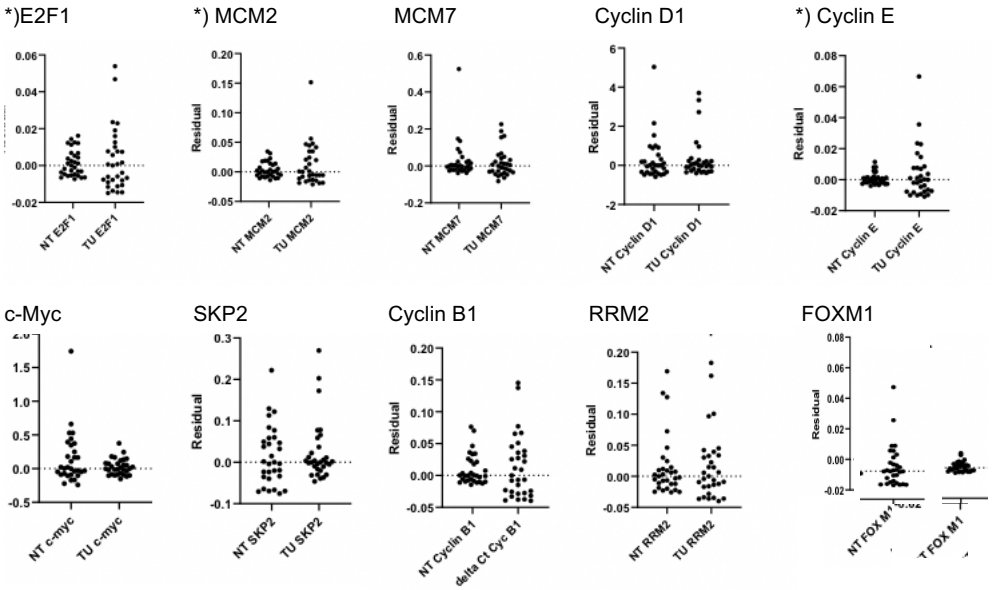

Figure 14:

Relative RNA levels of E2F1, Cyclin D1, C-Myc, MCM2, MCM7, RRM2, FOXM1, SKP2, Cyclin B and Cyclin E normalized to GAPDH of paired cholangiocarcinoma tissue (TU) and corresponding normal liver tissue (NT), *) p<0.05

To investigate a possible correlation between the E2F1 expression and the target genes, a correlation analysis was performed, demonstration a relation of E2F1 with MCM2, MCM7, Cyclin E, FOXM1, Cyclin B1 and RRM2 (Table 24).
Table 24 shows the correlation analysis of each gene with associated p-value, to indicate statistical significance.

correlationscoeffizient |ρ|		**p-values**	
	E2F1		E2F1
E2F1	1	**E2F1**	
MCM2	0,729435484	**MCM2**	3,23561E-06*
MCM7	0,483064516	**MCM7**	0,005910755*
Cyclin D1	-0,127419355	**Cyclin D1**	0,494556633
Cyclin E	0,903629032	**Cyclin E**	3,38123E-12*
c-Myc	0,016532258	**c-Myc**	0,929661333
SKP2	-0,191129032	**SKP2**	0,303026685
FOXM1	0,837096774	**FOXM1**	4,37839E-09*
Cyclin B1	0,895564516	**Cyclin B1**	1,02804E-11*
RRM2	0,861576355	**RRM2**	1,9571E-09*

Table 24: Correlationanalysis, Spearman coeffizient |ρ|, p-value, * p<0.05

In summary, by examining RNA expression, more meaningful results were obtained than at protein levels.
RNA expression of E2F1 was found to be increased in CCA tissue compared to expression in tumor-free tissue. Furthermore, the data collected support the hypothesis that the expression of E2F1 does have an impact on the expression of the target genes mentioned above.

3.3 Silencing of E2F1 in CCA-Cell lines

After having found altered gene expression of E2F1 and some of its target genes in tumor tissues, we planned to investigate the effects of pharmacologic manipulation of E2F1 in vitro. The levels of the E2F1 and the tested targets in the four intrahepatic cholangiocarcinoma cell lines following the knockdown of E2F1 via specific small-interfering RNA (siRNA) were investigated. The effect of E2F1 silencing was assessed by RT-PCR.

The following figures show the effect of suppressing E2F1 and the resulting influence on the expression of the investigated genes. Shown here graphically is the relative effect of silencing compared to the negative control, which was set to one for all cell lines. The table on the right shows the percentage knockdown in all four cell lines. The mean (M) and standard deviation (SD) were calculated from the values of the four cell lines. Negative siRNA and control are combined under scramble.
Negative percentages here mean that the expression of the corresponding gene was even higher in the cells where E2F1 was suppressed.

A) E2F1

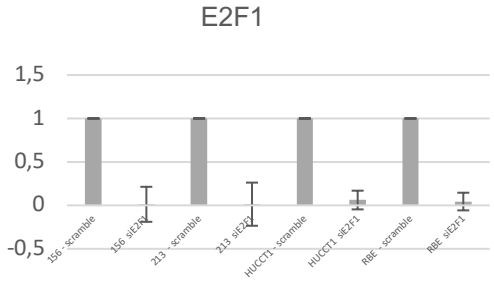

	E2F1
KKU-156	98,78%
KKU-213	98,64%
HUCCT1	93,86%
RBE	95,61%
M	**96,721**
SD	2,403

Figure 15A: RNA Expression of target genes, comparison under silencing of E2F1 and the control group (A), n=3

B)

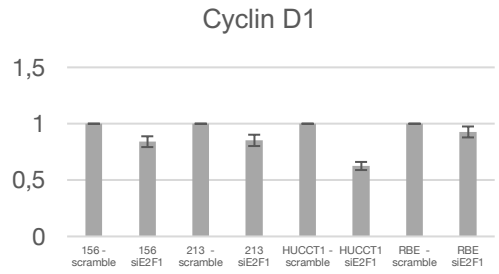

	Cyclin D1
KKU-156	15,93%
KKU-213	14,78%
HUCCT1	37,49%
RBE	7,29%
M	**18,87**
SD	12,99

C)

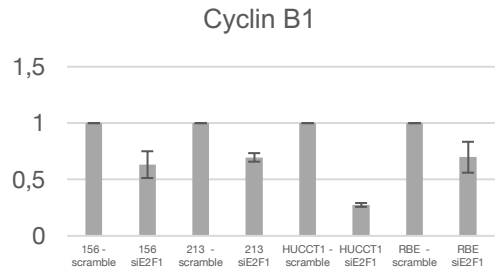

	Cyclin B1
KKU-156	36,81%
KKU-213	30,40%
HUCCT1	72,57%
RBE	30,25%
M	**42,51**
SD	20,28

D)

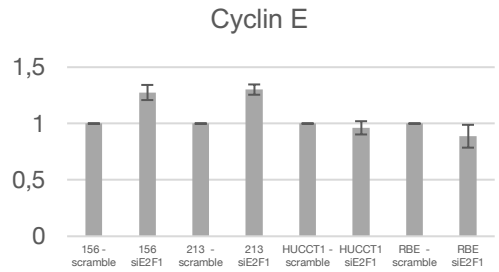

	Cyclin E
KKU-156	-27,56%
KKU-213	-30,14%
HUCCT1	3,79%
RBE	11,23%
M	**-10,67**
SD	21,24

E)

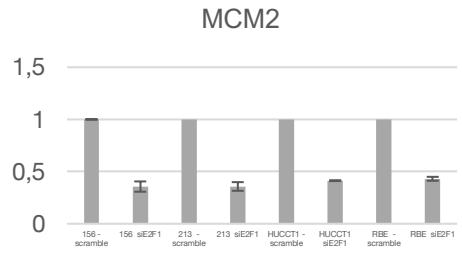

	MCM2
KKU-156	64,3591626
KKU-213	64,249688
HUCCT1	58,6758051
RBE	56,9046305
M	**61,0473216**
SD	3,8301184

Figure 15B: RNA Expression of target genes, comparison under silencing of E2F1 and the control group (B-E), n=3

F)

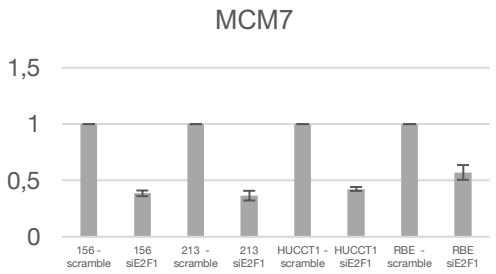

	MCM7
KKU-156	61,43%
KKU-213	63,46%
HUCCT1	57,58%
RBE	42,90%
M	**56,35**
SD	9,29

G)

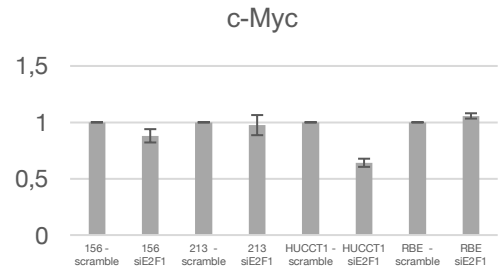

	C-Myc
KKU-156	11,95%
KKU-213	2,47%
HUCCT1	35,89%
RBE	-5,69%
M	**11,16**
SD	17,99

H)

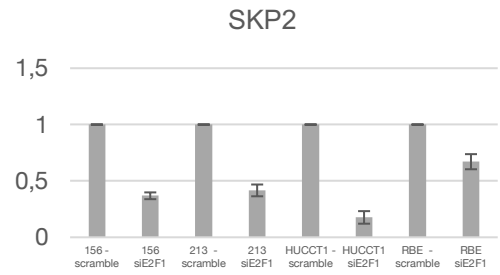

	SKP2
KKU-156	63,17%
KKU-213	58,40%
HUCCT1	82,36%
RBE	32,94%
M	**59,22**
SD	20,35

I)

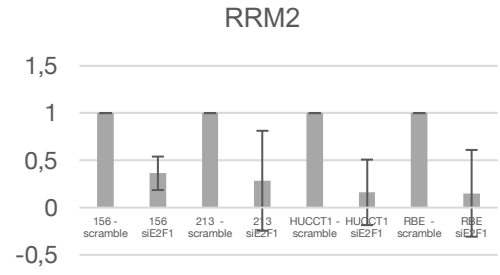

	RRM2
KKU-156	**63,70%**
KKU-213	**71,58%**
HUCCT1	**83,86%**
RBE	**84,87%**
M	**76,00**
SD	**10,19**

Figure 15C: RNA Expression of target genes, comparison under silencing of E2F1 and the control group (F-I), n=3

The following figure summarizes the absolute knockdown in percent (%). Logically, this was strongest in E2F1 itself with an average of 96.72%. A suppression of the respective expression above an average of 50% was also observed in MCM2, MCM7, SKP2 and RRM2.

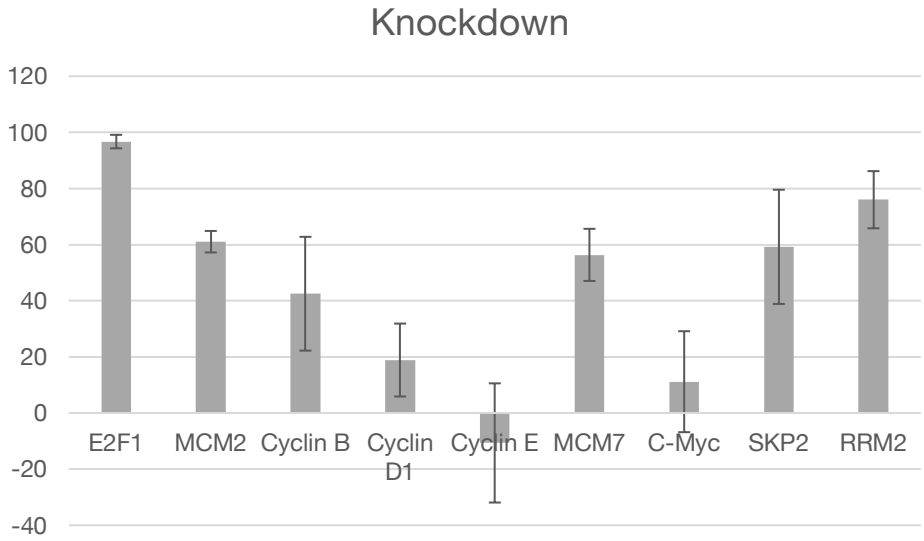

Figure 16: Knockdown effect in target genes after silencing E2F1

As can be appreciated graphically, the expression of all target genes examined decreased in the cells in which E2F1 was silenced, consistent with the notion that these genes are indeed E2F1 targets. The only exceptions were Cyclin E and c-Myc, where higher expression in the silenced group was observed only in the cell line RBE.

Table 25 shows the $2^{-\Delta CT}$ value calculated from RT-PCR for all genes studied for each cell line for control group (=scramble) and silencing group respectively.

	2-ΔCT-E2F1	2-ΔCT-MCM2	2-ΔCT - Cyclin B1	2-ΔCT - CYC D1	2-ΔCT-CYC E1	2-ΔCT-MCM7	2-ΔCT-CMyc	2-ΔCT - SKP2	2-ΔCT-RRM2
156 scramble	0,0039	0,0124	0,0557	0,0201	0,0040	0,0298	0,1393	0,0253	0,3924
156 siE2F1	0,0000	0,0044	0,0352	0,0169	0,0051	0,0115	0,1227	0,0093	0,1424
213 scramble	0,0040	0,0126	0,0516	0,0244	0,0038	0,0301	0,1756	0,0263	0,0338
213 siE2F1	0,0001	0,0045	0,0359	0,0208	0,0050	0,0110	0,1712	0,0109	0,0096
HUCCT1 scramble	0,0115	0,0194	0,0737	0,0835	0,0047	0,0279	0,1038	0,0106	0,0313
HUCCT1 siE2F1	0,0007	0,0080	0,0202	0,0522	0,0045	0,0119	0,0666	0,0019	0,0050
RBE scramble	0,0096	0,0152	0,0179	0,1609	0,0059	0,0294	0,1070	0,0096	0,0011
RBE siE2F1	0,0004	0,0083	0,0125	0,1491	0,0053	0,0168	0,1131	0,0064	0,0002

Table 25: Overview of $2^{-\Delta CT}$ values for the different target genes in the KKU 156, KKU 213, RBE, and HUCCT1 cells.

The following table shows the statistical comparison of the silenced cells compared to the control group. A significant difference in expression in the silenced group could be detected for E2F1, MCM2, and MCM7, underlining the influence of E2F1 expressionlevels on the expression of these genes.

Target	p-value
E2F1	**0,002***
MCM2	**0,001***
Cyclin B1	0,102
CYC E1	0,177
CMyc	0,326
SKP2	0,149
MCM7	**<,001***
Cyclin D1	0,808**
RRM2	0,683**

* values to be regarded as significant, as p< 0.05

** for cyclin D1 and RRM2, the Mann-Whitney U test was used to calculate the p-value, as the prerequisite of normal distribution was not met.

Table 26: statistic evaluation of comparison the silencing group against the control group

3.4 Real-time cell analysis under treatment with HLM006474

Finally, E2F1 was inhibited by HLM006474 in the four CCA cell lines and the effects on cell growth and proliferation was measured.

The results of the real-time cell analysis experiments are shown below. For each cell line, the curve under treatment with the inhibitor is shown. The cell index on the y-axis is plotted against the time in hours on the x-axis. In addition, the cell index is tabulated in bar charts with the corresponding numerical values.

In the cell line KKU-213, the proliferation curve of the cells treated with 20 µM HLM006474 was slightly above the DMSO control curve after application of the inhibitor. The proliferation curves of the cells treated with 50 µM and 100 µM HLM006474 ran significantly below, as shown in Figure 17.

The following graph shows the proliferation curves of the individual treatment groups of the cell line KKU-213 with the normalized cell index plotted against time in hours.

A) KKU-213

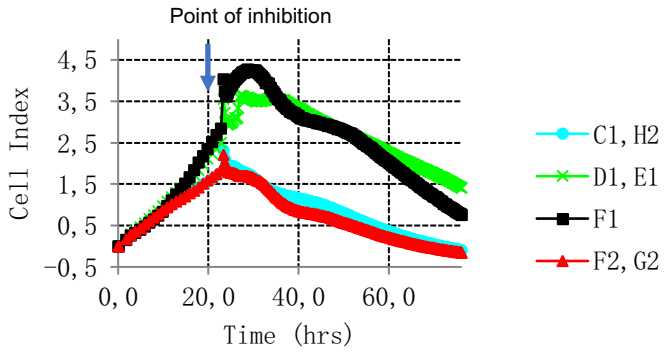

green c= 20µM (D1,E1), **blue**= 50µM (C1,H1), **red**= 100µM (F2,G2) of HLM006474, **black (F1)**= DMSO

B) KKU-213

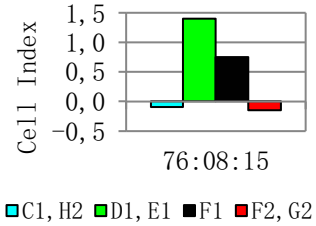

C) KKU-213

	Cellindex
DMSO	0,7481
20µM	1,4018
50µM	-0,0977
100µM	-0,1521

Figure 17: graph of the cell index for cell line KKU-213 under the treatment with HLM006474(top), as well as the representation of the cell index in the bar chart after 48 hours of treatment (below) with the values listed in a table

The proliferation curves of the treated KKU-156 showed a similar course, although the growth behavior was basically worse. The proliferation curve of the cells treated with 20 µM exceeded the DMSO control group, whereas the curves of the cells treated with 50µM and 100µM HLM006474 dropped relatively parallel.

The graph below shows the proliferation curves of each treatment group in the KKU-156 cell line, again the normalized cell index is plotted against time in hours. The cell index is negative in all concentration levels, as well as the DMSO, which means that there was no more increase in cell number after addition of the inhibitor. Nevertheless, differences between the individual groups could be shown, the cells treated with 50 µM showed the worst course.

A)KKU-156

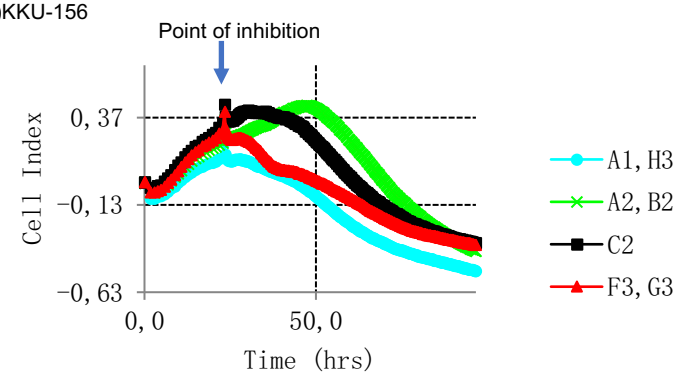

green c= 20µM (D1,E1), **blue**= 50µM (C1,H1), **red**= 100µM (F2,G2) of HLM006474, **black (F1)**= DMSO

B) KKU-156

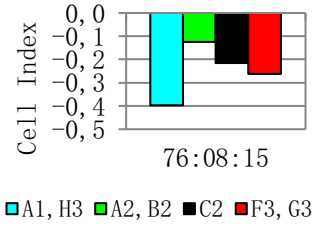

C) KKU-156

	Cell Index
DMSO	-0,2161
20µM	-0,1257
50µM	-0,3982
100µM	-0,2626

Figure 18: graph of the cell index for cell line KKU-156 under the treatment with HLM006474 (top), as well as the representation of the cell index in the bar chart after 48 hours of treatment (below) with the values listed in a table, n=3

In HUCCT1 cell line, the flattest curve was seen with a negative cell index for the cells treated with 100µM. The highest cell index was for the cells treated with 20 µM, the curve was above that of those treated with DMSO. This may be due to the fact that the cells can also react to DMSO, should there be an unintentionally high concentration.

A) HUCCT1

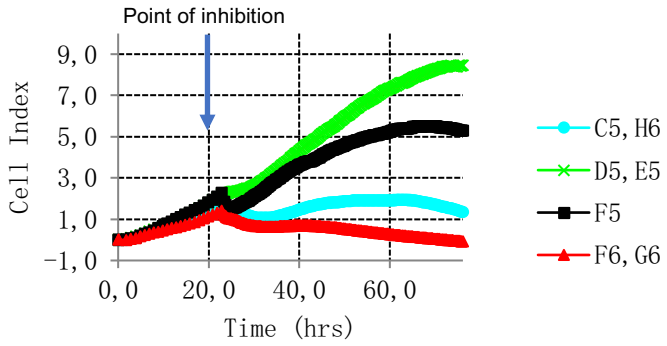

green c= 20µM, **blue**= 50µM, **red**= 100µM of HLM006474, **black**= DMSO

B) HUCCT1

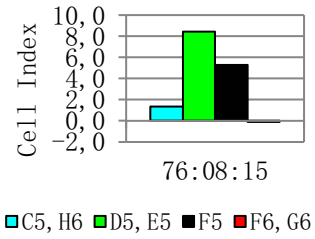

C) HUCCT1

	Cellindex
DMSO	5,275
20µM	8,4634
50µM	1,338
100µM	-0,0731

Figure 19: graph of the cell index for cell line HUCCT1 under the treatment with HLM006474 (top), as well as the representation of the cell index in the bar chart after 48 hours of treatment (below) with the values listed in a table, n=3

The same is true for the cell line RBE, below the concentration of 100µM the cell index was negative, whereas the cell indexes did not differ much between 50µM and 100µM.

A) RBE

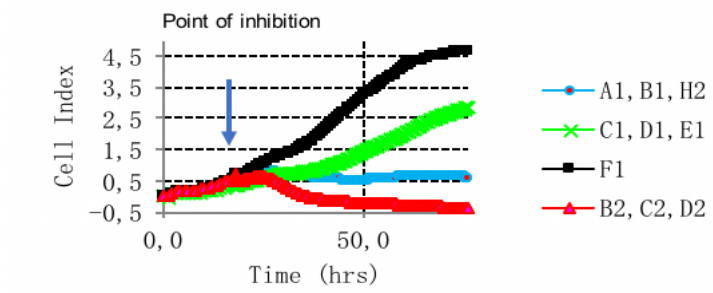

green c= 20µM, **blue**= 50µM, **red**= 100µM of HLM006474, **black**= DMSO

B) RBE

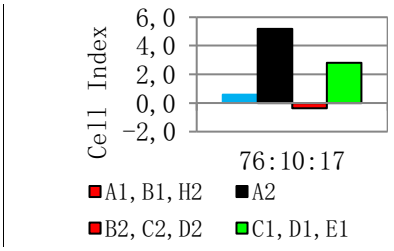

C) RBE

	Cellindex
DMSO	5,2078
20µM	2,8284
50µM	0,5849
100µM	-0,3789

Figure 20: graph of the cell index for cell line RBE under the treatment with HLM006474 (top), as well as the representation of the cell index in the bar chart after 48 hours of treatment (below) with the values listed in a table, n=3

The table below shows the IC50 values comparing the different cell lines. On average the IC50 was 32.94 µM, which is close to the biochemical IC50 value (30µM) of HLM006474. This value means that at a concentration of 32,94 µM, the E2F1 inhibitor HLM006474 blocks 50% of the vital CCA cells, which means cell death. This is indicating that the inhibition of E2F1 by HLM006474 resulted in decreased cell proliferation of the CCA cells studied here.

	IC50 (M)	IC50 (µM)		
KKU-213	2,86E-05	28,609	Mean(µM)	SD
KKU-156	2,09E-05	20,094	32,94425	9,16464662
RBE	4,51E-05	40,059		
HUCCT1	4,30E-05	43,015		

Table 27: IC50-values for the four cell lines, with mean- and standarddeviation

This experiment showed that inhibition by HLM006474 was effective in the CCA cell lines and affected growth behavior as shown. What effects this inhibition might have been already suggested in part by the preceding experiments at the cell biological level. Although these results suggest that E2F1 can be suppressed by drugs in CCA cell lines, they do not yet allow conclusions to be drawn as to whether this represents a therapeutic approach that can be transferred to the clinic in this form. There will be further experiments are required.

4. Discussion

4.1 E2F1 and regulation of its targets in CCA

CCA is a very aggressive disease with limited therapeutic options and a poor prognosis (1,-15). Since complete resection, the only curative approach, is often no longer possible at the time of diagnosis, there is an urgent need to develop new therapeutic options or target therapies.

Mounting evidence indicates that E2F1 has a key position in cancer cells concerning the cell cycle, metabolism, apoptosis, and metastasis (107). An abnormal activation of E2F1 is associated with a poor clinical outcome in many human cancers, but it has also been reported that E2F1 can take part in tumor suppression (107).

There are already studies in various tumor entities that describe the relationship between E2F1 expression levels and patient survival. For example, in liver cancer, a high expression of E2F1 is associated with a 5-year survival rate of 38%, whereas a low expression is associated with a 5-year survival rate of 62% (108). Also, in endometrial cancer, a nearly 20 percent higher 5-year survival rate (87%) was found in patients with a lower E2F1 expression than patients with a higher E2F1 expression (5-year survival rate of 68%) (109). In renal carcinoma, high levels of E2F1 are also an unfavorable prognostic factor concerning the 5-year survival rate (110). As already mentioned, E2F1 plays a controversial role in tumorgenesis. A possible tumor suppressor function in E2F1 has been suggested in cervical carcinoma, in which patients with a higher expression level of E2F1 present a higher 5-year survival rate (73%) (58). In contrast, patients with a lower E2F1 expression had a bad prognosis and showed a 5-year survival rate of 35%, suggesting that higher E2F1 levels are a good prognostic factor in this cancer type. Similarly, a high E2F1 expression level was recognized as a favorable prognostic factor in thyroid cancer (59).

The aim of this work was to show whether the inhibition of the transcription factor E2F1 by the inhibitor HLM006474 could represent a new approach in tumor therapy in cholangiocarcinoma. Thus, the expression of E2F1 in human CCA samples was investigated, as well as that of some genes that are in close synergism with E2F1, in order to verify whether this hypothesized relationship can be transferred to CCA

samples. To test the effect of inhibition of E2F1, CCA cell lines were treated with HLM006474 and their growth behavior was subsequently monitored.
Suprisingly, Western Blot analysis on protein levels of E2F1 and its targets did not show the expected differences between tumor samples and tumor-free tissue.
This result must also be examined from the point of view of the error-proneness of the Western blotting method. On the one hand, the samples are susceptible due to extraction and purification procedures. Furthermore, protein structure can be altered by denaturation processes, which can have an influence on the results of the Western blot. It also turned out that no satisfactory reproducible results could be obtained, which makes a statistically relevant statement difficult.
Another vulnerability is the antibodies. For different targets, several available antibodies from different manufacturers were tested, all of which did not produce satisfactory results
By studying human cholangiocarcinoma samples in comparison with tumor-free tissue, the primary aim was to demonstrate a presumed overexpression of E2F1 in tumor tissue. Unfortunately, this hypothesis does not translate at the protein level to the patient population studied.
Also the co-investigated targets show no significant difference between the tumor samples and the tumor-free tissue in the examination by Western blot. Thus, the results of Western blot analysis of human samples must be interpreted with great caution and should be redone in another setting. Examination of RNA expression by PCR yielded better results and appears to be the more sensitive method of investigation for the present study population compared with examination of protein expression by Western blot.

Again, the priority was to verify whether there was a difference in E2F1 expression between the tumor tissue and the tumor-free tissue, as has already been shown in multiple other tumor entities (111). In this work, it was shown that E2F1 RNA-expression was significantly higher in tumor tissue ($p=0.033$), confirming the suspected overexpression of E2F1 and leading tothe possibility of using E2F1 as a therapeutic target.

Since E2F1 activity is dependent on Cyclin D1/CDK4 conditional phosphorylation of the Rb-protein, it was of interest to see how Cyclin D1 expression behaved in CCA tumor samples. Other studies have already shown that both Cyclin D1 and E2F1 can act as tumor suppressors or oncogenes, depending on the tissue type (65).

Increased Cyclin D1 expression has also been described in many other tumor entities (112), in the collective studied in this work, contrary to expectations, higher Cyclin D1 expression was found in tumor-free tissue than in tumor tissue, with a significant difference ($p=0.008$).

Although this result would not highlight the intrinsic oncogenic activity of Cyclin D1, it could be explained by a negative feedback mechanism. In a study by Watanabe et al. it was shown that overexpression of E2F1 led to decreased Cyclin D1-dependent kinase activity and thus to lower protein levels of Cyclin D1 (113).

Conversely, one would expect that reduced E2F1 expression would lead to increased Cyclin D1, but this hypothesis cannot be supported by the cell culture experiments performed in this study, where silencing of E2F1 did not lead to a significant change in Cyclin D1 expression. However, the regulation of Cyclin D1 also depends on other pathways. Unfortunately, this work does not allow to make a clear statement about the interaction of E2F1 and Cyclin D1 in cholangiocarcinoma and thus neither the supposed consequences of an inhibition of E2F1.

Another cyclin of particular importance is Cyclin E. Its already known that Cyclin E overexpression is associated with increased resistance of tumor cells to therapeutic agents (114). Since cholangiocarcinoma is also known for responding poorly to chemotherapies (115) and also that the genes coding for Cyclin E are dependent on E2F1 (116) the study of this Cyclin E was of interest in this work.

Increased Cyclin E RNA expression was also detected in the present samples, this difference between tumor and tumor-free tissue at a significant level ($p=0.049$), supporting both the fact of poor response to chemotherapeutic agents, and the oncogenic potential of Cyclin E overexpression. It has also been previously described that the Cyclin E complex together with E2F1 forms a positive feedback loop that initiates the transition from G1 phase to S phase (114, 116-119) and thus has an important influence on cell division and proliferation. In the cell culture experiments, increased Cyclin E expression was measured in two cell lines when E2F1 was suppressed, and in two others it was only minimally decreased, showing on average

increased expression without significance under E2F1 suppression, suggesting but not proving the feedback mechanism of E2F1 and Cyclin E in cholangicellular carcinoma. The dependence of Cyclin E1 on E2F1 and the overexpression of Cyclin E1 demonstrated here in CCA suggest that inhibition of E2F1 may also have an inhibitory effect on the oncogenic activity of Cyclin E1 in this tumor type, as shown previously in hepatocellular carcinoma (120). RNA expression of Cyclin B1 was higher in tumor tissue in the studied collective, but they did not differ at a significant level from tumor-free tissue, suppression of E2F1 resulted in lower expression of Cyclin B, which is consistent with findings from other groups showing that E2F1 suppresses Cyclin B and the function of this cell cycle regulator appears to be closely linked to the activities of the E2F/Rb axis also in CCA (121) providing hope that druggable inhibition of E2F1 could simultaneously attenuate the cancer-promoting properties of Cyclin B1 overexpression.

It is already known that the oncogene c-Myc is involved in the pathogenesis of multiple tumor types (122). c-Myc has also been previously studied in cholangiocarcinoma, with a paper by Luo et al. describing high protein levels of c-Myc in CCA cells (123) and a correlation between c-Myc mediated loss of contact of CCA tumor cells is postulated, which could promote tumor proliferation. This result could not be reproduced in this work, protein expression levels measured by Western blot hardly differed between tumor tissue and tumor-free tissue ($p=0.38$). When examining the RNA expression levels, even the tumor-free tissue showed a higher value ($p=0.005$). The feedback mechanism between c-Myc and E2F1 has also been described previously (77-79). A paper by Li et al. postulates that long noncoding RNA sequences should influence the oncogenic potential of c-Myc via the regulation of E2F1 and thus have an important function in tumorgenesis and -progression (124). In the CCA samples studied in this work, no significant conclusion can be drawn about the correlation of E2F1 and c-Myc expression, because the cell culture experiments also show that silencing of E2F1 does not affect the expression of c-Myc in the CCA cell lines in this case.

Since it is known that E2F1 affects the activity of mini-chromosome maintenance proteins (58) and furthermore, MCM2 has already been shown to function as a proliferation and prognostic marker in other tumor entities (84-86), this work aimed to verify whether such a correlation can also be shown in cholangiocarcinoma in the present celllines or tumor samples. It has been already shown in other work that MCM2

expression is higher in CCA tumor tissue than in non-tumor tissue (125). At the protein level, this result could not be confirmed here; but at the RNA level, the experiments performed here also showed that the expression of MCM2 was significantly higher in tumor tissue than in tumor-free tissue ($p=0.029$), and the suspected proregulatory relationship between E2F1 and MCM2 was also confirmed, as the cell culture experiments showed that suppression of E2F1 leads to significantly reduced expression of MCM2. As MCM2 promotes proliferation and invasion of CCA tumor cells (125) and thus contributes to tumor proliferation by downregulating the p53 pathway (125), it is shown that downregulation of E2F1 also decreases MCM2 expression. Thus drug inhibition of E2F1 could thus decrease the tumor-promoting activity of MCM2.

For another member from the MCM7, there was no significant difference between the tumor and tumor-free tissue at both the protein and RNA levels. However, a correlation between E2F1 expression and MCM7 expression was demonstrated, in the cells with suppressed E2F1 by showing significantly lower MCM7 expression ($p<0.001$). The lower expression of MCM7 induced by inhibition of E2F1 may nevertheless have an anticarcinogenic effect on cholangiocarcinoma cells, as MCM7 has been associated with the ability of CCA cells to evade attack by anticancer agents by entering a quiescent phase, while retaining the potential for reactivation (126). Indeed, in this context, a work by Jia et al showed that knockdown of MCM7 inhibited transcription of G1/S- phase genes and consequently caused inhibition of reactivation of proliferation from dormancy (126), which in turn suggests that inhibition of E2F1 results in lower expression of MCM7 and thus reduces the ability of CCA cells to render themselves inaccessible to anticancer agents.

The higher SKP2 expression in tumor tissue postulated in other studies could not be reproduced in this study: in fact, a higher SKP2 expression was found in tumor-free tissue. SKP2 expression did decrease when E2F1 expression was inhibited, but not at a significant level. There are already studies that showed a higher SKP2 expression in CCA and thus SKP2 was also a possible prognostic marker (127), this approach can unfortunately not be applied to the CCA samples studied based on the data collected in the present work.

The same was shown for FOXM1 expression: there was no increase in tumor tissue, similar to SKP2, even in tumor-free tissue there was a significant increase. The original question was whether FOXM1 could be used as a therapeutic target by regulating E2F1 in a similar way as in ovarian cancer, where the suppression of certain E2F1-dependent DEAD-box RNA helicases could be used as a therapeutic target (128).
Although, based on the data collected here, such an approach in CCA does not seem promising, there is nevertheless already work using FOXM1 as a medial approach point in CCA. For example, Gao et. al. are investigating the FOXM1/AKR1C1 axis as a potential therapeutic target through the pharmacological inhibition by Avasimibe, a bioav(ACAT) inhibitor (129).
Further studies are needed on the role of FOXM1 in CCA to see if targeted therapy at this site could be of clinical benefit.
Also, an increase in RRM2 expression, as in other tumor entities (96-99), could not be shown in the present work, however, suppression of E2F1 showed an effect on RRM2 expression, which also decreased significantly under suppression. This correlation has also been described previously (130) showing that suppression of E2F1, could also suppress the thereby activated oncogenic properties of RRM2 (96).

Finally, to assess the effect on growth and viability of CCA cell lines after inhibition of E2F1 by HLM006474, real-time cell analysis was performed. Differences in cell viability, reflected by cell index, could be detected at the different concentration levels. Cell lines treated with HLM006474 at 20 µM showed a similar curve to cells treated with DMSO as a control. The curves and the associated cell indices were lower under treatment with 50 and 100 µM, but no longer differed greatly among themselves. The biochemical IC50 of HLM006474 is relatively high and amounts to 30µM (in melanoma cell line A375), which could also be reproduced as averaged here.
In NSCLC and SCLC, in addition to the efficacy of HLM006474, a synergism of efficacy was shown when used together with paclitaxel (101). Thus HLM006474 thus appears to be able to increase sensitivity to certain cancer therapeutics.
The results show an influence of the E2F1 inhibitor on the growth behavior and viability of the CCA cell lines. Clear differences can be seen between the growth curves and cell indices of the cell lines treated with DMSO or with the lowest concentration level (20µM), where similar to experiments on NSCLC and SCLC cell lines (101). No

pronounced difference was observed between the higher concentration levels 50µM and 100 µM.

At this point, it is necessary to further test the E2F1 inhibitor on CCA samples in the future, both in cell culture experiments and in vivo experiments, and also in a combination with common chemotherapeutic agents used in CCA, like gemcitabin or cisplatin, should be tested in the future.

The most recent reports on the use of HLM006474 are currently available from experiments in the HCC in the context of a paper by Liu et al. (131). Cell culture experiments were first performed with two specific inhibitors against E2F1(HLM006474) and SMAD3 (SIS3), where a clear inhibition of the investigated genes could be shown. Subsequently, the experiments were transferred to an in vivo model and the E2F1 inhibitor was investigated in mouse livers with promising results regarding the use of this target therapy in HCC subtypes with different oncofetal characteristics (131).

To date, there have been no reports of experiments with HLM006474 beyond experiments in mice or even whether its use in clinical trial setups is possible. There are reports that have examined the biochemical properties of HLM006474 in more detail and show that the R-enantiomeric form of the molecule has greater biological activity and thus a stronger inhibitory effect, and this could lead to better clinical outcomes when HLM006474 is used (132). But beyond that, the substance would need to be tested further.

In conclusion, the basic assumption of the expression behavior of E2F1 and the behavior target genes in CCA has not been comprehensively confirmed. This work was intended to demonstrate a clear overexpression of E2F1 and the associated possibility as a therapeutic target. At the protein level, no meaningful results could be obtained in the studied samples, which may be due to the performance, susceptibility of the reagents, quality of the antibodies and last but not least the sample size.

Indeed, with the same samples at the RNA level, clearer results could be obtained and showed at least a higher expression of E2F1 in tumor tissue, supporting the basic hypothesis. However, here only the expression of Cyclin E and MCM2 was significantly increased in tumor tissue. Cyclin D1, c-Myc, SKP2 and FOXM2 showed significantly higher RNA levels even in tumor-free tissue, contrary to expectations. At this point, it must be summarized that different results would have been expected when the CCA

samples were examined. Both at the protein and at the RNA level, one would have expected a clear overexpression of E2F1 in the tumor tissue, as already described elsewhere. Furthermore, if E2F1 overexpression was assumed, one would have expected that especially the cell cycle controlling cyclins would show a clear overexpression, but this was not the case, except for Cyclin E.

Thus, the collective of 33 CCA tumor samples studied here in direct comparison to healthy tissue does not allow clear conclusions regarding the E2F1 expression status and that of its target genes. At this point, it is necessary to significantly increase the number of samples to be studied in order to obtain a more representative cohort to finally assess E2F1 expression as well as the behavior of the other genes.

The existence of a correlation between E2F1 expression and the expression of the target genes, however, was corroborated by the cell culture experiments and that the method of silencing itself works was shown by a near 100% suppression of E2F1 expression shown in the four different CCA cell lines. Here, a clearer correlation with the investigated target genes could also be shown, especially for MCM2, MCM7, SKP2 and RRM2 expression. The suppression of E2F1 showed a significantly reduced expression and a knockdown effect of more than 50%, which in turn would support the possible effect of drug inhibition of E2F1 on the target genes and thereby also an effect on the respective oncogenic potential of the respective target genes, which has already been disscussed.

The drug effect itself was tested by using the synthetic inhibitor HLM006474 on the four CCA cell lines, which showed an effect on cell viability and growth behavior. The use of a dose between 50 and 100 µM seems to lead to a significant attenuation of cell growth. In contrast, a dose of 20 µM HLM006474 leads to a less pronounced flattening of the growth curve compared to the DMSO control group. However, it is critical to note that the growth behavior of the cell lines under real-time measurement was not particularly good, as shown by the relatively low cell indexes from the beginning and the curve progression of the DMSO control group, as well as the relatively low IC50 values. Nevertheless, the differences between the cells treated with the inhibitor and the untreated cells can be clearly seen.

At this point, the experimental conditions would have to be optimized to achieve a fundamentally better growth behavior of the cell lines.

There is now need to investigate the influence of the inhibition of E2F1 by HLM00674 on the protein and RNA level and in which way this affects in particular the expression of E2F1 and regulatory genes, especially those that are relevant for the cell cycle.
Of further interest would be a flow cytometric apoptosis measurement to test the impact of HLM006474 on cell viability.

Finally, the extensive influence of E2F1 and the E2F1/RB pathway on the cell cycle and, consequently, on uncontrolled cell division, cell proliferation and tumorigenesis and proliferation has been described many times. Targeting this transcription factor with drugs could significantly change tumor therapy, especially in conventionally poorly treatable tumor diseases such as CCA.
The results of this study do not provide a clear answer to the question of whether inhibition of E2F1 by HLM006474 could represent a valid therapeutic approach and are inconclusive, particularly in that expression patterns or correlations already investigated in other studies could not be reproduced or proven, especially in the human CCA samples. Nevertheless, in cell culture experiments a clear expression correlation between E2F1 and the genes involved in carcinogenesis in CCA investigated here could be shown, which does not allow to reject the working hypothesis to be completely. The fact that cell proliferation was influenced by the inhibition of E2F1 and that differences could be shown between different concentration levels at least offer starting points for further experiments and experimental models to evaluate the clinical suitability of HLM006474.

4.2 Summary

Cholangiocarcinoma is a very aggressive form of tumor, which still has a very poor prognosis, due in part to the often late time of diagnosis and the limited response to current forms of therapy.

Therefore, it is necessary to work on new therapeutic approaches to improve the therapy and consequently the prognosis of CCA.

This work was focused on the transcription factor E2F1, which is known to play a key role in cell cycle progression through its position in the Rb-pathway. As being a master regulator, E2F1 has a lot of target genes with complex interactions. By occupying such a key position in cell division and proliferation, E2F1 is also important in the proliferation of tumor cells. In many tumor entities an overexpression of E2F1 has already been described, although the role seems to be complex with contradictory results.

In principle, this work can be divided into two experimental areas, based on the question of whether E2F1 can be used therapeutically in CCA:

On the one hand, human CCA samples were examined, always in direct comparison with healthy liver tissue from identical patients. Here, the expression of E2F1 and several target genes (Cyclin E, Cyclin B1, MCM2, MCM7, c-Myc, Cyclin D1, SKP2 and FOXM1) was investigated. In conclusion, no meaningful results could be obtained at the protein level; there were no clear expression differences between tumor tissue and tumor-free tissue. At the RNA level, clearer differences could be obtained in some cases, whereby the expected correlation could only be confirmed for E2F1 itself and MCM2. Most of the other target genes even showed increased expression patterns in healthy tissue, concluding that the investigation of 33 CCA tumor samples did not lead to support the hypothesis that E2F1 is a promising therapeutic target.

The second major experimental complex involved cell culture experiments with four CCA cell lines. In order to demonstrate the dependence of target genes on E2F1, E2F1 was suppressed by silencing and then the expression of target genes underneath was examined. From these results, it could be deduced that suppression of E2F1 significantly affects the expression of the target genes. Suppression over 50% starting from the expression in the control groups was detected here for MCM2,MCM7, SKP2 and RRM2.

Furthermore, the cell lines were treated with the E2F1 inhibitor HLM006474 at different concentration levels and subsequently their growth behavior was monitored. Basically, based on this experimental model, it can be concluded that the application of HLM006474 has effects on the growth behavior of the CCA cell lines, and the difference between 50 and 100 µM was mostly not large anymore. Together with the results from the silencing experiments, it can be supposed that a therapeutic inhibition of E2F1 is possible and should also affect some genes involved in tumorigenesis and proliferation.

Finally, the results of this work can be summarized by the fact that the investigation of the human CCA samples, although not allowing clear conclusions about the role of E2F1 and its target genes in CCA, the cell culture experiments nevertheless showed that E2F1 in CCA has an influence on the expression of the other target genes. Inhibition of E2F1 by HLM006474 affects growth behavior, so the results provide at least a starting point that the use of HLM006474 should be further investigated and new experimental models should be tested in vitro and in vivo and also should be expanded to include combination with already established CCA therapies to see if clinical use of HLM006474 could achieve good results in tumor treatment and if its use in humans would eventually be feasible.

4.3 Zusammenfassung

Das cholangiozelluläre Karzinom ist ein äußerst aggressiver Tumor, welcher nach wie vor eine sehr schlechte Prognose hat, was unter anderem auf den oftmals späten Diagnosezeitpunkt und das bedingte Ansprechen auf die gängigen Therapieformen zurückzuführen ist.

Daher ist es notwendig an neuen therapeutischen Ansätzen zu arbeiten, um die Therapie und damit einhergehend auch die Prognose des CCA zu verbessern.

Fokus dieser Arbeit war der Transkriptionsfaktor E2F1, von dem bekannt ist, dass er beim Voranschreiten des Zellzyklus durch seine Stellung im Rb-Pathway eine zentrale Rolle einnimmt. E2F1 beeinflusst die Expression vieler Gene bzw. tritt mit ihnen in Wechselwirkungen.

Durch die Einnahme einer solchen Schlüsselposition bei Zellteilung und Zellproliferation hat E2F1 auch bei der Proliferation von Tumorzellen eine große Bedeutung. In vielen Tumorentitäten wurde bereits eine Überexpression von E2F1 beschrieben, wenn die Rolle dennoch komplex scheint und es auch Tumorerkrankungen gibt auf die das nicht bzw. Gegenteiliges zu trifft.

Diese Arbeit lässt sich in zwei Versuchsbereiche aufteilen, basierend auf der Fragestellung, ob E2F1 im CCA therapeutisch genutzt werden kann.

Dafür wurden zum einen humane CCA Proben auf die Expression von E2F1 und einiger Zielgene (Cyclin E, Cyclin B1, MCM2, MCM7, c-Myc, Cyclin D1, SKP2 und FOXM1) untersucht, immer im direkten Vergleich mit gesunden Lebergewebe vom identischen Patienten. Auf Proteinebene konnten keine aussagekräftigen Ergebnisse erzielt werden, da sich keine deutlichen Expressionsunterschiede zwischen Tumorgewebe und tumorfreien Gewebe nachweisen ließen. Auf RNA-Ebene ließen sich zum Teil deutlichere Unterschiede herausarbeiten, wobei sich der erwartete Zusammenhang nur für E2F1 selbst und MCM2 auf signifikantem Niveau bestätigen ließ. Die meisten anderen Zielgene zeigten sogar widersprüchliche Expressionsmuster, wodurch sich abschließend kritisch ableiten lässt, dass die Untersuchung von 33 CCA Tumorproben in dieser Arbeit nicht dazu geführt hat, die Hypothese zu stützen, dass E2F1 ein vielsprechender therapeutischer Ansatzpunkt im CCA ist.

Der zweite große Versuchskomplex beinhaltete Zellkulturversuche mit vier CCA Zelllinien. Um hier die Abhängigkeit der Zielgene von E2F1 aufzuzeigen, wurde E2F1 mittels Silencing unterdrückt und dann die Expression der Zielgene darunter untersucht. Aus diesen Ergebnissen ließ sich ableiten, dass eine Unterdrückung von E2F1 die Expression der Zielgene deutlich beeinflusst, eine Unterdrückung über 50% ausgehend von der Expression in den Kontrollgruppen wurde hier für MCM2, MCM7, SKP2 und RRM2 nachgewiesen.

Des weiteren wurden die Zelllinien mit dem E2F1-Inhibitor HLM006474 in unterschiedlichen Konzentrationsstufen behandelt und anschließend ihr Wachstumsverhalten untersucht. Grundsätzlich kann anhand dieses Versuchmodells gesagt werden, dass die Anwendung von HLM006474 Auswirkungen auf das Wachstumsverhalten der CCA-Zelllinien hat, wobei der Unterschied zwischen 50 und 100 µM meist nicht mehr groß war. Zusammen mit den Ergebnissen aus den Silencing Versuchen, kann aber der Schluss gezogen werden, dass eine therapeutische Inhibierung von E2F1 zum einem möglich ist und zum anderen auch einige mit in die Tumorentstehung und-proliferation involvierte Gene beeinflussen dürfte.

Abschließend können die Ergebnisse dieser Arbeit dahingehend zusammengefasst werden, dass die Untersuchungen der humanen CCA Proben zwar keine eindeutigen Schlüsse über die Rolle von E2F1 und seine Zielgenen im CCA zulassen, aber die Zellkulturversuche dennoch zeigten, dass E2F1 im CCA Einfluss auf die Expression anderer Schlüsselgene hat. Eine Inhibierung von E2F1 durch HLM006474 beeinflusst das Wachstumsverhalten, so dass die Ergebnisse zumindest einen Ausgangspunkt dafür liefern, dass der Einsatz von HLM006474 weiter untersucht werden sollte. Neue Versuchsmodelle in vitro und in vivo sollten dafür zur Anwendung kommen und diese sollten auch um die Kombination mit bereits etablierten Therapieformen erweitert werden, um zu sehen, ob ein klinischer Einsatz von HLM006474 gute Ergebnisse in der Tumorbehandlung erzielen könnte und ein Einsatz im Menschen schlussendlich realisierbar wäre.

5. Attachment

5.1 List of figures

Figure 1: Classification and appearance of CCA
Figure 2: Worldwide incidence of cholangiocarcinoma
Figure 3: Therapeutic algorithmus biliary carcinoma
Figure 4: Cell cycle
Figure 5: E2F1 related Transcription
Figure 6: Structure of E2F1
Figure 7: Structure of HLM006474
Figure 8a: E2F1 and GAPDH levels in 33 human cholangiocarcinoma samples
Figure 8b: Protein levels of E2F1 in pairs in tumor and tumor-free tissue (= normal)
Figure 9a: C-Myc and GAPDH levels in 33 human cholangiocarcinoma samples
Figure 9b: Protein levels of C-Myc in pairs in tumor and tumor-free tissue (= normal)
Figure 10a: Cyclin D1 and GAPDH levels in 33 human cholangiocarcinoma samples
Figure 10b: Protein levels of Cyclin D1 in pairs in tumor and tumor-free tissue (= normal)
Figure 11a: MCM2 and GAPDH levels in 33 human cholangiocarcinoma samples
Figure 11b: Protein levels of MCM2 in pairs in tumor tissue and tumor-free (= normal)
Figure 12a: MCM7 and GAPDH levels in 33 human cholangiocarcinoma samples
Figure 12b: Protein levels of MCM7 in pairs in tumor tissue and tumor free tissue (= normal)
Figure 13a: Cyclin E and GAPDH levels in 33 human cholangiocarcinoma samples
Figure 13b: Protein levels of Cyclin E in pairs in tumor tissue and tumor-free tissue (= normal)
Figure 14: Relative RNA levels of E2F1, Cyclin D1, C-Myc, MCM2, MCM7, and Cyclin E normalized to GAPDH of paired cholangiocarcinoma tissue (TU) and corresponding normal liver tissue (NT)
Figure 15A: RNA Expression of target genes, comparison under silencing of e2f1 and the control group, A
Figure 15B: RNA Expression of target genes, comparison under silencing of e2f1 and the control group, B-E

Figure 15C: RNA Expression of target genes, comparison under silencing of e2f1 and the control group, F-I

Figure 16: Knockdown effect in target genes after silencing E2F1

Figure 17: graph of the cell index for cell line KKU-213 under the treatment with HLM006474(top), as well as the representation of the cell index in the bar chart after 48 hours of treatment (below) with the values listed in a table

Figure 18: graph of the cell index for cell line KKU-156 under the treatment with HLM006474 (top), as well as the representation of the cell index in the bar chart after 48 hours of treatment (below) with the values listed in a table

Figure 19: graph of the cell index for cell line HUCCT1 under the treatment with HLM006474 (top), as well as the representation of the cell index in the bar chart after 48 hours of treatment (below) with the values listed in a table

Figure 20: graph of the cell index for cell line RBE under the treatment with HLM006474 (top), as well as the representation of the cell index in the bar chart after 48 hours of treatment (below) with the values listed in a table

5.2 List of tables

Table 1: Classification of small duct type and large duct type intrahepatic cholangiocarcinoma

Table 2: Clinical TNM classification of tumors of the intrahepatic bile ducts: T- Primary Tumor

Table 3: Clinical TNM classification of tumors of the intrahepatic bile ducts: N- Regional Lymph Nodes

Table 4: Clinical TNM classification of tumors of the intrahepatic bile ducts: M- Distant Metastasis

Table 5: Stages classification according to UICC

Table 6: CDKs and their cyclin partners

Table 7: CKIs

Table 8: E2F family genes and role in cell cycle, transcription, and other biological features

Table 9: List of Equipment

Table 10: List of reagents

Table 11: CCA cell lines

Table 12: Primary antibodies

Table 13: Secondary antibodies

Table 14: Software

Table 15: Clinicopathological features of the patients

Table 16: Composition of the master mix

Table 17: Device settings of the T100 Thermal cycler for rewriting RNA into cDNA

Table 18: Master mix composition of the target gene in direct comparison to the housekeeper gene

Table 19: Device settings of the CFX96™ Real-Time System for a run

Table 20: The settings in the RTCA 2.1.0 software for the measurements of cell lines growth after the treatment with HLM006474 with xCELLigence™

Table 21: Statistical evaluation of the Western Blot

Table 22: PCR results

Table 23: Statistical evaluation of the PCR results, p- values calculated by Mann-Whitney- U-Test

Table 24: Correlationanalysis, Spearman coeffizient |p|, p-value

Table 25: Overview of $2^{-\Delta CT}$ values for the different target genes in the KKU-156, KKU 213, RBE, and HUCCT1 cells.

Table 26: statistic evaluation of comparison the silencing group against the control group

Table 27: IC50-values for the four celllines, with mean- and standarddeviation

Table 28: Identity of tumor and non-tumorous specimens

Table 29: TaqMan™Gene Expression Assays of the different target genes studied in the PCR

Table 30: $2^{-\Delta\Delta CT}$- values CCA samples

Table 31: $2^{\wedge-\Delta\Delta CT}$- values CCA samples

5.3 List of abbrevations

%= percent
°C= Degree Celsius
18-FDG-Pet= 18-F-fluorodeoxyglucose positron emission tomography
3D-CRT= 3D conformal radiotherapy
ACTB= Actin Beta
AJCC= American Joint Committee on Cancer
BEC= biliary epithelial cells
BSA= bolvine serum albumin
CA19-9= Carbohydrate antigen 19-9
CCA= cholangiocarcinoma
CDK= cyclin dependent kinase
cDNA= complementary deoxyribonucleic acid
ce-CT= contrast-enhanced computer tomography
ce-MR= contrast-enhanced magnetic resonance
CEUS= contrast-enhanced ultrasound
CI= cell index
CK= Cytokeratin
CKI= cyclin dependent kinase inhibitor
cm^2= square centimeter
CSC=Cancer stem cells
CT= cycle threshold
cTNM= clinical TNM classification
CTRL= Control
dCCA= distal cholangiocarcinoma
DMEM= dulbeccos modified eagles medium
DMSO= dimethylsulfoxid
DNA= deoxyribonucleic acid
DP= dimerization partner
E2F1= E2F Transcription Factor 1
EBRT= External- beam radiation
eCCA= extrahepatic cholangiocarcinoma

ECL= enhanced chemiluminisence

ECOG= Eastern Cooperative Oncology Group),

EDTA = Ethyldiamintetraacetat

EpCAM =epithelial cell adhesion molecule

ERCP= endoscopic retrograde cholangiopancreatography

FCS= fetal calf serum

FGFR= fibroblast growth factor

FISH= fluorescent in situ hybridization

FOXM1= forkhead box M1

G1-phase/ G2-phase = first gap phase/second gap phase

GAPDH= Glycerinaldehyd-3-phosphate-Dehydrogenase

GART= Trifunctional purine biosynthetic protein adenosine-3

GMP= GMP synthase [glutamine-hydrolyzing

HCC= hepatocellular carcinoma

iCCA= intrahepatic cholangiocarcinoma

IDH1= Isocitrate dehydrogenase 1

IG= intraductal growing

IMRT= intensity-modulated radiotherapy

kDa= Kilodalton

M-phase= mitotic phase

MCM= mini-chromosome maintenance

MF= mass-forming

ml= milliliter

mM= millimolar

MMP= matrix metalloproteinase

MOC= mechanisms of chemoresistance

MPF= maturation-promoting factor

MRCP= magnetic resonance cholangiopancreatography

MRI= magnetic resonance imaging

mRNA= messenger ribonucleic acid

MUC= Mucin

NCAM = neutral cell adhesion molecule

PBD= percutane biliary drainage

PBS= phosphate Buffered Saline
pCCA= perihilar cholangiocarcinoma
PCR= polymerase chain reaction
PHLF= post-hepatectomy liver failure
PI= periductal infiltrating
PI3K= phosphoinositide 3-kinase
pRb= phosphorylated retinoblastoma protein
PSC= primary sclerosing cholangitis
pTNM= pathological TNM classification
q-RT-PCR= quantitative real-time polymerase chain reaction
Rb= retinoblastoma protein
rcf= relatice centrifugal force
RCTA= Real-time Cell Analysis
RNA= ribonucleic acid
rpm= revolutions per minute
RRM2= ribonucleotide reductase regulatory subunit M2
S-phase= synthetic phase
SDS-Page= sodium dodecyl sulfate polyacrylamide gel electrophoresis
SDS= sodium dodecyl sulfate-
siRNA= small interfering RNA
SKP2= s phase kinase-associated protein 2
TACE= transarterial chemoembolization
TARE= transarterial radioembolization
TBS= tris-bufferd saline
TFF= TreFoil Factor 1
UICC=Union for International Cancer Control)
V= Volt
VEGFR= vascular endothelial growth factor
WHO= World Health Organisation
µg= microgram
µl= microliter
µM= micromolar

5.4 Additional tables

1. ECOG Performance Status

0: Fully active, able to carry on all pre-disease performance without restriction
1: Restriceted in physically strenuous activity but ambulatory and able to carry out work of a light or sedentary nature, e.g., light house work, office work
2: ambulatory and capable of all selfcare but unable to carry out any work activities. Up and about more than 50 % of waking hours
3: capable of only limited selfcare, confindes to bed or chair more than 50% of waking hours
4: completely disabled. Cannot carry on any selfcare. Totally confined to bed or chair
5: dead

2. Sample List according to patients

Sample number	Patient	Tissue	Sample number	Patient	Tissue	Sample number	Patient	Tissue
1	1	Tu	**23**	12	Tu	**45**	23	Tu
2	1	No	**24**	12	No	**46**	23	No
3	2	Tu	**25**	13	Tu	**47**	24	Tu
4	2	No	**26**	13	No	**48**	24	No
5	3	Tu	**27**	14	Tu	**49**	25	Tu
6	3	No	**28**	14	No	**50**	25	No
7	4	Tu	**29**	15	Tu	**51**	26	Tu
8	4	No	**30**	15	No	**52**	26	No
9	5	Tu	**31**	16	Tu	**53**	27	Tu
10	5	No	**32**	16	No	**54**	27	No
11	6	Tu	**33**	17	Tu	**55**	28	Tu
12	6	No	**34**	17	No	**56**	28	No
13	7	Tu	**35**	18	Tu	**57**	29	Tu
14	7	No	**36**	18	No	**58**	29	No
15	8	Tu	**37**	19	Tu	**59**	30	Tu
16	8	No	**38**	19	No	**60**	30	No
17	9	Tu	**39**	20	Tu	**61**	31	Tu
18	9	No	**40**	20	No	**62**	31	No
19	10	Tu	**41**	21	Tu	**63**	32	Tu
20	10	No	**42**	21	No	**64**	32	No
21	11	Tu	**43**	22	Tu	**65**	33	Tu
22	11	No	**44**	22	No	**66**	33	No

Tu= tumor sample, No= tumor free sample

Table 28: Identity of tumor and non-tumorous specimens

3. List of Taqman Assays for PCR

Target	TaqMan™Gene Expression Assay	Company	ID
E2F1	E2F1 Human TaqMan™Gene Expression Assay (FAM)	Thermo Fisher Scientific Biosciences GmbH	Hs00153451_m1
c-Myc	TaqMan™Gene Expression Assay (FAM-MGB) Gene Name: MYC	Thermo Fisher Scientific Biosciences GmbH	Hs00153408_m1
Cyclin B1	Cyclin B1 (CCNB1) Human TaqMan™Gene Expression Assay (FAM)	Thermo Fisher Scientific Biosciences GmbH	Hs01030099_m1
MCM7	MCM7 Human TaqMan™Gene Expression Assay (FAM)	Thermo Fisher Scientific Biosciences GmbH	Hs00428518_m1
MCM2	MCM2 TaqMan™Gene Expression Assay (FAM)	Thermo Fisher Scientific Biosciences GmbH	Hs01091564_m1
ACTB	ACTB TaqMan Assay VIC-MBG-PL	Thermo Fisher Scientific Biosciences GmbH	HS99999903_M1
Cyclin E1	Cyclin E1 TaqMan™Gene Expression Assay (FAM)	Thermo Fisher Scientific Biosciences GmbH	Hs01026536_m1
RRM2	RRM2 Human TaqMan™Gene Expression Assay (FAM)	Thermo Fisher Scientific Biosciences GmbH	Hs00357247_g1
SKP2	SKP2 Human TaqMan™Gene Expression Assay (FAM)	Thermo Fisher Scientific Biosciences GmbH	Hs01021864_m1
GAPDH	GAPDH TaqMan™ Gene Expression Assay, VIC-MGB	Thermo Fisher Scientific Biosciences GmbH	Hs02786624_g1
FOXM1	FOXM1 Human TaqMan™Gene Expression Assay (FAM)	Thermo Fisher Scientific Biosciences GmbH	Hs01073586_m1
Cyclin D1	Cyclin D1 Human TaqMan™Gene Expression Assay (FAM)	Thermo Fisher Scientific Biosciences GmbH	Hs00765553_m1

Table 29: TaqMan™Gene Expression Assays of the different target genes studied in the PCR

4. $2^{-\Delta\Delta CT}$- values CCA samples

	Cyclin E	E2F1	MCM2	MCM7	Cyclin D1	c-Myc	SKP2	FOXM1	Cyclin B1	RRM2
Pateint 1	1,7445	0,2984	0,8131	0,5691	0,6740	0,6268	0,6476	0,6383	0,6425	0,6406
Pateint 2	8,2596	0,0033	0,9977	0,5008	0,7067	0,6127	0,6540	0,6355	0,6437	0,6401
Pateint 3	1,7508	0,2971	0,8139	0,5689	0,6742	0,6267	0,6477	0,6383	0,6425	0,6406
Pateint 4	0,8270	0,5637	0,6766	0,6257	0,6481	0,6381	0,6426	0,6406	0,6415	0,6411
Pateint 5	6,1618	0,0140	0,9904	0,5034	0,7055	0,6132	0,6537	0,6356	0,6437	0,6401
Pateint 6	0,9664	0,5118	0,7014	0,6150	0,6529	0,6360	0,6435	0,6402	0,6416	0,6410
Pateint 7	2,2846	0,2052	0,8674	0,5481	0,6839	0,6225	0,6496	0,6375	0,6428	0,6405
Pateint 8	0,7516	0,5939	0,6625	0,6318	0,6454	0,6393	0,6420	0,6408	0,6413	0,6411
Pateint 9	2,0905	0,2348	0,8498	0,5549	0,6807	0,6239	0,6489	0,6378	0,6427	0,6405
Pateint 10	0,0196	0,9865	0,5047	0,7048	0,6135	0,6536	0,6357	0,6436	0,6401	0,6417
Pateint 11	0,0197	0,9865	0,5047	0,7048	0,6135	0,6536	0,6357	0,6436	0,6401	0,6417
Pateint 12	0,3352	0,7927	0,5773	0,6702	0,6284	0,6469	0,6387	0,6423	0,6407	0,6414
Pateint 13	0,0019	0,9987	0,5005	0,7069	0,6126	0,6540	0,6355	0,6437	0,6401	0,6417
Pateint 14	0,3497	0,7847	0,5805	0,6688	0,6291	0,6466	0,6388	0,6423	0,6407	0,6414
Pateint 15	0,4868	0,7136	0,6098	0,6553	0,6349	0,6440	0,6400	0,6417	0,6409	0,6413
Pateint 16	0,3529	0,7830	0,5812	0,6684	0,6292	0,6465	0,6388	0,6422	0,6407	0,6414
Pateint 17	0,3930	0,7616	0,5899	0,6644	0,6309	0,6458	0,6392	0,6421	0,6408	0,6414
Pateint 18	0,0012	0,9992	0,5003	0,7070	0,6126	0,6540	0,6355	0,6437	0,6401	0,6417
Pateint 19	2,7293	0,1508	0,9008	0,5356	0,6899	0,6199	0,6507	0,6370	0,6431	0,6404
Pateint 20	1,4535	0,3651	0,7764	0,5838	0,6672	0,6297	0,6463	0,6389	0,6422	0,6407
Pateint 21	2,4949	0,1774	0,8843	0,5418	0,6869	0,6212	0,6501	0,6372	0,6430	0,6404
Pateint 22	0,0012	0,9992	0,5003	0,7070	0,6126	0,6540	0,6355	0,6437	0,6401	0,6417
Pateint 23	0,6633	0,6314	0,6455	0,6393	0,6420	0,6408	0,6414	0,6411	0,6412	0,6412
Pateint 24	0,7679	0,5873	0,6656	0,6304	0,6460	0,6391	0,6421	0,6408	0,6414	0,6411
Pateint 25	1,9498	0,2589	0,8357	0,5603	0,6782	0,6250	0,6484	0,6380	0,6426	0,6406
Pateint 26	5,0375	0,0304	0,9791	0,5073	0,7035	0,6141	0,6534	0,6358	0,6436	0,6401
Pateint 27	6,0583	0,0150	0,9897	0,5036	0,7053	0,6133	0,6537	0,6356	0,6437	0,6401
Pateint 28	2,1330	0,2280	0,8538	0,5533	0,6815	0,6235	0,6491	0,6377	0,6427	0,6405
Pateint 29	3,2893	0,1023	0,9316	0,5243	0,6953	0,6176	0,6518	0,6365	0,6433	0,6403
Pateint 30	2,2623	0,2084	0,8655	0,5489	0,6836	0,6226	0,6495	0,6375	0,6428	0,6405
Pateint 31	3,5725	0,9858	7,1694	0,2866	1,7338	0,8840	2,3029	6,4976	7,6651	5,8523
Pateint 32	4,6214	0,0406	0,9722	0,5097	0,7024	0,6146	0,6531	0,6359	0,6435	0,6401
Pateint 33	1,2896	0,4091	0,7531	0,5933	0,6628	0,6316	0,6454	0,6393	0,6420	0,6408

Table 30: $2^{-\Delta\Delta CT}$- values CCA samples

5. $2^{-\Delta\Delta CT}$- values Celllines

	2^-deltadelta neg. siRNA	2^-deltadelta siRNA
E2F1 KKU-156	1,5695	0,0192
E2F1 KKU-213	1,5869	0,0216
E2F1 RBE	1,7524	0,0770
E2F1 HUCCT1	1,8331	0,1126
MCM2 KKU-156	0,9904	0,3530
MCM2 KKU-213	1,1665	0,4170
MCM2 HUCCT1	1,5129	0,6252
MCM2 RBE	1,4066	0,7737
Cyclin B1 KKU-156	0,9872	0,6238
Cyclin B1 KKU-213	0,9937	0,6917
HUCCT1 Cyclin B1	1,3130	0,3601
Cyclin B1 RBE	1,6581	1,1566
Cyclin D1 KKU156	1,2000	1,0088
Cyclin D1 KKU-213	1,1481	0,9784
Cyclin D1 HUCCT1	1,6077	1,0049
Cyclin D1 RBE	0,9818	0,9102
Cyclin E1 KKU-156	0,9313	1,1880
Cyclin E KKU-213	0,8855	1,1524
Cyclin E1 HUCCT1	1,2750	1,2267
Cyclin E1 RBE	1,2987	1,1528
MCM7 KKU-156	1,1771	0,4540
MCM7 KKU-213	1,2436	0,4544
MCM7 HUCCT1	1,3041	0,5532
MCM7 RBE	1,5356	0,8768
c-Myc KKU-156	0,7591	0,6684
c-Myc KKU-213	0,7379	0,7197
c-Myc HUCCT1	1,1515	0,7383
c-Myc RBE	0,7105	0,7508
SKP2 KKU-156	1,5840	0,5838
SKP2 KKU-213	1,5914	0,6611
SKP2 HUCCT1	3,4017	0,6001
SKP2 RBE CTRL	1,5139	1,0153

Table 31: $2^{-\Delta\Delta CT}$- values CCA samples

6. References

1. Kendall T, Verheij J, Gaudio E, Evert M, Guido M, Goeppert B, et al. Anatomical, histomorphological and molecular classification of cholangiocarcinoma. Liver Int. 2019 May;39(S1):7–18.
2. Banales JM, Marin JJG, Lamarca A, Rodrigues PM, Khan SA, Roberts LR, et al. Cholangiocarcinoma 2020: the next horizon in mechanisms and management. Nat Rev Gastroenterol Hepatol. 2020 Sep;17(9):557–88.
3. Sinn et. al. Onkopedia Leitlinie-Biliäre Karzinome [Internet]. DGHO; 2021 [cited 2022 Nov 23]. Available from: https://www.onkopedia.com/de/onkopedia/guidelines/biliaere-karzinome/@@guideline/html/index.html#litID0E26CI
4. Banales JM, Cardinale V, Macias RIR, Andersen JB, Braconi C, Carpino G, et al. Cholangiocarcinoma: State-of-the-art knowledge and challenges. Liver Int. 2019 May;39(S1):5–6.
5. Banales JM, Cardinale V, Carpino G, Marzioni M, Andersen JB, Invernizzi P, et al. Cholangiocarcinoma: current knowledge and future perspectives consensus statement from the European Network for the Study of Cholangiocarcinoma (ENS-CCA). Nat Rev Gastroenterol Hepatol. 2016 May;13(5):261–80.
6. Vijgen S, Terris B, Rubbia-Brandt L. Pathology of intrahepatic cholangiocarcinoma. HepatoBiliary Surg Nutr. 2017 Feb;6(1):22–34.
7. Nakanuma Y, Kakuda Y. Pathologic classification of cholangiocarcinoma: New concepts. Best Pract Res Clin Gastroenterol. 2015 Apr;29(2):277–93.
8. Krasinskas AM. Cholangiocarcinoma. Surg Pathol Clin. 2018 Jun;11(2):403–
9. Nakanuma Y. Pathological classification of intrahepatic cholangiocarcinoma based on a new concept. World J Hepatol. 2010;2(12):419.
10. Aishima S, Oda Y. Pathogenesis and classification of intrahepatic cholangiocarcinoma: different characters of perihilar large duct type versus peripheral small duct type. J Hepato-Biliary-Pancreat Sci. 2015 Feb;22(2):94–100.
11. Komuta M, Govaere O, Vandecaveye V, Akiba J, Van Steenbergen W, Verslype C, et al. Histological diversity in cholangiocellular carcinoma reflects the different cholangiocyte phenotypes. Hepatology. 2012 Jun;55(6):1876–88.
12. Liau JY, Tsai JH, Yuan RH, Chang CN, Lee HJ, Jeng YM. Morphological

subclassification of intrahepatic cholangiocarcinoma: etiological, clinicopathological, and molecular features. Mod Pathol. 2014 Aug;27(8):1163–73.

13. Nakanuma Y, Xu J, Harada K, Sato Y, Sasaki M, Ikeda H, et al. Pathological spectrum of intrahepatic cholangiocarcinoma arising in non-biliary chronic advanced liver diseases: ICC in chronic liver disease. Pathol Int. 2011 May;61(5):298–305.

14. Wittekind C, Union for International Cancer Control, editors. TNM - Klassifikation maligner Tumoren. Achte Auflage. Weinheim: Wiley-VCH Verlag GmbH & Co. KGaA; 2017. 313 p.

15. Rizvi S, Gores GJ. Pathogenesis, Diagnosis, and Management of Cholangiocarcinoma. Gastroenterology. 2013 Dec;145(6):1215–29.

16. Cardinale V. Multiple cells of origin in cholangiocarcinoma underlie biological, epidemiological and clinical heterogeneity. World J Gastrointest Oncol. 2012;4(5):94.

17. Fan B, Malato Y, Calvisi DF, Naqvi S, Razumilava N, Ribback S, et al. Cholangiocarcinomas can originate from hepatocytes in mice. J Clin Invest. 2012 Aug 1;122(8):2911–5.

18. Vicent S, Lieshout R, Saborowski A, Verstegen MMA, Raggi C, Recalcati S, et al. Experimental models to unravel the molecular pathogenesis, cell of origin and stem cell properties of cholangiocarcinoma. Liver Int. 2019 May;39(S1):79–97.

19. DeOliveira ML, Cunningham SC, Cameron JL, Kamangar F, Winter JM, Lillemoe KD, et al. Cholangiocarcinoma: Thirty-one-Year Experience With 564 Patients at a Single Institution. Ann Surg. 2007 May;245(5):755–62.

20. Fitzmaurice C, Dicker D, Pain A, Hamavid H, Moradi-Lakeh M, MacIntyre MF, et al. The Global Burden of Cancer 2013. JAMA Oncol. 2015 Jul 1;1(4):505.

21. Massarweh NN, El-Serag HB. Epidemiology of Hepatocellular Carcinoma and Intrahepatic Cholangiocarcinoma. Cancer Control. 2017 Sep;24(3):107327481772924.

22. Razumilava N, Gores GJ. Cholangiocarcinoma. The Lancet. 2014 Jun;383(9935):2168–79.

23. Razumilava N, Gores GJ. Cholangiocarcinoma. The Lancet. 2014 Jun;383(9935):2168–79.

24. Razumilava N, Gores GJ. Classification, Diagnosis, and Management of Cholangiocarcinoma. Clin Gastroenterol Hepatol. 2013 Jan;11(1):13-21.e1.

25. Forner A, Vidili G, Rengo M, Bujanda L, Ponz-Sarvisé M, Lamarca A. Clinical

presentation, diagnosis and staging of cholangiocarcinoma. Liver Int. 2019 May;39(S1):98–107.
26. Cillo U, Fondevila C, Donadon M, Gringeri E, Mocchegiani F, Schlitt HJ, et al. Surgery for cholangiocarcinoma. Liver Int. 2019 May;39(S1):143–55.
27. Marin JJG, Lozano E, Briz O, Al-Abdulla R, Serrano MA, Macias RIR. Molecular Bases of Chemoresistance in Cholangiocarcinoma. Curr Drug Targets. 2017 May 4;18(8):889–900.
28. Adeva J, Sangro B, Salati M, Edeline J, La Casta A, Bittoni A, et al. Medical treatment for cholangiocarcinoma. Liver Int. 2019 May;39(S1):123–42.
29. Lamarca A, Hubner RA, David Ryder W, Valle JW. Second-line chemotherapy in advanced biliary cancer: a systematic review. Ann Oncol. 2014 Dec;25(12):2328–
30. Primrose JN, Fox RP, Palmer DH, Malik HZ, Prasad R, Mirza D, et al. Capecitabine compared with observation in resected biliary tract cancer (BILCAP): a randomised, controlled, multicentre, phase 3 study. Lancet Oncol. 2019 May;20(5):663–73.
31. Edeline J, Benabdelghani M, Bertaut A, Watelet J, Hammel P, Joly JP, et al. Gemcitabine and Oxaliplatin Chemotherapy or Surveillance in Resected Biliary Tract Cancer (PRODIGE 12-ACCORD 18-UNICANCER GI): A Randomized Phase III Study. J Clin Oncol. 2019 Mar 10;37(8):658–67.
32. Ebata T, Hirano S, Konishi M, Uesaka K, Tsuchiya Y, Ohtsuka M, et al. Randomized clinical trial of adjuvant gemcitabine chemotherapy *versus* observation in resected bile duct cancer. Br J Surg. 2018 Feb 5;105(3):192–202.
33. Shi X qi, Zhang J yu, Tian H, Tang L na, Li A lin. Role of adjuvant (chemo)radiotherapy for resected extrahepatic cholangiocarcinoma: a meta-analysis. J Zhejiang Univ-Sci B. 2020 Jul;21(7):549–59.
34. Kim BH, Kwon J, Chie EK, Kim K, Kim YH, Seo DW, et al. Adjuvant Chemoradiotherapy is Associated with Improved Survival for Patients with Resected Gallbladder Carcinoma: A Systematic Review and Meta-analysis. Ann Surg Oncol. 2018 Jan;25(1):255–64.
35. Rizvi S, Khan SA, Hallemeier CL, Kelley RK, Gores GJ. Cholangiocarcinoma — evolving concepts and therapeutic strategies. Nat Rev Clin Oncol. 2018 Feb;15(2):95–
36. Abou-Alfa GK, Sahai V, Hollebecque A, Vaccaro G, Melisi D, Al-Rajabi R, et al. Pemigatinib for previously treated, locally advanced or metastatic cholangiocarcinoma:

a multicentre, open-label, phase 2 study. Lancet Oncol. 2020 May;21(5):671–84.
37. Groot Koerkamp B, Wiggers JK, Allen PJ, Besselink MG, Blumgart LH, Busch ORC, et al. Recurrence Rate and Pattern of Perihilar Cholangiocarcinoma after Curative Intent Resection. J Am Coll Surg. 2015 Dec;221(6):1041–9.
38. Dickson PV, Behrman SW. Distal Cholangiocarcinoma. Surg Clin North Am. 2014 Apr;94(2):325–42.
39. Pollard TD, Earnshaw WC, Lippincott-Schwartz J, Seidler L. Cell biology: das Original mit Übersetzungshilfen. 2. Aufl. Heidelberg: Spektrum Akad. Verl; 2007. 917 p. (Easy reading).
40. Rassow J, Hauser K, Netzker R, Deutzmann R. Biochemie. 4. Auflage. Stuttgart: Thieme; 2016. 879 p. (Duale Reihe).
41. Lim S, Kaldis P. Cdks, cyclins and CKIs: roles beyond cell cycle regulation. Development. 2013 Aug 1;140(15):3079–93.
42. Schafer KA. The Cell Cycle: A Review. Vet Pathol. 1998 Nov;35(6):461–78.
43. Waldmann T. p21 Is Necessary for the p53-mediated G1 Arrest in Human Cancer Cells. Cancer Res. 1995 Nov 1;(Volume 55, Issue 22):5187–90.
44. Blagosklonny MV, Pardee AB. The Restriction Point of the Cell Cycle. Cell Cycle. 2002 Mar;1(2):102–9.
45. Campisi J, Medrano EE, Morreo G, Pardee AB. Restriction point control of cell growth by a labile protein: evidence for increased stability in transformed cells. Proc Natl Acad Sci. 1982 Jan 1;79(2):436–40.
46. Miller DM, Thomas SD, Islam A, Muench D, Sedoris K. c-Myc and Cancer Metabolism. Clin Cancer Res. 2012 Oct 15;18(20):5546–53.
47. Bartek J, Lukas J. Pathways governing G1/S transition and their response to DNA damage. FEBS Lett. 2001 Feb 16;490(3):117–22.
48. Nevins JR. The Rb/E2F pathway and cancer. Hum Mol Genet. 2001 Apr 1;10(7):699–703.
49. Attwooll C, Denchi EL, Helin K. The E2F family: specific functions and overlapping interests. EMBO J. 2004 Dec 8;23(24):4709–16.
50. Black EP, Hallstrom T, Dressman HK, West M, Nevins JR. Distinctions in the specificity of E2F function revealed by gene expression signatures. Proc Natl Acad Sci. 2005 Nov 1;102(44):15948–53.
51. Li J, Ran C, Li E, Gordon F, Comstock G, Siddiqui H, et al. Synergistic Function

of E2F7 and E2F8 Is Essential for Cell Survival and Embryonic Development. Dev Cell. 2008 Jan;14(1):62–75.

52. UniProtKB- Q96AV8 (E2F7_HUMAN). In 2020. Available from: https://www.uniprot.org/uniprot/Q96AV8

53. Poppy Roworth A, Ghari F, La Thangue NB. To live or let die – complexity within the E2F1 pathway. Mol Cell Oncol. 2015 Jan 2;2(1):e970480.

54. Narita M, Nuñez S, Heard E, Narita M, Lin AW, Hearn SA, et al. Rb-Mediated Heterochromatin Formation and Silencing of E2F Target Genes during Cellular Senescence. Cell. 2003 Jun;113(6):703–16.

55. Di Fiore R, D'Anneo A, Tesoriere G, Vento R. RB1 in cancer: Different mechanisms of RB1 inactivation and alterations of pRb pathway in tumorigenesis: RB1/pRb INACTIVATION IN CANCER. J Cell Physiol. 2013 Aug;228(8):1676–87.

56. Phillips AC, Vousden KH. [No title found]. APOPTOSIS. 2001;6(3):173–82.

57. Wang H, Wang X, Xu L, Zhang J, Cao H. Integrated analysis of the E2F transcription factors across cancer types. Oncol Rep [Internet]. 2020 Feb 17 [cited 2020 Dec 13]; Available from: http://www.spandidos-publications.com/10.3892/or.2020.7504

58. E2F1 cervical cancer. In 2020. Available from: https://www.proteinatlas.org/ENSG00000101412-E2F1/pathology/cervical+cancer

59. E2F1 thyroid cancer. In 2020. Available from: https://www.proteinatlas.org/ENSG00000101412-E2F1/pathology/thyroid+cancer

60. E2F1 cancer. In 2020. Available from: https://www.proteinatlas.org/ENSG00000101412-E2F1/pathology

61. Hollern DP, Swiatnicki MR, Rennhack JP, Misek SA, Matson BC, McAuliff A, et al. E2F1 Drives Breast Cancer Metastasis by Regulating the Target Gene FGF13 and Altering Cell Migration. Sci Rep. 2019 24;9(1):10718.

62. Liang YX, Lu JM, Mo RJ, He HC, Xie J, Jiang FN, et al. E2F1 promotes tumor cell invasion and migration through regulating CD147 in prostate cancer. Int J Oncol. 2016 Apr;48(4):1650–8.

63. Ohtani K, DeGregori J, Nevins JR. Regulation of the cyclin E gene by transcription factor E2F1. Proc Natl Acad Sci. 1995 Dec 19;92(26):12146–50.

64. Musgrove EA, Caldon CE, Barraclough J, Stone A, Sutherland RL. Cyclin D as a therapeutic target in cancer. Nat Rev Cancer. 2011 Aug;11(8):558–72.

65. Mega S, Miyamoto M, Ebihara Y, Takahashi R, Hase R, Li L, et al. Cyclin D1, E2F1 expression levels are associated with characteristics and prognosis of esophageal squamous cell carcinoma. Dis Esophagus. 2005 Jun 1;18(2):109–13.
66. Wang X, Qi X, Ming X, Wang L, Wang Y, Zhao X. Prognostic value of cyclin E expression in patients with ovarian cancer: a Meta-analysis. J BUON Off J Balk Union Oncol. 2017 Feb;22(1):64–71.
67. Nielsen N, Arnerlöv C, Emdin S, Landberg G. Cyclin E overexpression, a negative prognostic factor in breast cancer with strong correlation to oestrogen receptor status. Br J Cancer. 1996 Sep;74(6):874–80.
68. Fukuse T, Hirata T, Naiki H, Hitomi S, Wada H. Prognostic significance of cyclin E overexpression in resected non-small cell lung cancer. Cancer Res. 2000 Jan 15;60(2):242–4.
69. Wang A, Yoshimi N, Ino N, Tanaka T, Mori H. Overexpression of cyclin B1 in human colorectal cancers. J Cancer Res Clin Oncol. 1997 Feb;123(2):124–7.
70. Soria JC, Jang SJ, Khuri FR, Hassan K, Liu D, Hong WK, et al. Overexpression of cyclin B1 in early-stage non-small cell lung cancer and its clinical implication. Cancer Res. 2000 Aug 1;60(15):4000–4.
71. Kawamoto H, Koizumi H, Uchikoshi T. Expression of the G2-M checkpoint regulators cyclin B1 and cdc2 in nonmalignant and malignant human breast lesions: immunocytochemical and quantitative image analyses. Am J Pathol. 1997 Jan;150(1):15–23.
72. Sarafan-Vasseur N, Lamy A, Bourguignon J, Le Pessot F, Hieter P, Sesboüé R, et al. Overexpression of B-type cyclins alters chromosomal segregation. Oncogene. 2002 Mar 27;21(13):2051–7.
73. Cyclin B1 gencard. In Internet; 2021. Available from: https://www.ncbi.nlm.nih.gov/gene/891
74. Russo AJ, Magro PG, Hu Z, Li WW, Peters R, Mandola J, et al. E2F-1 Overexpression in U2OS Cells Increases Cyclin B1 Levels and cdc2 Kinase Activity and Sensitizes Cells to Antimitotic Agents. Cancer Res. 2006 Jul 15;66(14):7253–60.
75. Farhana L, Dawson M, Rishi AK, Zhang Y, Van Buren E, Trivedi C, et al. Cyclin B and E2F-1 expression in prostate carcinoma cells treated with the novel retinoid CD437 are regulated by the ubiquitin-mediated pathway. Cancer Res. 2002 Jul 1;62(13):3842–9.

76. cmyc gencard. In [cited 2021 Mar 13]. Available from: https://www.ncbi.nlm.nih.gov/gene/4609
77. Elliott MJ, Dong YB, Yang H, McMasters KM. E2F-1 up-regulates c-Myc and p14(ARF) and induces apoptosis in colon cancer cells. Clin Cancer Res Off J Am Assoc Cancer Res. 2001 Nov;7(11):3590–7.
78. Ladu S, Calvisi DF, Conner EA, Farina M, Factor VM, Thorgeirsson SS. E2F1 Inhibits c-Myc-Driven Apoptosis via PIK3CA/Akt/mTOR and COX-2 in a Mouse Model of Human Liver Cancer. Gastroenterology. 2008 Oct;135(4):1322–32.
79. Zhang Y, Zhang A, Shen C, Zhang B, Rao Z, Wang R, et al. E2F1 acts as a negative feedback regulator of c-Myc-induced hTERT transcription during tumorigenesis. Oncol Rep. 2014 Sep;32(3):1273–80.
80. Zhang L, Wang C. F-box protein Skp2: a novel transcriptional target of E2F. Oncogene. 2006 Apr;25(18):2615–27.
81. Kipreos ET, Pagano M. The F-box protein family. Genome Biol. 2000;1(5):reviews3002.1.
82. Gstaiger M, Jordan R, Lim M, Catzavelos C, Mestan J, Slingerland J, et al. Skp2 is oncogenic and overexpressed in human cancers. Proc Natl Acad Sci U S A. 2001 Apr 24;98(9):5043–8.
83. mcm2 gencard. In Internet; 2021. Available from: https://www.ncbi.nlm.nih.gov/gene/4171
84. Yousef EM, Furrer D, Laperriere DL, Tahir MR, Mader S, Diorio C, et al. MCM2: An alternative to Ki-67 for measuring breast cancer cell proliferation. Mod Pathol Off J U S Can Acad Pathol Inc. 2017 May;30(5):682–97.
85. de Andrade BAB, León JE, Carlos R, Delgado-Azañero W, Mosqueda-Taylor A, de Almeida OP. Expression of minichromosome maintenance 2, Ki-67, and geminin in oral nevi and melanoma. Ann Diagn Pathol. 2013 Feb;17(1):32–6.
86. Czyzewska J, Guzińska-Ustymowicz K, Pryczynicz A, Kemona A, Bandurski R. Immunohistochemical evaluation of Ki-67, PCNA and MCM2 proteins proliferation index (PI) in advanced gastric cancer. Folia Histochem Cytobiol. 2009;47(2):289–96.
87. Guzińska-Ustymowicz K, Pryczynicz A, Kemona A, Czyzewska J. Correlation between proliferation markers: PCNA, Ki-67, MCM-2 and antiapoptotic protein Bcl-2 in colorectal cancer. Anticancer Res. 2009 Aug;29(8):3049–52.
88. Deng M, Sun J, Xie S, Zhen H, Wang Y, Zhong A, et al. Inhibition of MCM2

enhances the sensitivity of ovarian cancer cell to carboplatin. Mol Med Rep. 2019 Sep;20(3):2258–66.
89. MCM7 Gene Card. In Internet; 2021. Available from: https://www.ncbi.nlm.nih.gov/gene/4176
90. Qu K, Wang Z, Fan H, Li J, Liu J, Li P, et al. MCM7 promotes cancer progression through cyclin D1-dependent signaling and serves as a prognostic marker for patients with hepatocellular carcinoma. Cell Death Dis. 2017 Feb;8(2):e2603–e2603.
91. Ren B, Yu G, Tseng GC, Cieply K, Gavel T, Nelson J, et al. MCM7 amplification and overexpression are associated with prostate cancer progression. Oncogene. 2006 Feb 16;25(7):1090–8.
92. FOXM1. In Internet; [cited 2021 Mar 20]. Available from: https://www.ncbi.nlm.nih.gov/gene/2305
93. Kalathil D, John S, Nair AS. FOXM1 and Cancer: Faulty Cellular Signaling Derails Homeostasis. Front Oncol. 2021 Feb 15;10:626836.
94. de Olano N, Koo CY, Monteiro LJ, Pinto PH, Gomes AR, Aligue R, et al. The p38 MAPK-MK2 axis regulates E2F1 and FOXM1 expression after epirubicin treatment. Mol Cancer Res MCR. 2012 Sep;10(9):1189–202.
95. Wang N, Li Y, Zhou J. Downregulation of ribonucleotide reductase subunits M2 induces apoptosis and G1 arrest of cervical cancer cells. Oncol Lett. 2018 Mar;15(3):3719–25.
96. Zhuang S, Li L, Zang Y, Li G, Wang F. RRM2 elicits the metastatic potential of breast cancer cells by regulating cell invasion, migration and VEGF expression via the PI3K/AKT signaling. Oncol Lett. 2020 Apr;19(4):3349–55.
97. Fang Z, Gong C, Liu H, Zhang X, Mei L, Song M, et al. E2F1 promote the aggressiveness of human colorectal cancer by activating the ribonucleotide reductase small subunit M2. Biochem Biophys Res Commun. 2015 Aug 21;464(2):407–15.
98. Mazzu YZ, Armenia J, Chakraborty G, Yoshikawa Y, Coggins SA, Nandakumar S, et al. A Novel Mechanism Driving Poor-Prognosis Prostate Cancer: Overexpression of the DNA Repair Gene, Ribonucleotide Reductase Small Subunit M2 (RRM2). Clin Cancer Res. 2019 Jul 15;25(14):4480–92.
99. Jung CP, Motwani MV, Schwartz GK. Flavopiridol increases sensitization to gemcitabine in human gastrointestinal cancer cell lines and correlates with down-regulation of ribonucleotide reductase M2 subunit. Clin Cancer Res Off J Am Assoc

Cancer Res. 2001 Aug;7(8):2527–36.
100. Zhan Y, Jiang L, Jin X, Ying S, Wu Z, Wang L, et al. Inhibiting RRM2 to enhance the anticancer activity of chemotherapy. Biomed Pharmacother. 2021 Jan;133:110996.
101. Kurtyka CA, Chen L, Cress WD. E2F inhibition synergizes with paclitaxel in lung cancer cell lines. PloS One. 2014;9(5):e96357.
102. Ma Y, Kurtyka CA, Boyapalle S, Sung SS, Lawrence H, Guida W, et al. A Small-Molecule E2F Inhibitor Blocks Growth in a Melanoma Culture Model. Cancer Res. 2008 Aug 1;68(15):6292–9.
103. He F. Bradford Protein Assay. BIO-Protoc [Internet]. 2011 [cited 2020 Mar 8];1(6). Available from: https://bio-protocol.org/e45
104. Holschbach, Martin. Western Blot: Gelelktrophorese für Proteine [Internet]. Antikörper-online. [cited 2022 Nov 29]. Available from: https://www.antikoerper-online.de/resources/17/1224/western-blot-gelelektrophorese-fuer-proteine/
105. Real time quantitaive PCR [Internet]. bionity.com. [cited 2022 Nov 29]. Available from: https://www.bionity.com/de/lexikon/Real_time_quantitative_PCR.html#CT-Wert_oder_auch_Cp-Wert
106. Kho D, MacDonald C, Johnson R, Unsworth C, O'Carroll S, Mez E, et al. Application of xCELLigence RTCA Biosensor Technology for Revealing the Profile and Window of Drug Responsiveness in Real Time. Biosensors. 2015 Apr 16;5(2):199–
107. Chun JN, Cho M, Park S, So I, Jeon JH. The conflicting role of E2F1 in prostate cancer: A matter of cell context or interpretational flexibility? Biochim Biophys Acta BBA - Rev Cancer. 2020 Jan;1873(1):188336.
108. E2F1 in liver cancer. In Internet; 2021. Available from: https://www.proteinatlas.org/ENSG00000101412-E2F1/pathology/liver+cancer
109. E2F1 in endometrium cancer. In.
110. E2F1 in renal cancer. In Internet; 2021. Available from: https://www.proteinatlas.org/ENSG00000101412-E2F1/pathology/renal+cancer
111. Fang Z, Lin M, Li C, Liu H, Gong C. A comprehensive review of the roles of E2F1 in colon cancer. Am J Cancer Res. 2020;10(3):757–68.
112. O'Connor MJ, Thakar T, Nicolae CM, Moldovan GL. PARP14 regulates cyclin D1 expression to promote cell-cycle progression. Oncogene. 2021 Jul;40(30):4872–83.

113. Watanabe G, Albanese C, Lee RJ, Reutens A, Vairo G, Henglein B, et al. Inhibition of Cyclin D1 Kinase Activity Is Associated with E2F-Mediated Inhibition of Cyclin D1 Promoter Activity through E2F and Sp1. Mol Cell Biol. 1998 Jun;18(6):3212–22.
114. Chu C, Geng Y, Zhou Y, Sicinski P. Cyclin E in normal physiology and disease states. Trends Cell Biol. 2021 Sep;31(9):732–46.
115. Marin JJG, Lozano E, Herraez E, Asensio M, Di Giacomo S, Romero MR, et al. Chemoresistance and chemosensitization in cholangiocarcinoma. Biochim Biophys Acta Mol Basis Dis. 2018 Apr;1864(4 Pt B):1444–53.
116. Kikuchi K, Kaida D. CCNE1 and E2F1 Partially Suppress G1 Phase Arrest Caused by Spliceostatin A Treatment. Int J Mol Sci. 2021 Oct 27;22(21):11623.
117. Hwang HC, Clurman BE. Cyclin E in normal and neoplastic cell cycles. Oncogene. 2005 Apr 18;24(17):2776–86.
118. Siu KT, Rosner MR, Minella AC. An integrated view of cyclin E function and regulation. Cell Cycle Georget Tex. 2012 Jan 1;11(1):57–64.
119. Sherr CJ, Roberts JM. CDK inhibitors: positive and negative regulators of G1-phase progression. Genes Dev. 1999 Jun 15;13(12):1501–12.
120. Sonntag R, Giebeler N, Nevzorova YA, Bangen JM, Fahrenkamp D, Lambertz D, et al. Cyclin E1 and cyclin-dependent kinase 2 are critical for initiation, but not for progression of hepatocellular carcinoma. Proc Natl Acad Sci. 2018 Sep 11;115(37):9282–7.
121. Mouawad R, Himadewi P, Kadiyala D, Arnosti DN. Selective repression of the Drosophila cyclin B promoter by retinoblastoma and E2F proteins. Biochim Biophys Acta Gene Regul Mech. 2020 Jul;1863(7):194549.
122. Gabay M, Li Y, Felsher DW. MYC activation is a hallmark of cancer initiation and maintenance. Cold Spring Harb Perspect Med. 2014 Jun 2;4(6):a014241.
123. Luo G, Li B, Duan C, Cheng Y, Xiao B, Yao F, et al. c-Myc promotes cholangiocarcinoma cells to overcome contact inhibition via the mTOR pathway. Oncol Rep. 2017 Apr;38(4):2498–506.
124. Li B, Zhang G, Wang Z, Yang Y, Wang C, Fang D, et al. c-Myc-activated USP2-AS1 suppresses senescence and promotes tumor progression via stabilization of E2F1 mRNA. Cell Death Dis. 2021 Oct 27;12(11):1006.
125. Wang CL, Liu XY, Wang YH, Zhang Z, Wang ZD, Zhou GQ. MCM2 promotes

the proliferation, migration and invasion of cholangiocarcinoma cells by reducing the p53 signaling pathway. Yi Chuan Hered. 2022 Mar 20;44(3):230–44.
126. Jia M, Zheng D, Wang X, Zhang Y, Chen S, Cai X, et al. Cancer Cell enters reversible quiescence through Intracellular Acidification to resist Paclitaxel Cytotoxicity. Int J Med Sci. 2020;17(11):1652–64.
127. Luo J, Zhou Y, Wang B, Li Q, Chen Y, Lan H. Immunohistochemically detected expression of Skp2, p27 kip1, and p-p27 (Thr187) in patients with cholangiocarcinoma. Tumour Biol J Int Soc Oncodevelopmental Biol Med. 2015 Jul;36(7):5119–25.
128. Zhao C, Li Y, Qiu C, Chen J, Wu H, Wang Q, et al. Splicing Factor DDX23, Transcriptionally Activated by E2F1, Promotes Ovarian Cancer Progression by Regulating FOXM1. Front Oncol. 2021;11:749144.
129. Gao Y, Xu D, Li H, Xu J, Pan Y, Liao X, et al. Avasimibe Dampens Cholangiocarcinoma Progression by Inhibiting FoxM1-AKR1C1 Signaling. Front Oncol. 2021;11:677678.
130. Tabbal H, Septier A, Mathieu M, Drelon C, Rodriguez S, Djari C, et al. EZH2 cooperates with E2F1 to stimulate expression of genes involved in adrenocortical carcinoma aggressiveness. Br J Cancer. 2019 Aug;121(5):384–94.
131. Liu M, Yan Q, Sun Y, Nam Y, Hu L, Loong JH, et al. A hepatocyte differentiation model reveals two subtypes of liver cancer with different oncofetal properties and therapeutic targets. Proc Natl Acad Sci U S A. 2020 Mar 17;117(11):6103–13.
132. Rosales-Hurtado M, Lebeau A, Bourouh C, Cebrian-Torrejon G, Albalat M, Jean M, et al. Improved synthesis, resolution, absolute configuration determination and biological evaluation of HLM006474 enantiomers. Bioorg Med Chem Lett. 2019 Feb 1;29(3):380–2.

Declaration

I hereby declare that I have prepared this thesis without the unauthorized assistance of third parties and without the use of aids other than those indicated. The data and concepts taken directly or indirectly from other sources are marked with reference to the source. In particular, I have not made use of the paid assistance of intermediary or consulting services (doctoral advisors or other persons). No one has received from me, directly or indirectly, any monetary benefits for work related to the content of the thesis presented. The thesis has not been submitted to any other examination authority in the same or similar form, either in Germany or abroad.

Ich erkläre hiermit, dass ich die vorliegende Arbeit ohne unzulässige Hilfe Dritter und ohne Benutzung anderer als der angegebenen Hilfsmittel angefertigt habe. Die aus anderen Quellen direkt oder indirekt übernommenen Daten und Konzepte sind unter Angabe der Quelle gekennzeichnet. Insbesondere habe ich nicht die entgeltliche Hilfe von Vermittlungs- bzw. Beratungsdiensten (Promotionsberater oder andere Personen) in Anspruch genommen. Niemand hat von mir unmittelbar oder mittelbar geldwerte Leistungen für Arbeit erhalten, die im Zusammenhang mit dem Inhalt der vorgelegten Dissertation stehen. Die Arbeit wurde bisher weder im In- noch im Ausland in gleicher oder ähnlicher Form einer anderen Prüfungsbehörde vorgelegt.

_____

Tabea Globuschütz, Regensburg am 01.12.23